e-Zine for meteor observers meteornews.net

MeteorNews

ISSN 2570-4745 VOL 8 / ISSUE 6 / NOVEMBER 2023

The Super-Perseid of August 15, 2023 at 22h49m58s UT. Camera: Sony Alpha A7sII. Lens: Sigma ART 20mm F 1.4 lens. (credit:Koen Miskotte).

- IAU Shower Database
- 2023 Perseids
- "blue" trails
- CAMS reports
- Radio meteor work
- Fireballs

Contents

© eMeteorNews

Grading evaluation of meteor showers' report in the IAU Meteor Data Center Shower Database

Masahiro Koseki

The Nippon Meteor Society, 4-3-5 Annaka Annaka-shi, Gunma-ken, 379-0116 Japan
geh04301@nifty.ne.jp

We attempted to numerically evaluate the reports published in the Shower Database, SD (downloaded 2023 on March 29) using GMN video observation data (downloaded 2023 on February 25). Of the 1595 entries published in the SD, 1117 were investigated, excluding those from the same group or those with insufficient data. There were 67 entries that were evaluated to have been clearly captured by video observation (Grade 10 and 9), 147 where the existence could be confirmed (Grade 8 and 7), and 213 where further confirmation work was required (Grade 6 and 5). On the other hand, for 339 entries, no corresponding meteor shower could be found (Grade 4); 201 where the observed meteors are so small (N<10) and cannot be checked (Grade 3). In this survey, there were 78 cases in which it was impossible to investigate areas surrounding powerful meteor showers (Grade 2). There were also 99 cases that were determined to be duplicates of those that had already been reported (Grade 1).
It is highly anticipated that future GMN observations will help a lot clarifying the problems, especially in the southern hemisphere.

1 Introduction

The Shower Database (SD) list is a mixed bag, and the data posted cannot be taken as exact facts. Early publications included only visual observations or were based on a few orbits from photographic or radio observations. For example, 0300ZPU00 ~ 0318MVE00 are not numbered in the original SD, that is, in Jenniskens (2006), and are based on visual observations. Since then, many meteor showers have been discovered by using the rich data from radio and video observations. On the other hand, there are also claims for meteor shower discoveries which are so weak that it is indistinguishable from the sporadic background meteor activity. Furthermore, the SD has a problem with multiple shower activities which are included in one meteor shower, or conversely, the same activity is registered as a different meteor shower (Koseki, 2020a).

In response to this confusion, it would be meaningful to evaluate how relevant the individual reports published in the SD can be considered. It is best to use Global Meteor Network[1] data as GMN has sufficient video observations publicly available for this purpose.

2 Research step

2.1 Selection of the entries

We use the SD downloaded 2023 on March 29, which has 1595 entries. It is not necessary to survey all entries because this research intends to estimate the grade for each meteor shower. In fact, we made selections while looking at the radiant point distribution and the activity curve for the next step excluding 0290ALL00 ~ 0299OAR00 because they lack radiant data, and ultimately investigated 1117 out of 1595 entries. In this way, we use IAUNo + Code + AdNo as the CODE for distinguishing the entries in the same meteor shower, for example, 0023EGE00 for describing the first entry of EGE (epsilon-Geminids).

2.2 Plotting the radiant distribution of GMN meteors and the activity profile

Koseki (2019a) showed it is useful for us to plot the radiant distribution 10 degrees in solar longitude before and after the maximum listed in the entry and to calculate *DRs*: the sliding mean of the radiant density ratios within bins of 3 degrees in $\lambda_{\odot}$.

- *DR3*: the density ratio within a circle of 3 degrees relative to a ring of 3 to 6 degrees.
- *DR10*: the density ratio within a circle of 3 degrees relative to a ring of 6 to 10 degrees.
- *DR15*: the density ratio within a circle of 3 degrees relative to a ring of 10 to 15 degrees.
- *DR3_20*: the density ratio within a circle of 3 degrees relative to a ring of 15 to 20 degrees.
- *DR6_20*: the density ratio within a circle of 6 degrees relative to a ring of 15 to 20 degrees; this is only a reference value.
- *DR* = 1 means that the radiant density is flat.

Figures 1 to 3 and *Tables 1 and 2* are examples of this procedure for 0023EGE00. *Figure 1* shows the radiant distribution of GMN video meteors around $(\lambda - \lambda_{\odot}, \beta) = (253.48, 4.20)$ from $\lambda_{\odot} = 199.7°$ to $\lambda_{\odot} = 219.7°$; the radiant concentration is well within $r < 3$ degrees. *Figure 2* shows the radiant distribution given in the SD; boxes are classified as EGE and a cross represents others. We can judge whether the classification in the SD is adequate. If inadequate, we divide such entries into several groups. If some crosses are in the inner circle ($r < 3$), we should be cautious about whether they might be an

[1] Global Meteor Network. https://globalmeteornetwork.org/

Table 1 – The radiant distribution near the EGE shower activities in the SD.

CODE	$\lambda_\odot$	$\lambda - \lambda_\odot$	β	v_g	Distance	x	y
0023EGE00	209.7	253.48	4.2	69.4	0	0	0
0023EGE01	206	254.37	3.68	68.8	1	–0.9	–0.5
0023EGE02	198	255.36	4.71	69.6	1.9	–1.9	0.5
0537KAU00	208	244.63	9.79	65.5	10.4	8.7	5.7

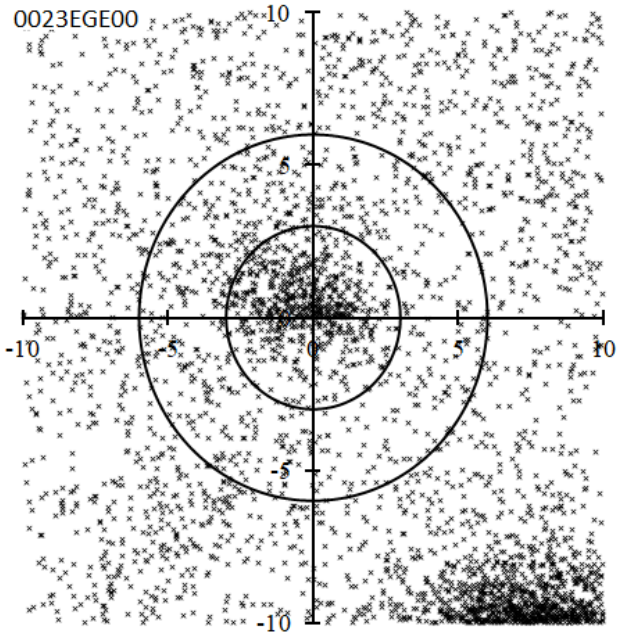

Figure 1 – Radiant distribution for 0023EGE03. The center is $(\lambda - \lambda_\odot, \beta) = (253.48, 4.20)$ and the period is $\lambda_\odot = 199.7°$ to $\lambda_\odot = 219.7°$. The radius of the inner circle is 3 degrees and the radius of the outer circle is 6 degrees, and the EGE radiants fall within the inner circle.

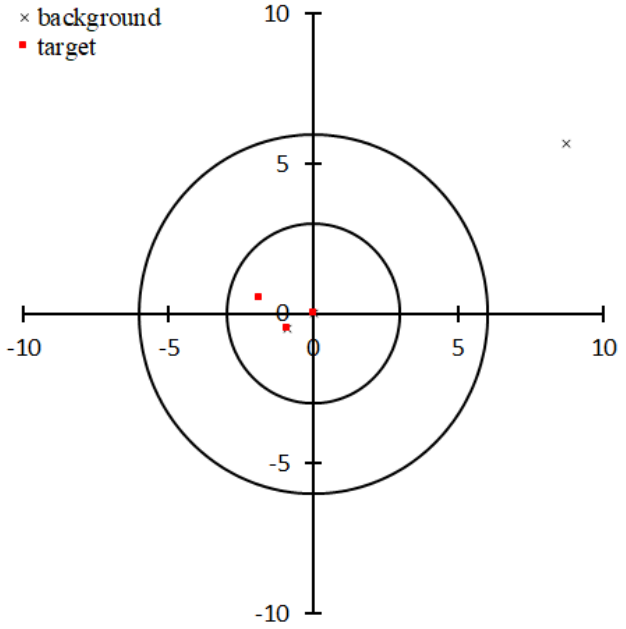

Figure 2 – Radiant distribution for meteor showers listed in the SD; the center and range are the same as in *Figure 1*. Filled squares are EGE, and one cross is the other.

indication for other, different, shower activities. *Table 1* gives some details of meteor activities plotted in *Figure 2*. *Figure 3* represents the activity profiles plotted according to the calculation of *DRs* and $Nr \leq 3$; *DR3_20* and *DR6_20* are omitted to simplify the figure; the graph for $Nr \leq 3$ represents the number of radiants counted within 3 degrees from the radiant position in steps of one degree in $\lambda_\odot$. The graph of *DR15* is quite different from the other three because the nearby strong activity of Orionids hinders *DR15* of EGE.

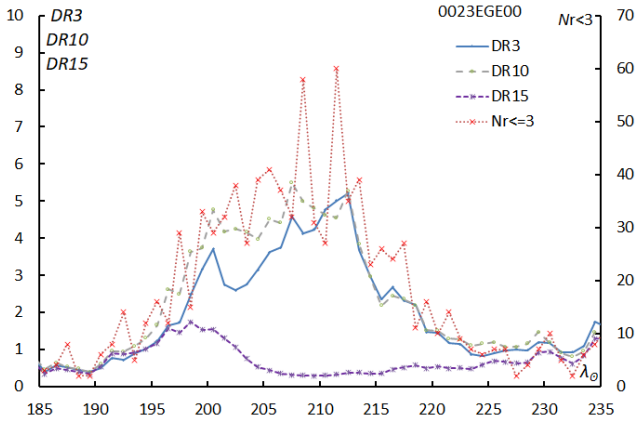

Figure 3 – Activity profiles of EGE using *DR*; the center used for calculation is the same as in *Figure 1*.

Table 2 – The peak values of the graphs in *Figure 3*; *DR3_20* and *DR6_20* are added and *N3* gives the total meteor number within $r \leq 3$ and $\lambda_\odot = 199.7$~$219.7°$.

	$\lambda_\odot$	Value
$Nr \leq 3$	211.5	60
DR3	212.5	5.22
DR10	207.5	5.49
DR15	200.5	1.54
DR3_20	200.5	4.61
DR6_20	202.5	2.35
N3		657

2.3 Check the peak rates of the raw number and the DR

When evaluating meteor showers, it is important that the radiant point and maximum activity are clearly defined. It seems useful to give another example to confirm the meaning of *DRs* and $Nr \leq 3$.

Figures 4 and 5 show the radiant distribution and the activity profiles for 0022LMI03 and *Table 3* gives the summary of its activity.

It is clear the radiants of LMI are concentrated within narrow areas and surrounding meteor activities are scarce. As a result, it can be seen that the values of *DRs* become larger and the variation in the maximum becomes smaller

 © eMeteorNews

than those of EGE though *N3* of LMI is smaller than EGE, that is, the total LMI activity is smaller than EGE. Therefore, the density of radiant points and the intensity of the meteor shower activity can be expressed by the magnitude of the *DR* values. On the other hand, it must be noted that in cases such as EGE, where the meteor shower is affected by surrounding meteor showers, $Nr \leq 3$ is a direct indicator of the strength of the meteor shower's activity.

Table 3 – Summary of the LMI activity profile (*Figure 5*).

	$\lambda\odot$	Value
$Nr \leq 3$	208.5	125
DR3	210.5	27.62
DR10	208.5	55.17
DR15	207.5	54.32
DR3_20	209.5	29.01
DR6_20	209.5	8.12
N3		827

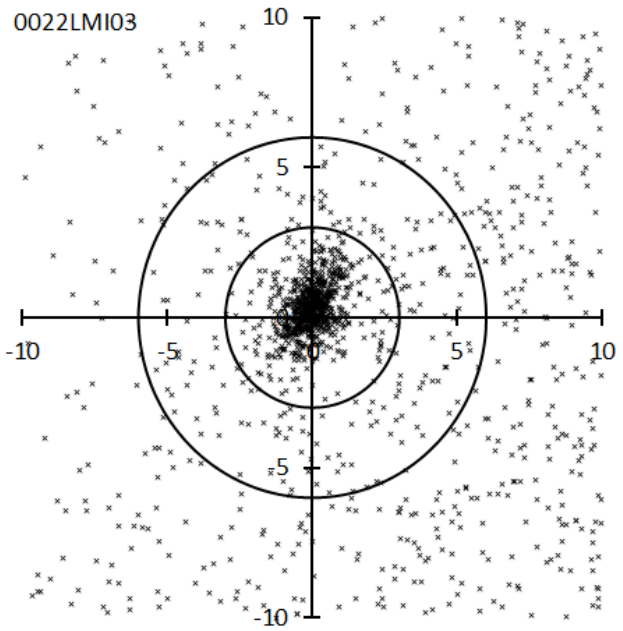

Figure 4 – Radiant distribution for 0022LMI03. The center is $(\lambda - \lambda\odot, \beta) = (297.96, 25.93)$ and the period is $\lambda\odot = 199°$ to $\lambda\odot = 219°$. Compared to EGE, the radiant points are concentrated, and the surrounding radiant point distribution is diffused.

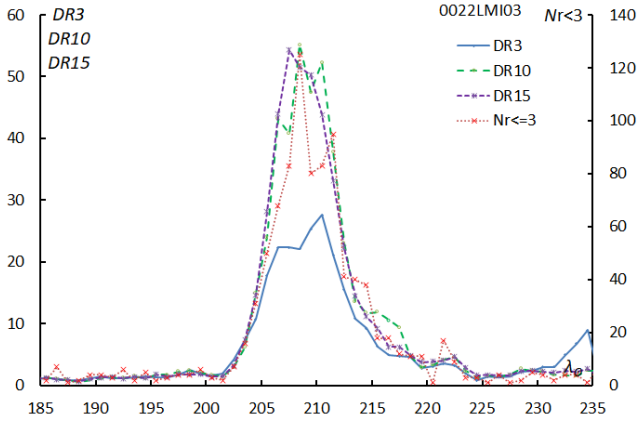

Figure 5 – Activity profiles of LMI using *DR*; the center used for calculation is the same as in *Figure 4*. The activity curves are narrower and higher than those of EGE.

2.4 Evaluation of the grading

There are three other issues when evaluating meteor shower activity.

Firstly, as is clear from the maps in the appendix, meteor showers around the Sun and deep in the southern hemisphere are difficult to observe with GMN video observations; that is, they have $N3 < 10$. Second, the method used here is not applicable around strong meteor showers. To handle such meteor showers, it is necessary to use specialized methods, so they are excluded from this study. The third problem is confusion in the SD itself, where the same meteor shower is listed separately, or different meteor showers are listed in one item. Taking these issues into consideration, meteor shower activity is evaluated on the following 10 scales. Below, the average value of *DRs* (excluded *DR6_20* because this is only a reference value) is abbreviated as *DR*, and $Nr \leq 3$ is abbreviated as *N*. *Figure 6* shows the summary of the evaluation.

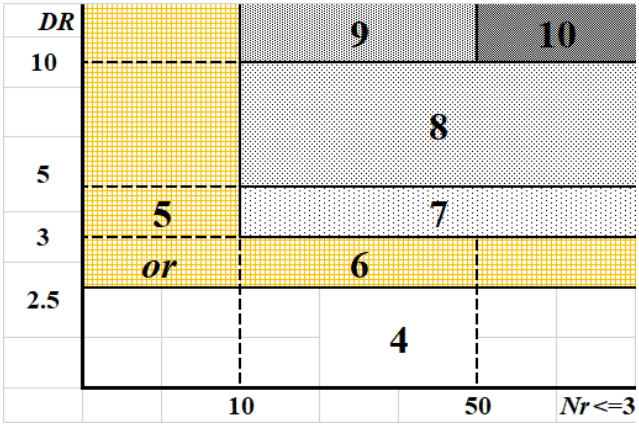

Figure 6 – Overview of the evalution for the classification in different Grades.

The grading criteria:

- 10: $DR > 10$ and $N > 50$, 39 cases.
- 9: $DR > 10$ and $10 < N < 50$, 28 cases.
- 8: $DR > 5$ and $N > 10$, 53 cases.
- 7: $DR > 3$ and $N > 10$, 94 cases.
- 5 and 6: $DR > 2.5$. If the difference between the date of the maximum listed in the SD and the average date of the maximum for *DR* is less than 5, the score is 6 else 5. 159 cases got Grade 6, 54 cases Grade 5.
- 4: $DR < 2.5$, 339 cases.
- 3: $N3 < 10$, 201 cases.
- 2: In case a strong shower (STA and NTA, ORI (with its tale; TORI), PER, GEM, COM, and SDA) influences the radiant area, 78 cases.
- 1: When there is confusion in the SD, 72 cases.

2.5 Preliminary grading of meteor showers listed in the SD

Although this evaluation is provisional as it does not consider the radiant point's drift, we believe it will be useful for readers. If the rating is not 9 or higher, it cannot be a target for visual observation, a rating of 8 can only be captured under favorable conditions. It is appropriate to limit meteor showers to those of 7 or higher levels when we

count the number of meteors and investigate the properties of meteor showers. Those with a stage of 4 or lower are those whose activity was not confirmed in this survey, and those with a stage of 5 and 6 require future investigation and consideration, including whether they exist as a meteor shower. The number of cases for each grade has been mentioned above with the grading criteria.

2.6 Classification of meteor showers

The number following the slash after the Code is the value of the 'shower status flags' by the SD. Particularly established showers are shown in bold in the list.

The shower status flags:

- –9: removed from the MDC, data not published
- –8: no Look up table
- –7: various faults: typo, suspicious ...
- –6: criterion *R3*; the shower has been found to be unreliable.
- –5: not used yet
- –4: criterion *R2*; duplicate, shower designation was changed; the data was added as another solution to the previously known stream
- –3: criterion *R4*; $N < 3$; only 1 or 2 members
- –2: criterion *R1*; missing or wrong data, or problems with references
- –1: to be removed from the list of established showers
- 0: single shower, working list
- 1: single established shower,
- 2: to be established shower

Criteria for moving showers to the List of removed showers (Hajduková et al., 2023):

- *R1*. The correct bibliographic information for the stream identification is absent.
- *R2*. The shower is found to be a duplicate of an earlier discovered shower.
- *R3*. The shower has been found to be unreliable.
- *R4*. The stream was identified using fewer than three meteoroids.

Meteor showers marked with * in parentheses have comments in the section *Additional notes* below, so please refer to the corresponding Code in this section. If * is followed by a different Code, please see the comments for that Code. For Grade 2, the meteor shower that had an influence is indicated by an abbreviation in parentheses; TORI means the tail of Orionids.

Grade 10

0001CAP06/1(*), **0002STA00/1**, **0004GEM00/1**, **0005SDA00/1**, **0006LYR00/1**, **0007PER00/1**, **0008ORI00/1**, **0010QUA00/1**, **0011EVI06/1(*)**, **0012KCG11/1(*)**, **0013LEO00/1**, 0015URS01/–2, **0016HYD01/1**, **0017NTA03/1**, **0019MON01/1**, **0020COM03/1**, **0022LMI03/1**, **0026NDA10/1**, **0031ETA07/1**, **0145ELY02/1**, **0164NZC01/1(*0164NZC00)**, **0175JPE02/1**, **0184GDR00/1**, **0191ERI02/1**, 0199ADC01/0, **0208SPE02/1(*)**, **0250NOO06/1**, **0281OCT00/1**, **0333OCU00/1**, **0336DKD01/1**, **0341XUM06/1**, **0404GUM04/1**, **0411CAN00/1**, 0429ACB00/2, **0431JIP00/1(*0367OPG00)**, 0444ZCS00/2, **0445KUM00/1**, 0458JEC00/0, 0623XCS00/0(*).

Grade 9

0018AND01/1, 0027KSE01/–3, **0027KSE02/1(*)**, **0110AAN04/1**, **0164NZC00/1(*)**, **0165SZC02/1(*)**, **0170JBO07/1**, **0171ARI03/1**, **0221DSX00/1**, 0255PUV00/–2(*), **0323XCB04/1**, **0331AHY00/1**, **0335XVI00/1(*)**, **0343HVI07/1**, **0362JMC02/1**, 0370MIC00/0(*0165SZC02), **0372PPS00/1(*)**, 0410DPI00/0, **0428DSV00/1(*)**, 0450AED00/0, 0497DAB00/0, **0510JRC00/1**, **0533JXA00/1(*)**, **0569OHY00/1(*0316BHD00)**, 0757CCY00/0, 0784KVE00/0(*0303LVL00), 0839PSR00/0(*0027KSE02), 0860PAN00/0.

Grade 8

0021AVB06/1(*), 0040ZCY02/2(*), **0069SSG03/1**, 0081SLY00/0(*), **0187PCA00/1(*)**, **0197AUD01/1(*0073ZDR00)**, **0206AUR03/1,** 0215NPI04/2(*), **0246AMO00/1(*)**, **0257ORS03/1(*)**, **0319JLE00/1**, **0334DAD00/1(*)**, **0337NUE00/1(*)**, **0338OER00/1(*)**, **0339PSU01/1**, 0340TPY00/0(*), 0340TPY01/0(*), **0346XHE01/1**, **0348ARC00/1**, **0372PPS01/1(*0372PPS00)**, 0394ACA00/2, **0427FED00/1**, 0459JEO01/0, 0465AXC00/0, 0480TCA00/0(*), 0481OML00/0, 0488NSU00/0(*0527UUM00), 0490DGE01/0(*), 0502DRV00/2(*), **0512RPU00/1**, 0515OLE00/0(*), 0519BAQ00/2, 0520MBC00/0, 0523AGC00/2, **0524LUM00/1**, **0526SLD00/1**, **0529EHY00/1**, 0531GAQ01/2, 0552PSO01/2(*), 0571TSB00/0, 0647BCO00/0, 0694OMG00/0(*), 0825XIE00/0, 0841DHE00/0, 0854PCY00/0, 0867FPE00/0(*0371APG00), 0893EOP00/0, 0915DNO00/0, 0924SAN00/0, 1032FHY00/0, 1096NAC00/0, 1133TCS00/0(*0187PCA00), 1166TTR00/0.

 © eMeteorNews

Grade 7

0012KCG07/1(*), **0023EGE00/1,** 0040ZCY00/2, 0047DLI02/0(*), 0049LVI00/–3, 0055ASC01/–6, 0081SLY01/0(*), **0096NCC00/1(*)**, **0096NCC02/1(*0096NCC00)**, **0096NCC03/1(*0096NCC00)**, **0096NCC06/1(*0096NCC00)**, **0096NCC08/1(*0096NCC00)**, **0097SCC03/1(*0096NCC00)**, **0097SCC05/1(*0096NCC00)**, 0101PIH00/0, 0136SLE00/0(*), 0139GLI00/0(*), 0149NOP02/0(*0150SOP00), 0150SOP00/0(*), 0150SOP03/0(*0150SOP00), 0150SOP05/0(*0150SOP00), 0167NSS01/0(*), 0168SSS00/0, **0183PAU00/1**, **0183PAU02/1**, **0197AUD00/1(*0073ZDR00)**, 0205XAU00/–3, 0253CMI03/0, 0371APG00/0(*), 0386OBC01/2, 0413MUL00/2, 0416SIC00/2, 0436GCP00/0, 0439ASX02/0(*), 0448AAL00/–6(*0139GLI00), 0456MPS00/2(*0150SOP00), 0460LOP00/2, 0464KLY00/0(*), 0470AMD02/2(*), 0472ATA01/–6, 0493DEC00/0, 0507UAN01/0, 0517ALO00/0, **0530ECV00/1(*)**, **0549FAN00/1**, 0556PTA00/0, 0557SFD00/0, 0563DOU00/0(*), 0567XHY00/0(*), 0568FCV00/0, 0570FBH00/0, 0581NHE00/0, 0582JBC00/0, 0587FNC00/0, 0601ICT00/0, 0610SGM00/0, 0644JLL00/0(*), 0645PHC00/0, 0651OAV00/0, 0653RLY00/0, 0665MUC00/0(*0359MZC00), 0686JRD00/0(*), 0708RLM00/0, 0710IOL00/0, 0729DCO00/0, 0738RER00/0(*), 0749NMV00/0(*0710IOL00), 0750SMV00/0, 0803LSA00/0, 0809USG00/0(*0150SOP00), 0814CVD00/0, 0817PCI00/0(*), 0829JSP00/0, 0830SCY00/0, 0833KOR00/0, 0837CAE00/0, 0849SZE00/0, 0874PXS00/0, 0877OHD00/0, 0886ACV00/0, 0891FSL00/0, 0897OUR00/0, 0920XSC00/0(*), 1075AGP00/0(*0817PCI00), 1088SEE00/0, 1093NCB00/0, 1106GAD00/0, 1120DUM00/0, 1131OZP00/0, 1165BCS00/0(*), 1180DAN00/0(*0340TPY01), 1185ESV00/–2, 1189TZA00/0(*), M2023–D2/0(*1099JED00).

Grade 6

0009DRA06/1, **0027KSE00/1**, **0061TAH00/1**, **0061TAH02/1**, 0067NSA00/0, 0093VEL02/–6(*0093VEL00), 0103TCE01/–3, 0134NGV00/0, 0150SOP01/0(*0150SOP00), **0151EAU00/1**, **0152NOC04/1(*)**, **0165SZC01/1(*)**, **0170JBO00/1**, 0186EUM01/0, 0200ESE00/0, **0212KLE00/1**, 0220NDR00/2, 0225SOR01/0, 0241OUI00/0, 0245NHD00/–3(*0558TSM00), 0252ALY00/0(*), **0254PHO01/1(*)**, 0269OCS00/–3, 0275CLI00/–2, 0308PIP00/0, 0313ECR00/0(*), **0324EPR00/1**, 0349LLY00/0, 0365BCM00/0, 0395GCM00/0, 0398DCM01/0, 0400BMO00/0, 0414ATR00/0(*), **0446DPC00/1**, 0462JGP00/0, 0472ATA00/–6, 0482NGP00/–6, 0491DCC00/0, 0501FPL00/–6, 0535THC00/0, 0536FSO00/0, 0545XCA00/0, 0559MCB00/0, 0575SAU00/0(*), 0580CHA00/0, 0583TTA00/0(*), 0605FHR00/0, 0655APC00/0, 0657GSG00/0, 0658EDR00/0(*), 0661OTH00/0, 0668JMP00/0, 0681OAQ00/0, 0683JTS00/0, 0688BTR00/0, 0689TAC00/0, 0693ANP00/0, 0707BPX00/0, 0709LCM00/0(*0093VEL00), 0709LCM01/0(*0093VEL00), 0712FDC00/0, 0713CCR00/0, 0716OCH00/0, 0720NGB00/0, 0727ISR00/0, 0732FGV00/0, 0734MOC00/0, 0736XIP00/0, 0739LAR00/0, 0752AAC00/0, 0770LCA00/0(*), 0771SCO00/0, 0780NPU00/0(*0761PPC00), 0781NLV00/0(*0761PPC00), 0790PVL00/0, 0795SUR00/0, 0800JCT00/0, 0802ADS00/0, 0807FLO00/0, 0812NAA00/0, 0815UMS00/–7, 0816CVT00/0, 0818OAG00/0, 0822NUT00/0, 0823FCE00/0(*), 0824DEX00/0(*0542DES00), 0826ILI00/0, 0827NPE00/0, 0831GPG00/0, 0834ACU00/0, 0840TER00/0, 0843DMD00/0, 0847BEL00/0, 0848OPE00/0, 0850MBA00/0, 0856EMO00/0, 0859MTB00/0, 0862SSR00/0, 0865JES00/0, 0866ECB00/0, 0870JPG00/0, 0875TEI00/0, 0879ATI00/0, 0880YDR00/0, 0882PLE00/0, 0884NBP00/0, 0887DZB00/0, 0889YOP00/0, 0890ESU00/0, 0892MCN00/0, 0906ETD00/0, 0907MCE00/0, 0917OVI00/0, 0922PPE00/0(*), 0927AAQ00/0, 1033OCR00/0, 1037MED00/0, 1045SUT00/0, 1046PIS00/0, 1047GCR00/0, 1052CAQ00/0, 1053FDE00/0, 1054TDE00/0, 1055TVL00/0, 1056AZC00/0, 1057SPG00/0, 1058TPS00/0, 1059MKQ00/0, 1065NAT00/0, 1066FOR00/0, 1067ESC00/0, 1074JAC00/0, 1078SFO00/0, 1079ANT00/0, 1089CTS00/0(*), 1094EMA00/0, 1095EPX00/0, 1100XLU00/0, 1101FAC00/0, 1105UPV00/0, 1138COH00/0, 1155FBC00/0, 1158TSX00/0, 1162DPV00/0(*1119LAV00), 1163PYX00/0, 1164NOR00/0, 1168DCN00/0, 1171JGC00/0, 1172OEC00/0, 1173VAC00/0, 1174DDO00/0, 1175FHL00/0, 1179OGE00/0, 1181SOS00/0, 1187TFE00/0, 1188TOU00/–2, 1191EIV00/0, 1192ZEV00/0, M2023–D1/0.

Grade 5

0039NAL00/–7, 0045PDF00/0, 0088ODR01/0, **0096NCC01/1(*0096NCC00)**, **0096NCC04/1(*0096NCC00)**, **0097SCC00/1(*0096NCC00)**, 0102ACE00/–2(*1165BCS00), 0121NHY00/0, 0133PUM01/0, 0136SLE01/–2(*0136SLE00), 0232BCN00/0(*0558TSM00), 0270FAO00/0, 0273PBO00/–2, 0307TPU00/0, 0314ACR00/0, 0318MVE00/0, **0326EPG00/1**, 0345FHE00/2, 0347BPG00/0, 0359MZC00/0(*), 0398DCM00/0, 0413MUL01/2, 0433ETP00/0, 0451CAM00/0, 0469AUS00/–6,

0487NRC00/–6, 0509KVI00/0, 0514OMC00/0(*), 0539ACP00/0, 0558TSM00/0(*), 0597TTS00/0(*0514OMC00), 0670JEP00/0, 0672HNJ00/0, 0677FCL00/0, 0703IOD00/0, 0733LAL00/0, 0766BAD00/0, 0786SXP00/0, 0798ACD00/0, 0799NEC00/0, 0805GSC00/0, 0806SGI00/0, 0836ABH00/0, 0842CRN01/0, 0868PSQ00/0, 0881TLE00/0, 0894JMD00/0, 0895OAB00/–3, 0899EMC00/0, 0909SEC00/0, 1099JED00/0(*), 1127ESL00/0, 1167FOD00/0, 1169IFR00/0.

Grade 4

0003SIA02/0(*), 0033NIA01/–2(*), 0034DSE00/0, 0038CUR00/–2, 0043ZSE02/–3, 0055ASC00/–6, 0065GDE00/0, 0066NSC00/0, 0073ZDR00/0(*), 0076KAQ00/0, 0076KAQ01/0, 0083OCG00/0, 0086OGC00/–3(*), 0088ODR00/0, 0089PVI00/–2, 0091JZA00/–3, 0094RGE00/0, **0096NCC05/1(*0096NCC00)**, **0097SCC01/1(*0096NCC00)**, **0097SCC02/1(*0096NCC00)**, 0103TCE00/–2, 0103TCE02/–3, 0104GBO00/–3, 0112NDL01/0(*), 0113SDL00/0(*0112NDL01), 0113SDL01/0(*0112NDL01), 0113SDL02/–2(*0112NDL01), 0121NHY01/–3, 0121NHY02/0, 0121NHY03/0, 0124SVI00/0, 0131DAL00/–3, 0133PUM02/–3, 0135SGV00/0, 0138ABO00/0, 0140XLI00/0, 0142MDR00/0, 0148MLV00/0, 0159TAQ00/0, 0161SSC00/–2, 0166JLY00/–2, 0167NSS00/0, 0169SCU00/0, 0177BCA00/0(*), 0179SCA00/2, 0182OCY00/0, 0185DBA00/0, **0187PCA01/1(*)**, 0190BPE00/0, 0192TRI00/0, 0193ZAR00/–3, 0199ADC00/0(*), 0207SCS00/–6, 0209EER00/0, 0210BAU00/–6, 0211AOR00/0, 0214BCP00/–3(*), 0216SPI03/2, 0217OPC00/–7, 0219SAR00/0, 0219SAR02/0(*), 0219SAR03/0(*), 0220NDR01/2, 0224DAU00/0, 0226ZTA00/0, 0226ZTA02/0, 0227OMO00/–2, 0228OLY00/0, 0229NAU00/0, 0230ICS00/0, 0231ACM00/–6, 0232BCN01/–3, 0234EPC00/0, 0235LCY00/0, 0236GPS00/0, 0237SSA01/2(*), 0241OUI01/–6, **0242XDR00/1**, 0244PAR00/0, 0248IAR00/0, 0249NAR00/–2, 0253CMI00/0, 0253CMI01/–2, 0258DAR00/0, 0260GTI00/0, 0266ACC00/0(*), 0267JNO00/0, 0268BCD00/–3, 0271MLY00/0, 0272ACO00/0, 0276ADR00/–2, 0279ZED00/–2, 0282DCY00/–2, 0283OPL00/0, 0284OMA00/0, 0287NER00/0, 0288DSA00/0, 0289DNA00/0, 0317TCN00/0, **0321TCB00/1(*)**, **0322LBO00/1**, **0327BEQ00/1**, **0328ALA00/1**, **0343HVI01/1**, 0350MAL00/0, 0352ZOP00/0, 0356MVL00/0, 0361TSR00/0, 0366JBP00/0, 0368JAD00/0(*0373TPR00), 0373TPR00/0(*), 0380KDR00/0, 0382BUM00/0, 0384OLP00/0, 0385AUM00/0(*), 0386OBC00/2, 0387OKD00/0(*0385AUM00), **0388CTA00/1(*0237SSA01)**, 0389OME00/0, 0391NDD00/0, 0396DTA00/0, 0397NGM00/0, 0399DHY00/0, 0401BSX00/0, 0402JHY00/0, 0403CVN00/0, 0406FCB00/0, 0407OEE00/0(*0086OGC00), 0412FOP00/0, 0417ETT00/0(*0237SSA01), 0418BHE00/0, 0420CCA00/0, 0422NLL00/–3, 0423SLL00/0, 0424SOL01/–2(*), 0425PSA00/0, 0432NBO00/0, 0434BAR00/0, 0435MPR00/0, 0437NLY00/0, 0438MLE00/0, 0440NLM00/0, 0442RLE00/0, 0443DCL00/0, 0449ABS00/–6, 0452TVI00/–6(*), 0454MPV00/–6, 0455MAC00/–6, 0461JGS00/–6, 0463JRH00/–6, 0466AOC00/0, 0467ANA00/–6, 0470AMD00/2(*0470AMD02), 0471ABC00/–6(*0214BCP00), 0471ABC01/–6, 0473LAQ00/–6(*), 0474ABA00/–6, 0475SAQ00/–6, 0476ICE00/–6, 0477SRP00/–6, 0484IOA00/–6, 0485NZT00/–6, 0486NZP01/0, 0489ZLE00/–6, 0492DTH00/–6, 0494DEL00/0(*), 0495DMT00/–6, 0496DED00/–6, 0511FLY00/0, 0516FMV00/0, 0518AHE00/0, 0525ICY00/0, 0528JZD00/0, 0534FOA00/0, 0537KAU00/0, 0538FFA00/0, 0540TCR00/0, 0541SSD00/0, 0542DES00/0(*), 0543TTB00/0, 0544JNH00/0, 0546FTC00/0, 0547KAP00/0, 0551FSA00/0, 0553DPE00/0, 0554APE00/0, 0555OCP00/0, 0555OCP01/0, 0560SES00/0, 0561SSX00/0, 0562BCT00/0, 0564SUM00/0, 0565FUM00/0, 0566BCF00/0, 0572TOH00/0, 0573TLM00/0, 0574GMA00/0, 0574GMA01/0, 0576FOB00/0, 0577FPI00/0, 0578TUM00/0, 0579TCV00/0, 0584GCE00/0, 0585THY00/0, 0586TLA00/0, 0588TTL00/0, 0590VCT00/0, 0591ZBO00/0, 0592PON00/0, 0593TOL00/0, 0594RSE00/0, 0595TTT00/0, 0596MUS00/0, 0599POS00/0, 0600FAU00/0, 0602KCR00/0, 0603FCR00/0, 0604ACZ00/0, 0606JAU00/0, 0607TBO00/0, 0608FAR00/0, 0609BOT00/0, 0611VCF00/0, 0612NCA00/0, 0615TOR00/0, 0616TOB00/0, 0617IUM00/0, 0618THD00/0, 0619SLM00/0, 0620SBO00/0, 0621SUA00/0, 0622PUA00/0, 0648TAL00/0, 0652OSP00/0, 0660EPS00/0, 0669CHP00/0, 0671MCY00/0, 0684NUP00/0, 0685JPS00/0, 0687KDP00/0, 0691ZCE00/0, 0696OAU00/0, 0698AET00/0, 0701BCE00/0, 0702ASP00/0, 0704OAN00/0, 0706ZPI00/0(*0219SAR03), 0714RPI00/0(*0219SAR02), 0715ACL00/0, 0719LGM00/0, 0721DAS00/0, 0722FLE00/0(*), 0728PGE00/0, 0730ATV00/0(*0452TVI00), 0731JZB00/0, 0737FNP00/0, 0745OSD00/0, 0751KCE00/0, 0754POD00/0, 0755MID00/0, 0759THO00/0, 0791IAN00/0, 0796SED00/0, 0810XCD00/0, 0813OAC00/0, 0819SPS00/0, 0820TRD00/0, 0821DRP00/0, 0855ATD00/0, 0858FPB00/0, 0863TLR00/0, 0864JSG00/0, 0869UCA00/0, 0872ETR00/0, 0873OMI00/0, 0876ROR00/0, 0878OEA00/0, 0883NMD00/0, 0885DEV00/0, 0888SCV00/0(*), 0896OTA00/0, 0898SGP00/0, 0902DCT00/0, 0903OAT00/0, 0905MXD00/0, 0910BTC00/0, 0911TVU00/0, 0912BCY00/0, 0913FVI00/–3,

 © eMeteorNews

0916ATH00/0, 0918TAG00/0, 0919ICN00/0, 0921JLC00/0(*), 0923FBO00/0, 0925EAN00/0, 1038SND00/0, 1039FFD00/0, 1040SPD00/0, 1041FTD00/0, 1042SCP00/0, 1043OSG00/0, 1044EPU00/0, 1051AKC00/0, 1061EPO00/0, 1068TPE00/0(*0373TPR00), 1072AUA00/0, 1080ANE00/0, 1082DSG00/0, 1087OOE00/0, 1090EOR00/0, 1092FLM00/0, 1097DOH00/0(*), 1102GLU00/0, 1103FBI00/0, 1119LAV00/0(*), 1121LAD00/0, 1125FFL00/0, 1132TSA00/0, 1134PIE00/0, 1135JOM00/0, 1136AGA00/0, 1137AMP00/0, 1143SNS00/0(*0150SOP00), 1145DMI00/0, 1149OXP00/0, 1150GAC00/0, 1154DPU00/0, 1156GAE00/0, 1159CVI00/0, 1183JMH00/0, 1184RHC00/0, 1190JZL00/0, 1193JLG00/0, 1195SCD00/0, 1200ULI00/0, 1202MCD00/0, 1203LDM00/0, 1204CUA00/0, M2022–Q2/0.

Grade 3

0024PEG00/–6, 0046BCR01/–3, 0052OUM00/–2, **0063COR00/1**, **0063COR01/1**, 0092UER00/–6, 0093VEL00/0(*), 0093VEL01/0(*0093VEL00), 0098ECO00/–2, 0099JSC00/0, **0100XSA00/1**, **0100XSA01/1**, 0105OCN00/0, 0105OCN01/0(*0093VEL00), 0105OCN02/–2(*), 0106API00/0, 0107DCH00/2, 0107DCH01/2, 0107DCH02/2, 0108BTU00/0(*), 0109ACN00/–2, 0111FCM00/–2, 0114DXC00/0, 0115DCS00/2(*0115DCS05), 0115DCS03/2(*0115DCS05), 0115DCS05/2(*), 0116DEQ00/0, 0117DCQ00/0, 0118GNO01/0, 0118GNO03/0, 0118GNO04/–2, 0119LCE00/0, 0120DPA00/0, 0122APX00/–2, 0125SAL00/–6, 0126SGE00/–3, 0127MCA00/0, **0128MKA00/1**, 0129QPE00/0, 0133PUM00/0, **0137PPU00/1**, 0141DCP00/0, 0143LPE00/0, **0144APS01/1**, 0146CAU00/0, 0147PAQ00/0, **0153OCE00/1**, 0154DEA01/0, 0155NMA01/0, **0156SMA00/1(*)**, 0157ICA00/0, 0158CET00/0, 0162ACI00/–2, **0172ZPE04/1, 0173BTA03/1**, 0174TAS00/0, 0176PHE00/0(*), 0178JCE00/–2, 0180MSE00/0, 0181KPA00/0, 0186EUM00/0, **0188XRI00/1(*)**, 0189DMC00/0, 0195BIN00/0, 0196NPH00/–2, **0198BHY00/1**, 0201GDO00/0, **0202ZCA00/1**, **0202ZCA01/1**, 0203GLE00/0, 0204DXL00/0, 0213BRC00/–2, 0218GSA00/0, 0222DDl00/0, 0223GVI00/0, **0233OCC00/1**, **0233OCC01/1**, 0238DOR00/–2, 0239GPU00/0, 0240DFV00/0, 0251IVI00/0, **0254PHO00/1(*0254PHO01),** 0261DDC00/0, 0262KLI00/0, 0263NAN00/0, 0264XCE00/0, 0265JGD00/0, 0274NUM00/–3, 0277GCA00/–3, 0278MSR00/–2, 0280ADL00/–2, 0305SPU00/0, 0306COL00/0, 0309GVE00/0, 0310APY00/0, 0311DVE00/0, 0312ECA00/0(*0259CAR00), 0320OSE01/–3(*), **0325DLT00/1**, **0330SSE00/1(*0320OSE01)**, 0351DTR00/0, 0353SCT00/0, 0354DDT00/0, 0357PHP00/0, 0358TOP00/0, 0360PSP00/0, 0363ZER00/0, 0364KCT00/0, 0369JTR00/0, 0374ISC00/0, 0375AOE00/0, 0376ALN00/0, 0377DMO00/0, 0378GER00/0, 0381DPL00/0, 0393RBO00/0, 0405MHY00/0, 0408KHY00/0, 0419DAC00/0, 0421MMI00/0, 0426DCR00/0, 0453MML00/–6, 0457MDL00/–6, 0468AAH00/–6, 0478STC00/–6, 0503NNA00/0, 0532MLD00/0, 0656AAA00/0, 0664MXA00/0, 0679MUA00/0, 0724LAP00/0, 0725DZC00/–2, 0756RPH00/0, 0758VOL00/0(*), 0760OCD00/0, 0762OPA00/0, 0763UPA00/0, 0764TEL00/0, 0765ASG00/0, 0767APH00/0, 0768ZPH00/0, 0772GSE00/0, 0773THP00/0(*0761PPC00), 0774ECM00/0(*0761PPC00), 0775OBP00/0(*0761PPC00), 0776OAP00/0(*0761PPC00), 0777OPU00/0(*0761PPC00), 0778ZAN00/0, 0779OLV00/0(*0761PPC00), 0782IAD00/0, 0783ILU00/0, 0788NHR00/0, 0789JMV00/0, 0792MBE00/0, 0794GLY00/0, 0797EGR00/0, 0801JCD00/0, 0804DGR00/0, 0808PCS00/0, 0811LCP00/0, 0828TPG00/0, 0832LEP00/0, 0835JDP00/0, 0838ODS00/0, 0845OEV00/0, 0846TSC00/0, 0851BEC00/0, 0852AST00/0, 0853ZPA00/0, 0857EVO00/0, 0908XXL00/–3, 0926OMH00/–3, 1034GPA00/0, 1035SPH00/0, 1036CPH00/0, 1048JAS00/0, 1050MZE00/0, 1063EOC00/0(*), 1064JER00/0, 1069JOP00/0, 1071IHD00/0(*), 1073GGR00/0, 1091OEH00/0, 1104APO00/0, 1130ARD00/0, 1139JEG00/0, 1140ETM00/0, 1141IFO00/0, 1144JKV00/0, 1146DHO00/0, 1147NLI00/0, 1148SLI00/0, 1152NSB00/0, 1170LTM00/0(*0252ALY00), 1177IVO00/0, 1182XIN00/–2, 1199AFO00/0, 1207OMP00/0, 1209FOS00/0, 1210GAG00/0(*0188XRI00), 1211SFG00/0.

Grade 2

0025NOA00/2(NTA), 0025NOA01/2(NTA), 0028SOA00/2(STA), 0032DLM00/0(COM), 0090JCO00/0(COM), 0194UCE00/–3(*0583TTA00), 0216SPI00/2(STA), 0216SPI02/2(STA), 0226ZTA01/–7(ORI), 0237SSA00/2(STA), 0243ZCN00/–2(ORI), 0256ORN00/0(NTA), 0256ORN01/0(*), **0257ORS00/1(STA)**, 0285GTA00/–3(STA), 0286FTA00/0(STA), 0300ZPU00/0(*0255PUV00), 0301PUP00/0(*0255PUV00), 0302PVE00/0(*0255PUV00), 0303LVL00/0(*), 0304CVE00/0(*0303LVL00), 0316BHD00/0(*), **0327BEQ01/1(*)**, 0367OPG00/0(*), 0379ACT00/0(*), **0390THA00/1(*GEM)**, 0415AUP00/0(*), 0430POR00/–6(TORI), 0441NLD00/0(*), 0479SOO00/2(TORI), 0499DDL00/–4(COM), 0505AIC01/2(SDA), **0506FEV00/1(COM)**, 0548FAQ00/0(*0164NZC00), 0589FCA00/0(TORI*), 0598TCT00/0(*), 0614JOS00/0(*), 0624XAR00/0(STA), 0625LTA00/0(STA),

0626LCT00/0(STA), 0627NPS00/0(STA), 0628STS00/0(STA), 0629ATS00/0(NTA), 0630TAR00/0(NTA), 0631DAT00/0(NTA), 0632NET00/0(NTA), 0633PTS00/0(NTA), 0634TAT00/0(NTA), 0635ATU00/0(NTA), 0636MTA00/0(*0257ORS03), 0637FTR00/0(STA), 0638DZT00/0(*0257ORS03), 0640AOA00/0(SDA), 0641DRG00/0(GEM), 0642PCE00/0(SDA), 0667JTP00/0(*), 0680JEA00/0(*), 0692EQA00/0(*0001CAP06), 0695APA00/0(*0694OMG00), 0717LAU00/0(*0208SPE02), 0718XGM00/0(TORI), 0748JTL00/0(*0710IOL00), 0861JXS00/0(*0167NSS01), 0900BBO00/0(*), 0901TLC00/–3(*0424SOL01), 0914AGE00/0(GEM), 1060NSE00/0(*), 1085NCQ00/0(*), 1086SCQ00/0(*), 1098EMI00/0(*), 1142SNT00/0(*0583TTA00), 1176SSH00/0(*), 1194MAR00/0(NTA), 1197RTU00/0(*), 1198XRO00/0(ORI), 1201MSA00/0(*0167NSS01), 1205FLN00/0(*), 1206FDR00/0(*).

Grade 1

0033NIA07/1(*), 0123NVI00/0(*), 0130DME00/–2(*0108BTU00), 0136SLE02/0(*0021AVB06), 0259CAR00/–2(*), 0315OCA00/0(*0105OCN02), 0332BCB00/–2(*0321TCB00), 0342BPI00/–4(*), 0355XIC00/0(*0156SMA00), 0383LDR00/0(*), 0392NID01/2(*0334DAD00), 0409NCY00/0(*0040ZCY02), 0424SOL00/0(*), 0425PSA01/–2(*0081SLY01), 0462JGP01/–4(*), 0483NAS00/–4(*0439ASX02), 0498DMH00/0(*0340TPY01), 0500JPV02/0(*0428DSV00), 0507UAN00/0(*), 0508TPI00/–4(*), 0513EPV00/0(*0428DSV00), 0522SAP00/0(*0175JPE), 0527UUM00/0(*), 0550KPC00/0(*0187PCA01), 0613TLY00/0(*0081SLY01), 0643OLS00/0(*0515OLE00), 0705UYL00/0(*0081SLY00), 0726DEG00/0(*), 0746EVE00/0(*0255PUV00), 0747JKL00/0(*0644JLL00), 0753NED00/0(*0334DAD00), 0761PPC00/–2(*), 0769PPH00/0(*0176PHE00), 0785TCD00/0(*0313ECR00), 0787KVO00/0(*0758VOL00), 0793KCA00/0(*0515OLE00), 0844DTP00/0(*0340TPY00), 0871DCD00/0(*0177BCA00), 0904OCO00/0(*0770LCA00), 1046PIS01/0(*0254PHO01), 1049DIU00/0(*0494DEL00), 1070SCE00/0(*0738RER00), 1076APP00/0(*0922PPE00), 1077PIC00/0(*0545XCA00), 1081SUC00/0(*0823FCE00), 1083ETC00/0(*1063EOC00), 1084EPP00/0(*1069JOP00), 1107JID00/0(*1099JED00), 1108IHR00/0(*1071IHD00), 1110CEP00/0(*0658EDR00), 1111AQI00/0(*0164NZC00), 1112UPI00/0(*0372PPS00), 1113SJA00/0(*0533JXA00), 1114SGC00/0(*0480TCA00), 1115NXE00/0(*0338OER00), 1116NFL00/0(*0502DRV00), 1117NEV00/0(*0335XVI00), 1118MLT00/0(*0722FLE00), 1122UMN00/0(*0563DOU00), 1123FFH00/0(*0340TPY01), 1124HTV00/0(*0428DSV00), 1126SOV00/0(*0530ECV00), 1129JTT00/0(*0165SZC01), 1151NPA00/0(*0575SAU00), 1153TOD00/0(*0320OSE01), 1157FCD00/0(*1089CTS00), 1160JBH00/0(*0888SCV00), 1161THT00/0(*1097DOH00), 1178RDR00/0(*0686JRD00), 1186PSI00/0(*0152NOC04), 1196ZCM00/0(*0246AMO00), 1208OES00/0(*0115DCS05).

Additional notes

Notes for the meteor shower entries marked with (*) above:

- 0001CAP06: 0692EQA00 activity is difficult to distinguish from 0001CAP late-stage activities. CAP01 and 10 match XCS; see 0623XCS00.
- 0003SIA01: 0003SIA01 is too close to 0005SDA.
- 0011EVI06: 0011EVI00 is completely inconsistent with modern observations. 0011EVI01 is in error; Jenniskens (2006) listed an erroneous orbit (ω and Ω) and, therefore, *Los*, *S_LoR*, and *LaR* in the SD are errors. The SD considers 0011EVI02 to be "–7 various faults: typo ... suspicious", but this one shows the correct value.
- 0012KCG07: This represents the KCG activity in normal years and should be distinguished from the activity in active years for example 0012KCG11 (Koseki, 2014b and 2020b).
- 0021AVB06: This activity consists of 0021AVB04, 0021AVB06, and 0136SLE02. The first detection of this activity is 0136SLE02 (Koseki, 2020c).
- 0027KSE02: Although the activities surrounding KSE are complex (Koseki, 2019b), two activities are relatively clear; 0839PSR00 and KSE03: ($\lambda_\odot$, $\lambda - \lambda_\odot$, β) = (25.9, 216.7, 38.3), which has now been removed from the SD. The evaluation values of KSE01 and 02 are due to the influence of PSR.
- 0033NIA01: Classically, Northern ι-Aquariids are considered active from late July to mid-August, and NIA00, 01, and 04 are the final stages of this activity.
- 0033NIA07: NIA02, 03, 05, and 07 coincide with the activity of 0215NPI, which is completely different from the classical one. NPI was known before these NIA observations and should be integrated into 0215NPI.
- 0040ZCY02: 0409NCY00 matches 0040ZCY02.
- 0047DLI02: 0047DLI02 is near 0150SOP02, see 0150SOP00.
- 0073ZDR00: Jenniskens' meteor shower table (Jenniskens, 2006), which is the prototype of SD, had ZDR = θ-Herculids, which was later replaced by the

 © eMeteorNews

current observation report. In fact, the existence of ζ-Draconids has already been pointed out through photographic observations, and corresponding ones had been seen in Denning's visual observations (Denning, 1899), but this activity is incorrectly named AUD in the current SD. The author described this problem in detail (Koseki, 2014).

- 0081SLY00: 0081SLY00 is a different activity than 0081SLY01 (Koseki, 2023) and is an independent meteor shower along with 0705UYL00.
- 0081SLY01: 0081SLY01 is a diffuse activity that matches 0424SOL00, and 0425PSA01 and 0613TLY00 are also thought to be related.
- 0086OGC00: Although it is based on the observation of a sudden appearance through visual observations, there are no other sufficiently relevant observations to support it. It seems that the observation of 0407OEE00 by CMOR is consistent, but only extremely unclear activity has been observed.
- 0093VEL00: 0105OCN01 is near 0093 VEL00. The reports included in 0093VEL were compiled by Jenniskens on a meteor shower active from November 8th to February 24th (Jenniskens, 2006). 0093VEL02 was calculated by himself as an average value including visual observations. According to the figure in the appendix, there is a group of observations where the radiant appears to move southward from November to January, and VEL02 is close to the southern end of this radiant drift. Although not reported in the SD, meteor activity is clearly recognized in the appendix's figure even at the solar longitude of 260 degrees, which is blank in the table below; see also 0490DGE01.

Code	$\lambda_\odot$	$\lambda - \lambda_\odot$	β	v_g
0490DGE01	254	176.8	–29.9	24.7
0709LCM01	273.3	175.1	–45.9	25.1
0709LCM00	286	176.4	–54.6	25.4
0093VEL02	296	213.3	–65.1	33.1

- 0096NCC00: 0096NCC and 0097SCC are the typical ANT meteor activities and, therefore, all their entries are given here to show the problems about the evolution of meteor showers. See '*Discussions*'.
- 0105OCN02: 0105OCN02, 03, and 0315OCA00 are the same activity possibly based on the same source.
- 0108BTU00: 0130DME00 matches 0108BTU00.
- 0112NDL01: Both 0112NDL01 and 0113SDL01 are named simply δ-Leonids in the original papers (Sekanina, 1973; 1976). This is what was originally called 0029DLE but was split into two parts. 0112NDL02 is the first report of δ-Leonids. Lindblad searched meteor showers by using the D-criterion and he classified 24 photographic meteors in this shower including 3 meteors from the southern ecliptic hemisphere (Lindblad, 1971).
- 0115DCS05: 1208OES00 matches 0115DCS05. 0115DCS is classified as 'to be established shower', but it is further in addition to 0115DCS05's set divided into two groups; one is 0115DCS00, 0115DCS01, and 0115DCS02, and the other is 0115DCS03 and 0115DCS04. These later two groups are based on old observations and cannot be confirmed by modern CMOR observations, so it is inappropriate to refer to them as 'to be established' either.
- 0123NVI00: 0123NVI00 matches 0011EVI.
- 0136SLE00: Classically, σ-Leonids refers to the activity detected by Southworth and Hawkins using the D-criterion (Southworth and Hawkins, 1963). They got 27 σ -Leonid meteors from 360 meteor samples and they were very dispersed from February 5 to May 22; the maximum D(M, N) reaches 0.56. Their original σ-Leonids are located on the western side: $(\lambda - \lambda_\odot, \beta) = (171, 2)$ to the SLEs in the current SD. It seems to be better to list SLEs in the with another name.
- 0139GLI00: 0139GLI00 is near 0448AAL00 and 01 but the geocentric velocity is over 10km/s slower than the latter.
- 0150SOP00: The SOP reporting is mixed, with activity spreading from $\lambda_\odot = 47°$ in SOP02 to $\lambda_\odot = 70°$ in SOP05. There are reports of 0055ASC, 0149NOP, 0456MPS, and so on in the vicinity, which is an ambiguous area between meteor showers and sporadic meteor activity like 0096NCC and 0097SCC.
- 0152NOC04: 1186PSI00 matches 0152NOC04.
- 0156SMA00: 0355XIC00 matches 0156SMA00.
- 0164NZC00: NZC activity continues from solar longitude 85 degrees to 120 degrees, and NZC00 covers its early stage; 548FAQ00 covers the second half of 0164NZC activity. 1111AQI00 matches NZC.
- 0165SZC01: SZC00 and 01 are quite different activities from 0165SZC02 and 04 (Koseki, 2023). 1129JTT00 matches the former activity.
- 0165SZC02: 0370MIC00 matches this activity, but MIC observation reports are faster than SZC02 and 04, and this activity should be called MIC.
- 0167NSS01: Unlike 0167NSS00, 0167NSS01 can be considered as one activity along with 0861JXS00 and 01 and 1201MSA00, but it is unclear because it is within the domain of ANT.
- 0175JPE02: 0462JGP00 and 0522SAP00 match 0175JPE. 0462JGP01 was renamed 0175JPE04.
- 0176PHE00: 0769PPH00 coincides with 0176PHE.
- 0177BCA00: 0871DCD00 matches 0177BCA00.
- 0187PCA00: PCA00 and 02 are different activities from 01 but are rather close to 1133TCS00. The evaluation value shown here is based on the activity of 1133TCS00, and since PCA00&02 and TCS are seen as different activities from the activity profile, if we calculate the evaluation value of PCA00&02 again, it will be 7.
- 0187PCA01: 0550KPC00 matches 0187PCA01.
- 0188XRI00: 1210GAG00 matches 0188XRI01, but XRI is classified as established though both are highly inconsistent even within the SD.
- 0197AUD01: This should originally be called ZDR (Koseki, 2014b). See 0073ZDR00.

- 0199ADC00: This entry does not represent ADC activities and ADC01 and 02 show it best.
- 0208SPE02: 0717LAU00 covers 0208SPE final activities.
- 0214BCP00: 0471ABC00 matches 0214BCP00.
- 0215NPI04: 0033NIA02, 03, 05, and 07 should be included in 0215NPI.
- 0219SAR02: 0714RPI00 locates between 0219SAR01 and 02.
- 0219SAR03: 0706ZPI00 is near 0219SAR03.
- 0237SSA01: This activity, followed by 0417ETT00, probably exhibits the early stage of 0388CTA activities. Both SSA01 and ETT00 were published earlier than the first report of CTA.
- 0246AMO00: 1196ZCM00 matches 0246AMO.
- 0252ALY00: 1170LTM00 is near 0252ALY00.
- 0254PHO01: PHO is associated with comet 289P/Blanpain and was observed in 1956 and 2014. PHO00 corresponds to the former, and PHO01 corresponds to the latter, but due to changes in the comet's orbit, the radiant point has also changed significantly. In such cases, it is considered more appropriate to use the name of the comet rather than the name of the constellation as the name of the meteor shower. 1046PIS01 matches 0254PHO01.
- 0255PUV00: This is in an area of high meteor activity, and there are several other similar reports (0300ZPU, 0301PUP, 0302PVE, 0746EVE). There is still no analyzing report that integrates these (see Appendix).
- 0256ORN01: 0256ORN cannot be distinguished from 0017NTA as clearly as 0257ORS can from 0002STA. It is possible that ORN00 and 02 are terminal activities of NTA, and ORN01 and 04 are different shower activities that can be distinguished from them.
- 0257ORS03: 0257ORS listed in the SD are divided into two groups; ORS0~2 are all part of 0002STA though different in position, and ORS3 and 5 are considered as one shower activity. The latter is thought to include 0636MTA00 and 0638DZT00, but there is room for consideration as to whether to call this ORS or give it a new name.
- 0259CAR00: 0312ECA00 matches 0259CAR00. CAR is a duplicate registration with ECA.
- 0266ACC00: 0266ACC00 is near both 0096NCC and 0097SCC.
- 0303LVL00: 0303LVL00 is near 0304CVE00 but their activities are represented better by 0784KVE00.
- 0313ECR00: 0785TCD00 matches. 0313ECR00.
- 0316BHD00: 0316BHD is located on the outer edge of 0569OHY, and 0569OHY data provides a better picture of its activity.
- 0320OSE01: 1153TOD00 matches 0320OSE01. However, the number of meteors in OSE01 and OSE03 is 2 and 8, respectively, which is small, and the TOD is 21, which is not at all large. According to GMN observations, there are only 5 meteors within 3 degrees of the radiant point of OSE01 and within 10 degrees before and after the solar ecliptic longitude. In addition, the number of meteors in the original OSE00 was 60 (Brown et al., 2008), which is extremely low for CMOR observations, and moreover, OSE has not appeared in subsequent CMOR observations. OSE00 is about 9 degrees away from 01,03 and close to 0330SSE00; annually recorded by CMOR. There are many problems in treating OSE as an established shower.
- 0321TCB00: 0332BCB00 matches 0321TCB00.
- 0327BEQ01: The radiant point of 0327BEQ01 is an extension of the NZC's area of activity and is heavily influenced by NZC.
- 0334DAD00: 0753NED00 appears to capture activity in the very early stages of 0334DAD, and 0392NID appears to capture the activities of the first half of 0334DAD.
- 0335XVI00: 1117NEV00 captures the initial activity of 0335XVI, and the radiant point is an inverse extension of the movement of the XVI radiant drift.
- 0337NUE00: One of the strongest activities of the tale of the Orionids, though NUE01 and 03 are more than 4 degrees apart from the center; see 0552PSO01 also.
- 0338OER00: 1115NXE00 captures 338OER activities; NXE is on the path of the OER radiant drift. 0490DGE00 is also an extension of that pathway and may be related; see 0490DGE01.

Code	$\lambda_\odot$	$\lambda - \lambda_\odot$	β	v_g
0338OER03	230.5	184.6	–20.8	28
1115NXE00	241.88	180.7	–24.5	26.06
0490DGE01	254	176.8	–29.9	25

- 0340TPY00: 0340TPY00 is quite different activity from TPY01 and 02. 0844DTP00 matches TPY00.
- 0340TPY01: 0498DMH00, 01, and 1123FFH00 match the activity of 0340TPY01 and 02.; see 0567XHY00. 1180DAN00 may have been affected by the later stages of this activity.
- 0342BPI00: 0342BPI00 was renamed 0026NDA04, though August Beta-Piscids (BPI) seems to be the more appropriate name for this activity. The maximum seems to be too far apart for the shower activities currently considered to be NDA to be associated with SDA activities.
- 0359MZC00: The activity periods and radiant positions of 0359MZC00 and 0665MUC00 are almost the same, but their geocentric velocities are significantly different; $v_g = 29.2$ and $v_g = 57.1$ respectively for MZC and MUC. Although it is treated as ECY rather than MZC in CMOR, ECY showed only extremely weak activity in 2019 between 2018 and 2023.
- 0367OPG00: Although the radiant position of OPG matches that of 0431JIP, the peak of JIP activity is sharp, and the maximum of OPG is more than 5 degrees later than that of JIP. JIP data appears to better represent this activity.
- 0371APG00: The radiant position of OPG is near 0867FPE00. Although the peak of APG activity is not clear, FPE shows a clear maximum of about 10 degrees

 © eMeteorNews

earlier than the value indicated by APG. Careful observations are required for future surveys to check whether the two activities are the same.

- 0372PPS00: The radiant distribution of PPS is wide, the period of activity is long, and the two activities seem to overlap. 1112UPI00 corresponds to the latter half of PPS activities.
- 0373TPR00: Both 0368JAD00 and 1068TPE00 are near 0373TPR00, though they might be under the influence of 0411CAN.
- 0379ACT00: 0379ACT00 is adjacent to 0505AIC, which appears to be the final stage of 0005SDA.
- 0383LDR00: LDR00 is located only 4 degrees south of the 0281OCT, and the timing of its activity is also consistent, so the LDR is thought to be an observation of the OCT.
- 0385AUM00: 0387OKD00 is near 0385AUM00.
- 0390THA00: The radiant point of THA is an extension of the drift of the radiant point of 0004GEM, and at least the meteors determined to be THA by CAMS are considered to be the early activity of GEM (Koseki, 2018).
- 0414ATR00: ATR can also be seen as capturing the terminal activities of 0372PPS00.
- 0415AUP00: AUP probably covers 0175JPE final activities.
- 0424SOL00: 0424SOL00 matches 0081SLY01.
- 0424SOL01: 0424SOL01 seems to match 0901TLC00, but as the SD points out, the source of SOL01 cannot be found.
- 0428DSV00: 0428DSV, 0500JPV, 0513EPV, and 1124HTV00 constitute the DSV complex as one meteor activity.
- 0439ASX02: 0483NAS matches 0439ASX;0483NAS00 and 01 were renamed as 0439ASX01 and 02 respectively.
- 0441NLD00: The NLD radiant point is located at the edge of the 0392NID active area.
- 0452TVI00: 0730ATV00 is near 0452TVI00.
- 0462JGP01: This was renamed 0175JPE04.
- 0464KLY00: KLY is the earliest and southernmost part of 0012KCG activity, and it is necessary to consider whether it is an independent meteor shower activity.
- 0470AMD02: AMD is at the end of KCG's activity area, and it is necessary to consider whether it is an independent meteor shower activity. AMD00 and 01 are apart from 02 by about 4 degrees.
- 0473LAQ00: 0473LAQ01 is near both 0026NDA02 and 0033NIA05. See 0033NIA07.
- 0480TCA00: 1114SGC00 matches 0480TCA.
- 0490DGE01: DGE 00 and 01 may cover different activities, the former may be related to 0338OER and the latter to 0093VEL; see also 0093VEL00 and 0338OER00.
- 0494DEL00: 1049DIU00 matches 0494DEL.
- 0502DRV00: 1116NFL00 covers the initial activity of 0502DRV, and the radiant point is an inverse extension of the movement of the DRV radiant drift.
- 0507UAN00: 0507UAN00 probably matches 0411CAN.
- 0508TPI00: 0508TPI00 and 01 were renamed 0026NDA06 and 07 respectively.
- 0514OMC00: OMC corresponds to the late activity of 0597TTS.
- 0515OLE00: 0643OLS00 and 0793KCA00 also belong to OLE activities though OLS and KCA represent this activity better.
- 0527UUM00: 0527UUM00 matches 0488NSU, though the report of 0527UUM00 was published earlier than 0488NSU00.
- 0530ECV00: 1126SOV00 represents the late activity of 0530ECV.
- 0533JXA00: 1113SJA00 matches 0533JXA.
- 0542DES00: 0824DEX00 seems to represent this activity better.
- 0545XCA00: 1077PIC00 matches 0545XCA.
- 0552PSO01: PSO01 is about 10 degrees west of the tail of Orionids and can be distinguished as a separate meteor activity. 0337NUE01 belongs to this activity; see 0337NUE.
- 0558TSM00: It is thought that 0232BCN00 captures the earliest period of TSM's activities, and 0245NHD00 captures the latter half. 0245NHD00 is the first report.
- 0563DOU00: 1122UMN00 matches 0563DOU.
- 0567XHY00: This observation captures the later activities of 0498DMH00, 01, and 1123FFH00; see 0340TPY01. The activity profiles of DMH and FFH suggest the activity peaks twice around $\lambda_\odot = 265°$ and $\lambda_\odot = 273°$; future careful observations would reveal whether the activity is one or should be divided into two.
- 0575SAU00: 1151NPA00 matches 0575SAU00.
- 0583TTA00: 0194UCE00, 0583TTA00, and 1142SNT00 appear to be meteor shower activity moving northward parallel to the Orionids tail. Although not reported in the SD, meteor activity is clearly recognized in the appendix's figure even at the solar longitude of 150 degrees, which is blank in the table below.

Code	$\lambda_\odot$	$\lambda - \lambda_\odot$	β	v_g
0194UCE00	145.7	249.6	-17.1	61
0583TTA00	164	249.6	-17.4	65
1142SNT00	171.2	249.4	-15.5	65.5

- 0589FCA00: FCA is the final stage of the Orionids tail activity.
- 0598TCT00: TCT represents the earliest activity of 0191ERI.
- 614JOS00: 0614JOS00 is probably a member of the DSV complex (see also 0428DSV00).
- 0623XCS00: 0623XCS is located eastward about 5 degrees from 0001CAP and CAP01 and 10 match XCS. The maximum of XCS is about 5 degrees earlier in solar longitude than CAP, and it seems to be a

distinct activity from CAP. The score for XCS00 might be overestimated by the influence of CAP and its own score is estimated at about 8.

- 0644JLL00: 0747JKL00 matches 0644JLL.
- 0658EDR00: 1110CEP00 matches 0658EDR00.
- 0667JTP00: 0667JTP00 covers the 0031ETA final activities.
- 0680JEA00: 0680JEA00 activities fall within the scope of 0171ARI and are difficult to distinguish.
- 0686JRD00: 1178RDR00 is almost the same as 0686JRD00: the SD notes for JRD "Updated 2020.06.10 by email from PJ; data in MDC differ from those given in publication".
- 0694OMG00: 0695APA00 probably covers the 0694OMG early activities.
- 0710IOL00: 0748JTL00 and 0710IOL00 are probably the same shower activity. Moreover, this activity may continue weakly until 0749NMV00.
- 0722FLE00: 1118MLT00 probably matches 0722FLE00. The difference in location and timing is thought to be due to the radiant drift.
- 0726DEG00: 0726DEG00 matches 0256ORN01&04. See 0256ORN01.
- 0738RER00: 0738RER00 seems the 1070SCE00 early activity.
- 0758VOL00: 0787KVO00 coincides with 0758VOL00.
- 0761PPC00: The SD states for this entry "Group members:773/THP, 774/ECM, 775/OBP, 776/OAP, 777/OPU, 779/OLV, 780/NPU, 781/NLV. Removed, only mean values of parameters" but lists the same parameter of 0773THP in this line. The SD adds the comment in line 0773THP00 "Member of the Puppids-Pyxidids Complex 761/PPC".
- 0770LCA00: 0904OCO00 matches 0770LCA00.
- 0817PCI00: 1075AGP00 is near 0817PCI00 and seems to represent this activity better.
- 0823FCE00: 1081SUC00 matches 0823FCE00.
- 0888SCV00: 1160JBH00 matches 0888SCV00.
- 0900BBO00: 0900BBO00 is close to 0010QUA, and future detailed investigation is required on whether it can be considered as an independent shower activity.
- 0920XSC00: 0920XSC00 is in the area where 0149NOP and 0150SOP activities are claimed, and one should be cautious about recognizing it as an independent activity.
- 0921JLC00: 0921JLC00 is located between 0005SDA and 0026NDA, in an unclear location where 0003SIA activities are sometimes claimed.
- 0922PPE00: 1076APP00 matches 0922PPE00.
- 1060NSE00: 1060NSE00 locates on the outer edge where 0149NOP and 0150SOP activities are claimed. See 0150SOP00.
- 1063EOC00: 1083ETC00 matches 1063EOC00.
- 1069JOP00: 1069JOP00 matches 1084EPP00.
- 1071IHD00: 1108IHR00 matches 1071IHD00.
- 1085NCQ00: 1085NCQ is within 3 degrees of 0026NDA and is difficult to distinguish.
- 1086SCQ00: 1086SCQ00 is close to the terminal activity of 0005SDA and is difficult to distinguish.
- 1089CTS00: 1157FCD00 matches 1089CTS00.
- 1097DOH00: 1161THT00 matches 1097DOH00.
- 1098EMI00: 1098EMI00 is within 3 degrees of 0019MON and is difficult to distinguish.
- 1099JED00: 1107JID00 matches 1099JED00 and they are followed by M2023-D2 with a 10-day delay. Future research is required regarding the relationship between 1099JED00 and M2023-D2.
- 1119LAV00: 1162DPV00 seems to be the same one.
- 1165BCS00: 1165BCS00 can explain the activities of 0102ACE, which have not been well understood.
- 1176SSH00: 1176SSH00 is difficult to distinguish from 0346XHE.
- 1178RDR00: 1178RDR00 is almost the same as 0686JRD0: the SD notes for JRD "Updated 2020.06.10 by email from PJ; data in MDC differ from those given in publication".
- 1189TZA00: 1189TZA00 is near 0164NZC.
- 1197RTU00: 1197RTU00 is difficult to distinguish from the terminal activity of 0002STA.
- 1205FLN00: 1205FLN00 is located within the activity area of 0112NDL and 0113SDL.
- 1206FDR00: 1206FDR00 matches 0012KCG in its active years.

3 Discussions

Meteor showers gradually spread out in the process of evolution, eventually becoming sporadic meteor activity, this change is continuous and there are no milestones. In the ANT region, we often encounter meteor activity that is part of this continuous process. Koseki discussed NCC and SCC, which are representative examples of this, in detail (Koseki, 2023). In this paper, evaluation values are obtained for all NCC and SCC entries, and they are distributed between GRADE 4 and 7. Meteor activity that is in the process of continuous extinction has an evaluation value of this level. For other meteor showers in the ANT region for which there are multiple reports, only the characteristic ones were given evaluation values. It is up to each individual to decide where to set a break in the continuous process, and caution should be taken when meteor activity is given an evaluation value of this level, especially those in the ANT region.

On the other hand, it should be noted that the TCB and LBO evaluation values are 4 even though clear activities are recognized by CMOR[2] and they are considered established showers. This is because this study is based on video observations. It is natural that there are differences in the way meteor showers are perceived by radio observations and video observations (Koseki, 2014a). This evaluation value will directly serve as a reference for video observers,

[2] CMOR, The Canadian Meteor Orbit Radar (CMOR), https://fireballs.ndc.nasa.gov/cmor-radiants/earth.html

 © eMeteorNews

but those using other observation methods such as visual observation or radio waves should be aware of the differences.

The figures in the appendix show that while the SD indicates meteor shower activity in places where there is little concentration of radiant points, there are also cases where meteor shower activity has not yet been noted in places where radiant points are concentrated. In particular, it is expected that the efforts of observers in the southern hemisphere will reveal more detailed information about meteor activity in the south. Pointing out new meteor showers is not the purpose of this article, so we will not go into more detail.

Acknowledgment

We appreciate the daily efforts by all camera operators of the Global Meteor Network. This analysis owes to their work. This analysis relied upon the publicly available data from the GMN group under license[3] (Vida et al., 2019; 2020; 2021).

References

Brown P., Weryk R. J., Wong D. K., and Jones J. (2008). "A meteoroid stream survey using the Canadian Meteor Orbit Radar. I. Methodology and radiant catalogue". *Icarus*, **195**, 317–339.

Denning W.F. (1899). "General Catalogue of the Radiant Points of Meteoric Showers and of Fireballs and Shooting Stars observed at more than one station". *Memoirs of the Royal Astronomical Society*, **53**, 201–293.

Hajduková M., Rudawska R., Jopek T., Koseki M., Kokhirova G., and Neslušan L. (2023). "Modification of the Shower Database of the IAU Meteor Data Center". *Astronomy and Astrophysics*, **671**, A155. doi:10.1051/0004-6361/202244964.

Jenniskens P. (2006). Meteor Showers and their parent comets. Cambridge, Table 7, 'Working list of cometary meteors.

Koseki M. (2014a). "Various meteor scenes I: The perception and the conception of a 'meteor shower'". *WGN, Journal of the IMO*, **42**, 170–180.

Koseki M. (2014b). "Various meteor scenes II: Cygnid-Draconid Complex (κ-Cygnids)". *WGN, Journal of the IMO*, **42**, 181–197.

Koseki M. (2018). "Different definitions make a meteor shower distorted—the views from SonotaCo net and CAMS". *WGN, Journal of the IMO*, **46**, 119–135.

Koseki M. (2019a). "Showers of the IAU Meteor Data Center in the video data of SonotaCo: a simple and clear criterion for grading meteor showers". *WGN, Journal of the IMO*, **47**, 7–17.

Koseki M. (2019b). "Legendary meteor showers: Studies on Harvard photographic results". *WGN, Journal of the IMO*, **47**, 139–150.

Koseki M. (2020a). "Confusions in IAUMDC Meteor Shower Database (SD)". *eMetN*, **5**, 93–111.

Koseki M. (2020b). "Cygnid-Draconid Complex (κ-Cygnids) II: Call for observations, κ-Cygnids 2021". *WGN, Journal of the IMO*, **48**, 129–136.

Koseki M. (2020c). "Three Virginid showers". *eMetN*, **5**, 245–251.

Koseki M. (2023). "Remaining problems in IAUMDC Shower Database (SD)". *eMetN*, **5**, 288–309.

Lindblad B. A. (1971). "A Computerized Stream Search among 2401 Photographic Meteor Orbits". *Smithsonian Contributions to Astrophysics*, **12**, 14–24.

Sekanina Z. (1973). "Statistical Model of Meteor Streams. III. Stream search Among 19903 Radio Meteors". *Icarus*, **18**, 253–284.

Sekanina Z. (1976). "Statistical model of meteor streams. IV - A study of radio streams from the synoptic year". *Icarus*, **27**, 265–321.

Southworth R. B. and Hawkins G. S. (1963). "Statistics of meteor streams". *Smithsonian Contributions to Astrophysics*, **7**, 261–285.

Vida D., Gural P., Brown P., Campbell-Brown M., Wiegert P. (2019). "Estimating trajectories of meteors: an observational Monte Carlo approach - I. Theory". *Monthly Notices of the Royal Astronomical Society*, **491**, 2688–2705.

Vida D., Gural P., Brown P., Campbell-Brown M., Wiegert P. (2020). "Estimating trajectories of meteors: an observational Monte Carlo approach - II. Results". *Monthly Notices of the Royal Astronomical Society*, **491**, 3996–4011.

Vida D., Šegon D., Gural P. S., Brown P. G., McIntyre M. J. M., Dijkema T. J., Pavletić L., Kukić P., Mazur M. J., Eschman P., Roggemans P., Merlak A., Zubrović D. (2021). "The Global Meteor Network – Methodology and first results". *Monthly Notices of the Royal Astronomical Society*, **506**, 5046–5074.

[3] https://creativecommons.org/licenses/by/4.0/

Appendix

Full radiant distribution all year round; the crosses are the radiants in Sun-centered geocentric ecliptic coordinates obtained by Global Meteor Network and the red circles are radiants of the entries in the IAU working list of meteor showers (SD or Shower Database).

Circles are plotted based on the peak activity though the meteor shower is active some days long. To compare the concentration of radiant points in GMN and the radiant points in SD, please refer to the distribution charts before and after.

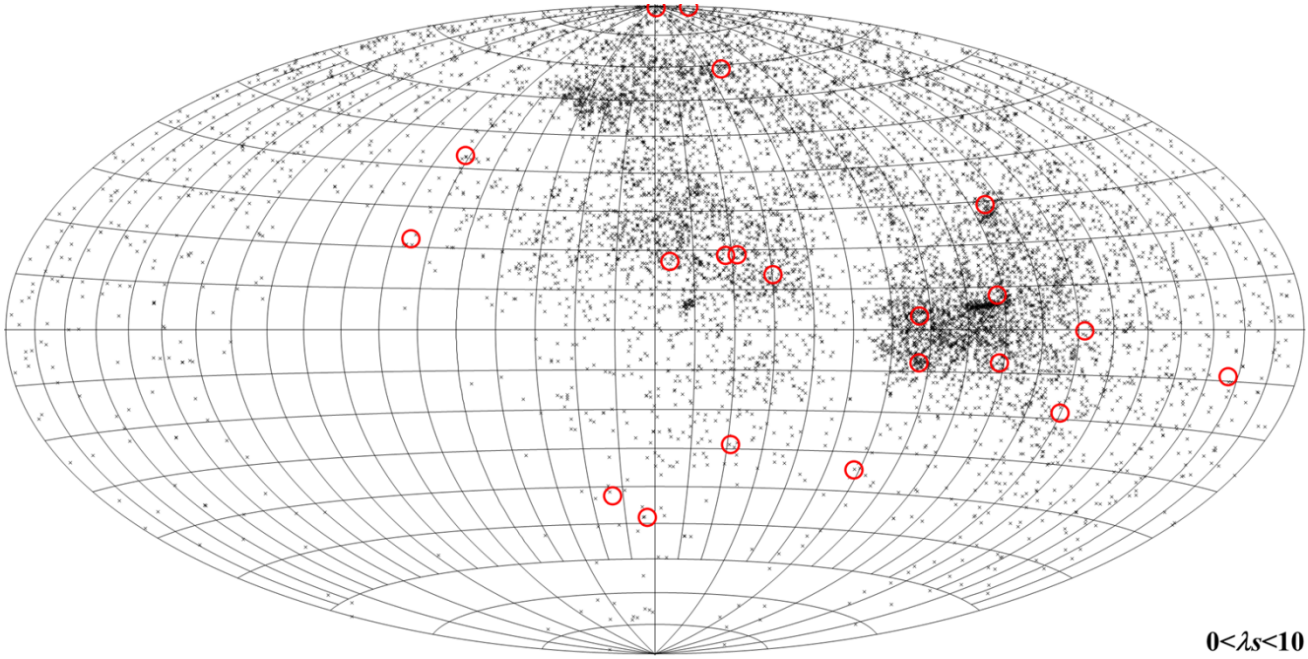

Figure 7 – Radiant distribution obtained by the Global Meteor Network during the interval $0° < \lambda_\odot < 10°$, the black crosses are the individual GMN radiants, the red circles the radiants according to the IAU shower database[4].

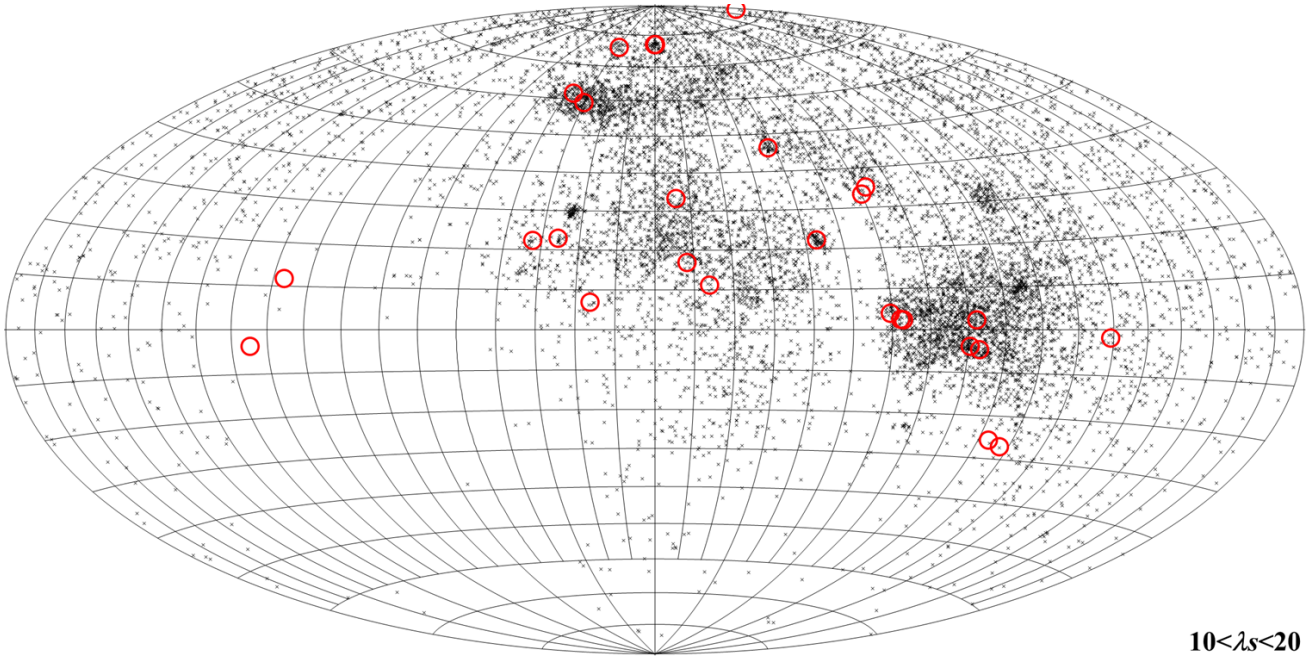

Figure 8 – Radiant distribution obtained by the Global Meteor Network during the interval $10° < \lambda_\odot < 20°$, the black crosses are the individual GMN radiants, the red circles the radiants according to the IAU shower database[4].

[4] https://www.ta3.sk/IAUC22DB/MDC2022/Roje/roje_lista.php?corobic_roje=0&sort_roje=0

 © eMeteorNews

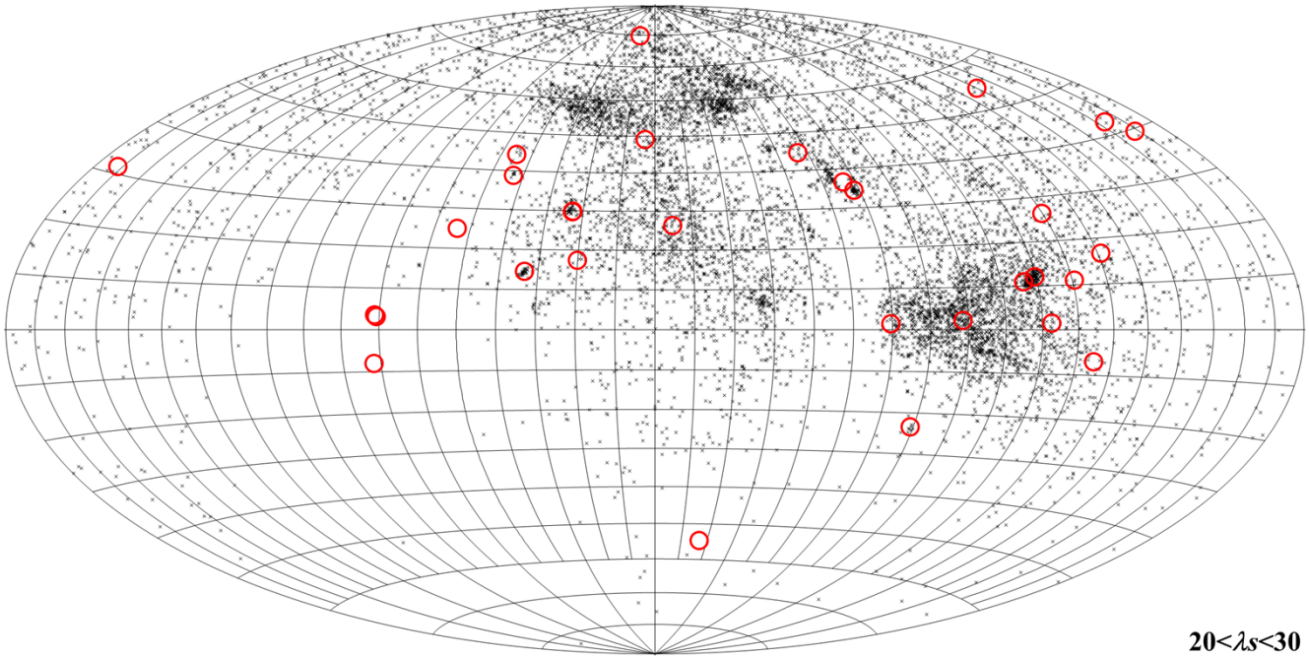

Figure 9 – Radiant distribution obtained by the Global Meteor Network during the interval $20° < \lambda_{\odot} < 30°$, the black crosses are the individual GMN radiants, the red circles the radiants according to the IAU shower database[5].

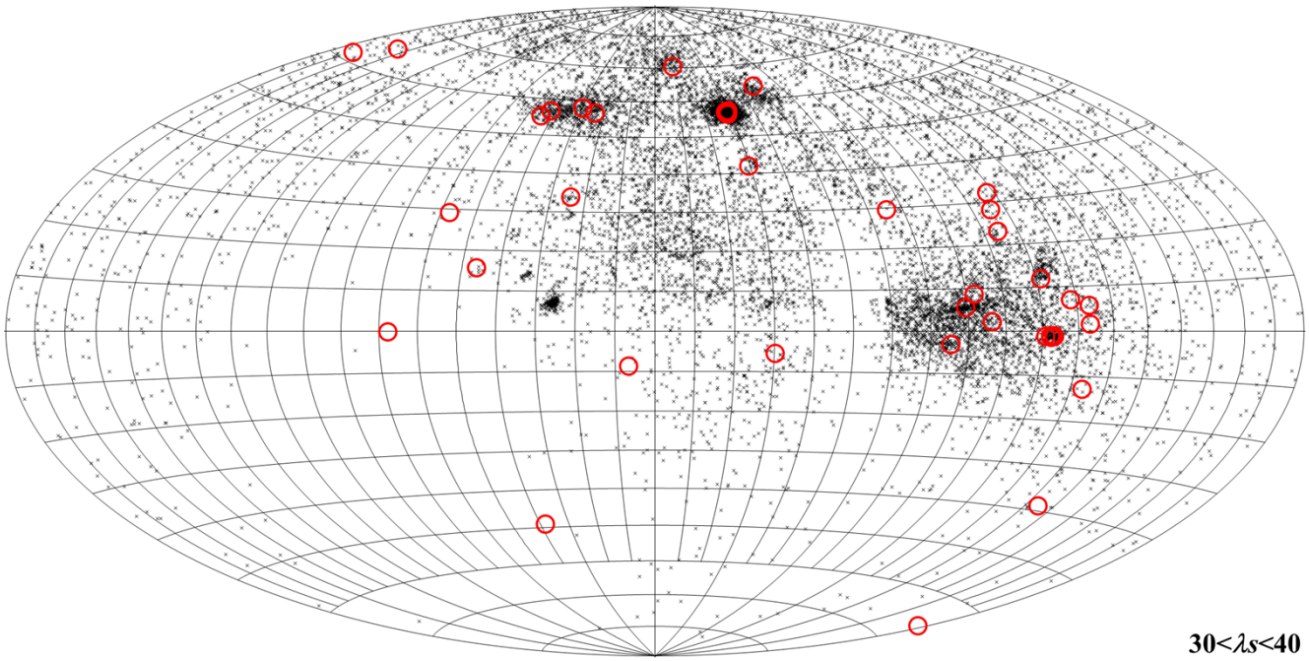

Figure 10 – Radiant distribution obtained by the Global Meteor Network during the interval $30° < \lambda_{\odot} < 40°$, the black crosses are the individual GMN radiants, the red circles the radiants according to the IAU shower database[5].

[5] https://www.ta3.sk/IAUC22DB/MDC2022/Roje/roje_lista.php?corobic_roje=0&sort_roje=0

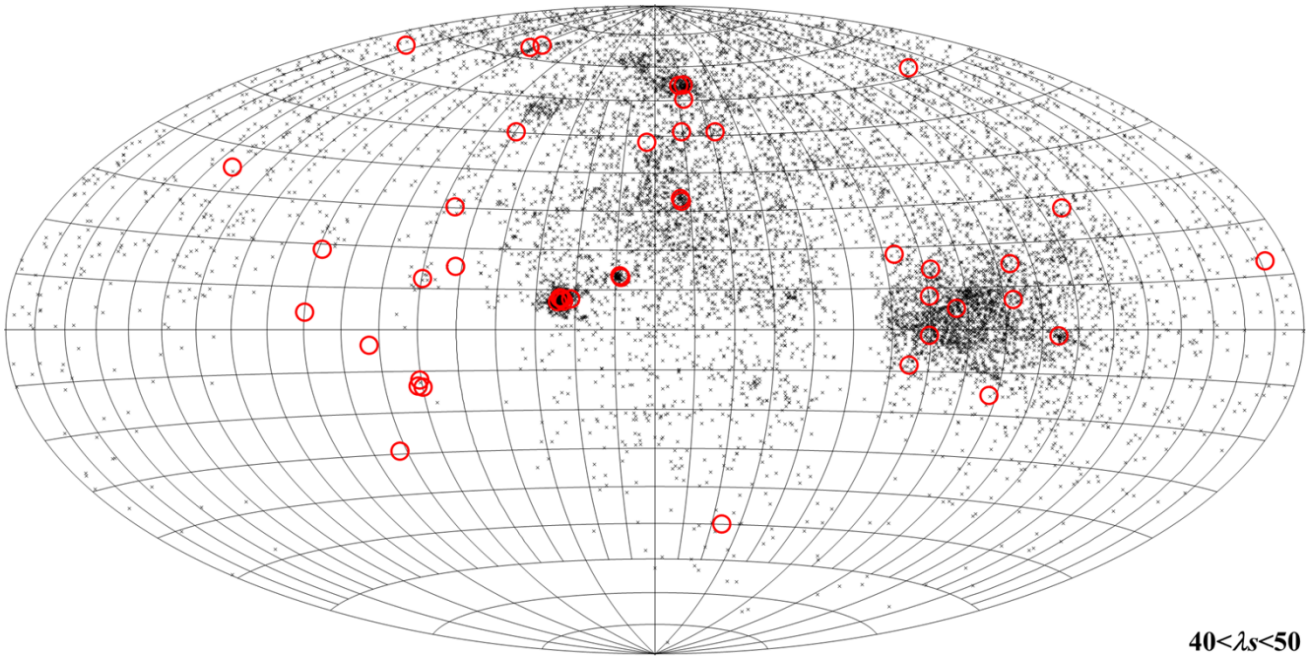

Figure 11 – Radiant distribution obtained by the Global Meteor Network during the interval 40° < $\lambda_{\odot}$ < 50°, the black crosses are the individual GMN radiants, the red circles the radiants according to the IAU shower database[6].

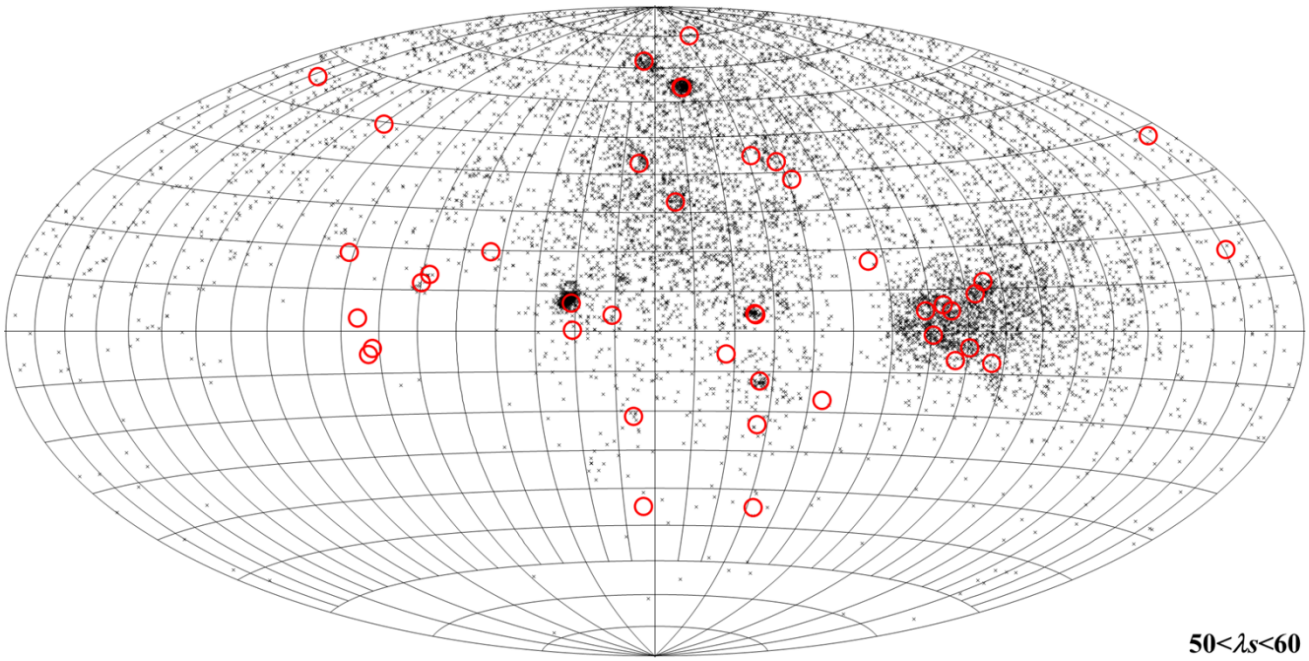

Figure 12 – Radiant distribution obtained by the Global Meteor Network during the interval 50° < $\lambda_{\odot}$ < 60°, the black crosses are the individual GMN radiants, the red circles the radiants according to the IAU shower database[6].

[6] https://www.ta3.sk/IAUC22DB/MDC2022/Roje/roje_lista.php?corobic_roje=0&sort_roje=0

 © eMeteorNews

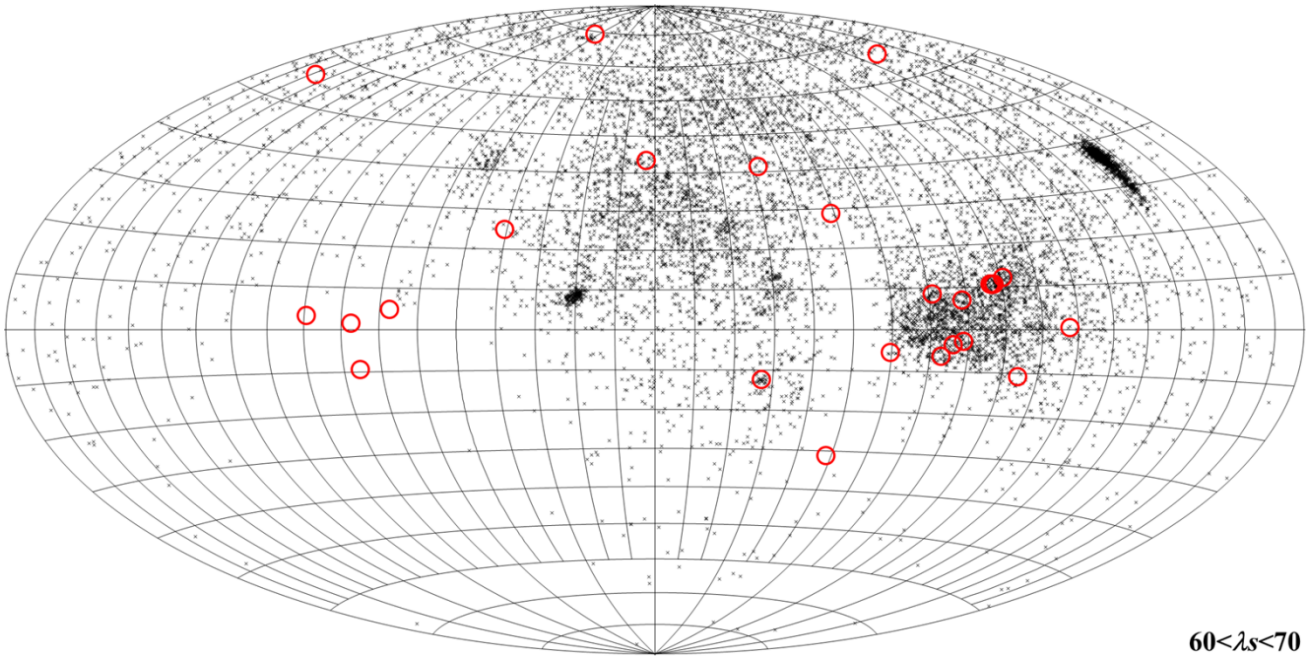

Figure 13 – Radiant distribution obtained by the Global Meteor Network during the interval 60° < $\lambda_{\odot}$ < 70°, the black crosses are the individual GMN radiants, the red circles the radiants according to the IAU shower database[7].

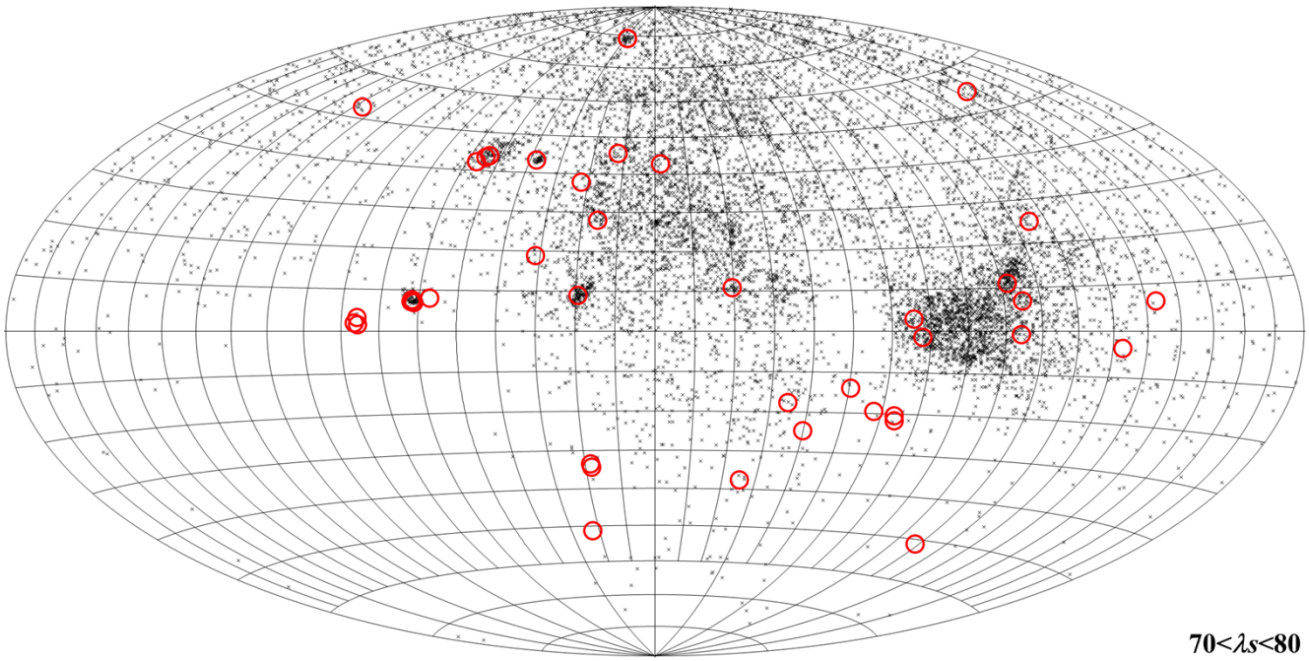

Figure 14 – Radiant distribution obtained by the Global Meteor Network during the interval 70° < $\lambda_{\odot}$ < 80°, the black crosses are the individual GMN radiants, the red circles the radiants according to the IAU shower database[7].

[7] https://www.ta3.sk/IAUC22DB/MDC2022/Roje/roje_lista.php?corobic_roje=0&sort_roje=0

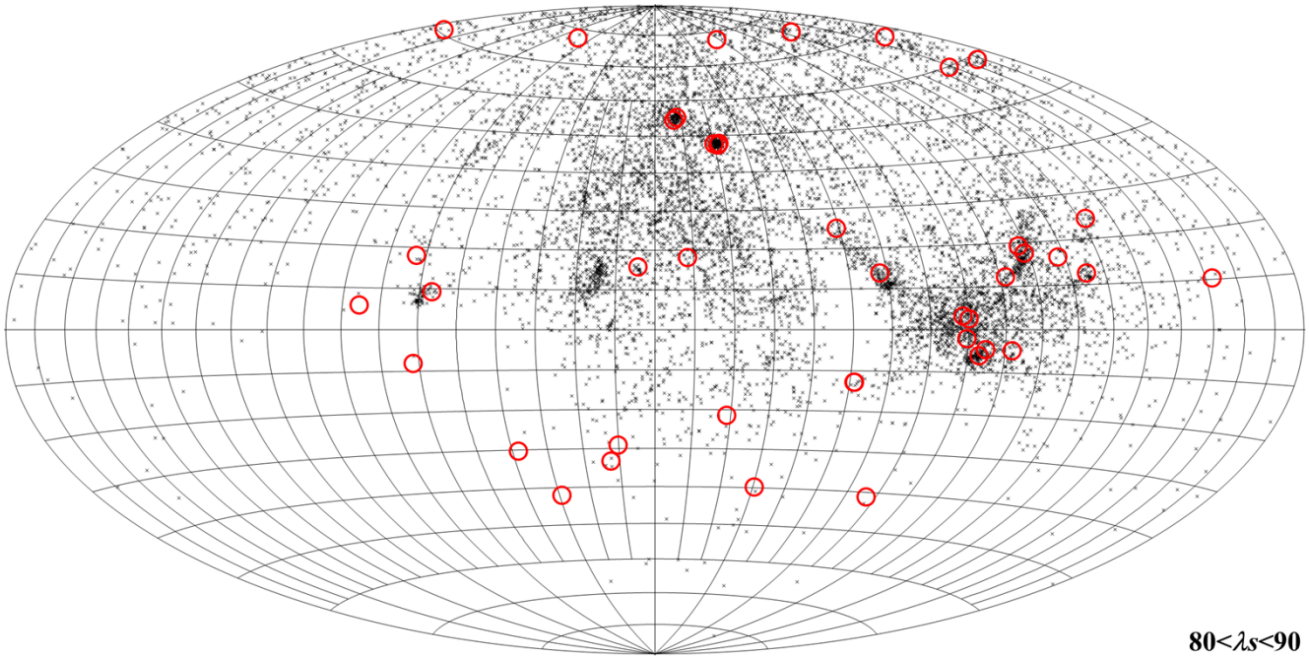

Figure 15 – Radiant distribution obtained by the Global Meteor Network during the interval 80° < $\lambda_\odot$ < 90°, the black crosses are the individual GMN radiants, the red circles the radiants according to the IAU shower database[8].

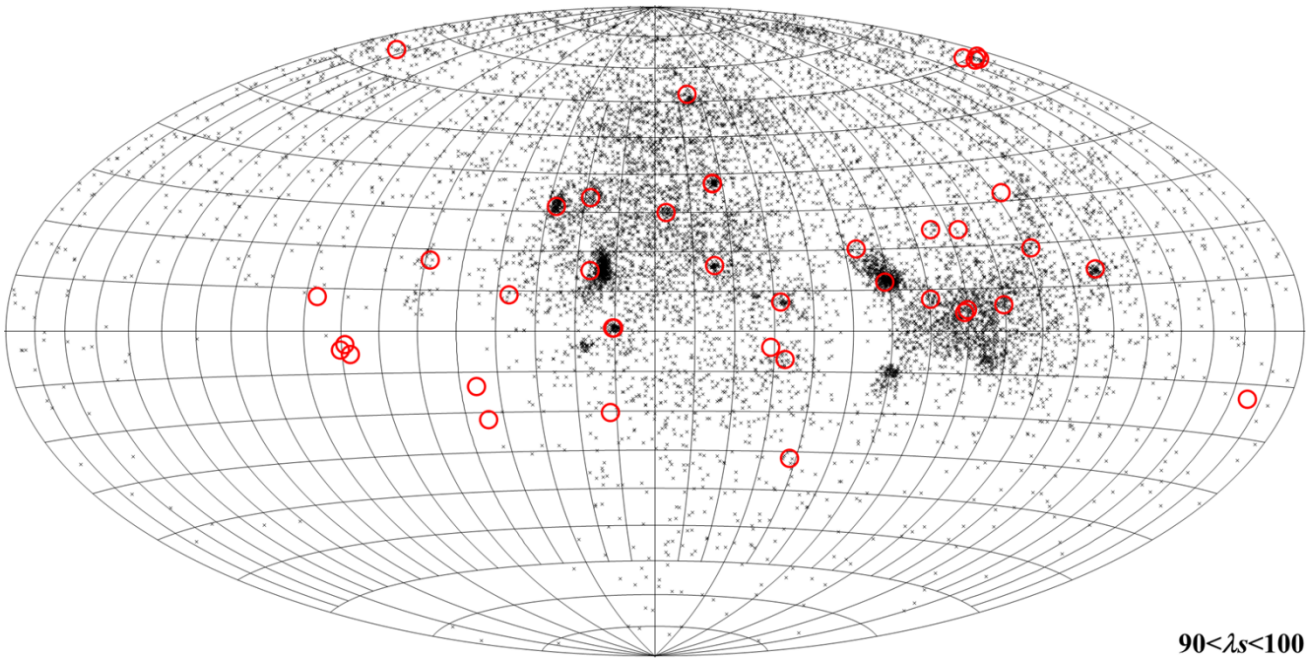

Figure 16 – Radiant distribution obtained by the Global Meteor Network during the interval 90° < $\lambda_\odot$ < 100°, the black crosses are the individual GMN radiants, the red circles the radiants according to the IAU shower database[8].

[8] https://www.ta3.sk/IAUC22DB/MDC2022/Roje/roje_lista.php?corobic_roje=0&sort_roje=0

 © eMeteorNews

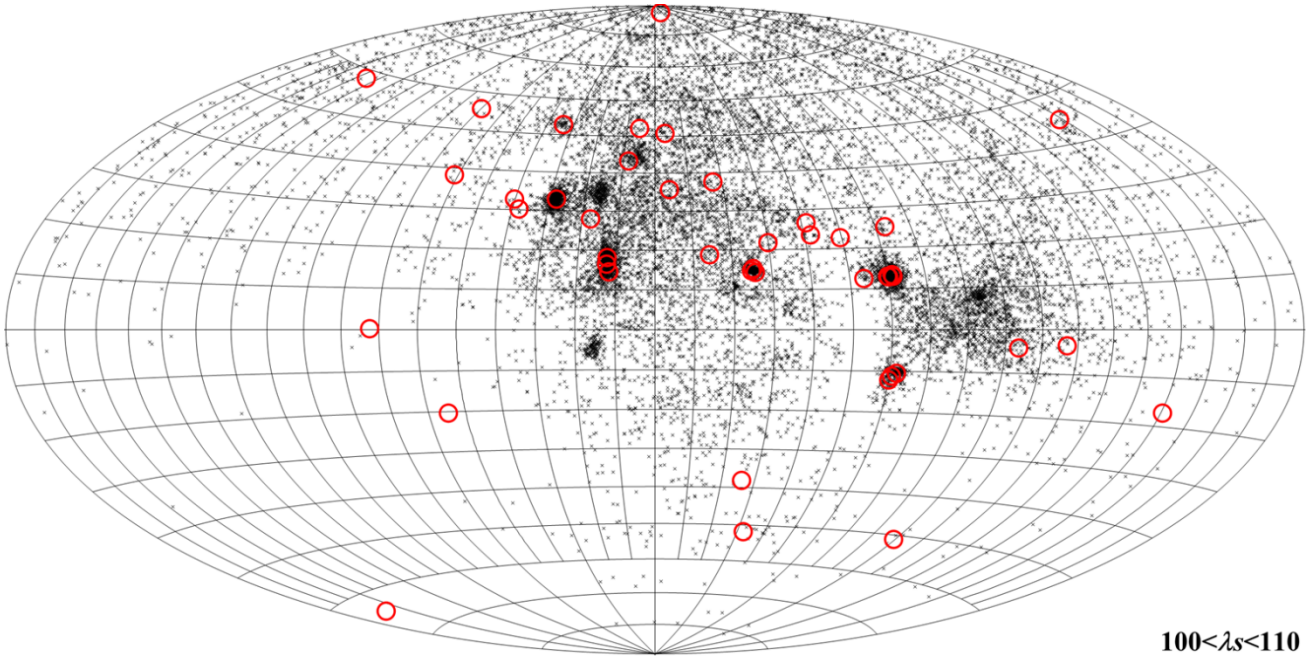

Figure 17 – Radiant distribution obtained by the Global Meteor Network during the interval 100° < $\lambda_\odot$ < 110°, the black crosses are the individual GMN radiants, the red circles the radiants according to the IAU shower database[9].

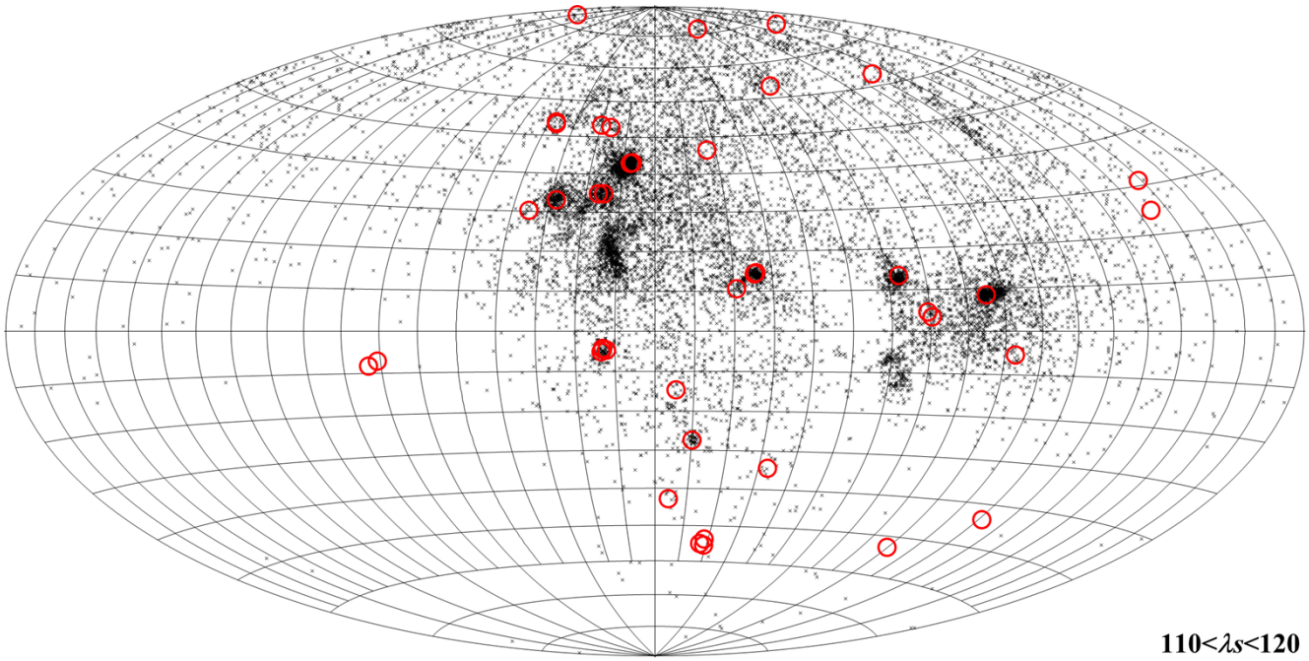

Figure 18 – Radiant distribution obtained by the Global Meteor Network during the interval 110° < $\lambda_\odot$ < 120°, the black crosses are the individual GMN radiants, the red circles the radiants according to the IAU shower database[9].

[9] https://www.ta3.sk/IAUC22DB/MDC2022/Roje/roje_lista.php?corobic_roje=0&sort_roje=0

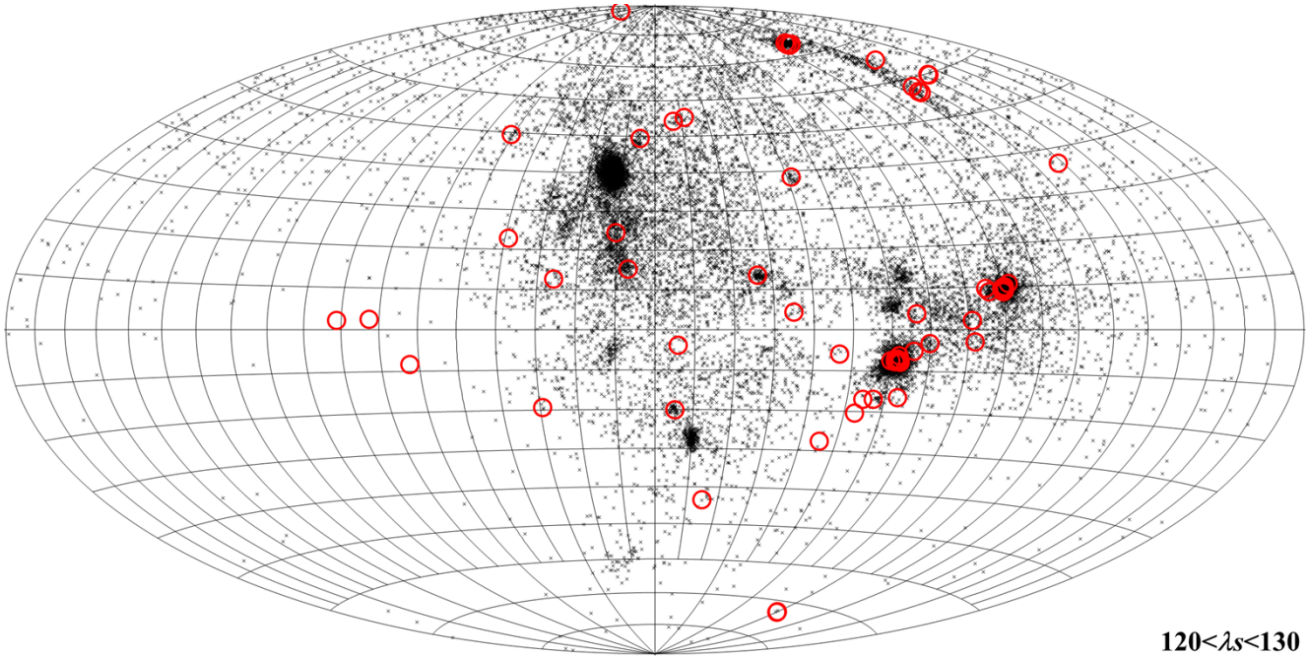

Figure 19 – Radiant distribution obtained by the Global Meteor Network during the interval 120° < $\lambda_{\odot}$ < 130°, the black crosses are the individual GMN radiants, the red circles the radiants according to the IAU shower database[10].

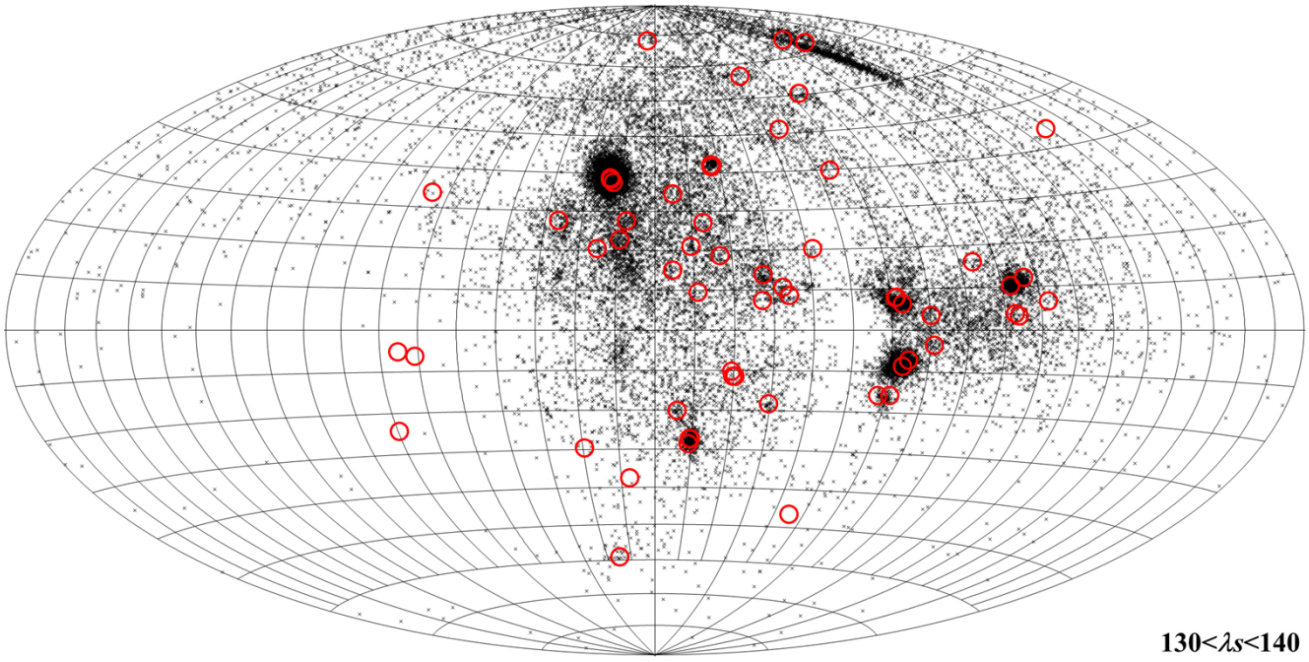

Figure 20 – Radiant distribution obtained by the Global Meteor Network during the interval 130° < $\lambda_{\odot}$ < 140°, the black crosses are the individual GMN radiants, the red circles the radiants according to the IAU shower database[10].

[10] https://www.ta3.sk/IAUC22DB/MDC2022/Roje/roje_lista.php?corobic_roje=0&sort_roje=0

 © eMeteorNews

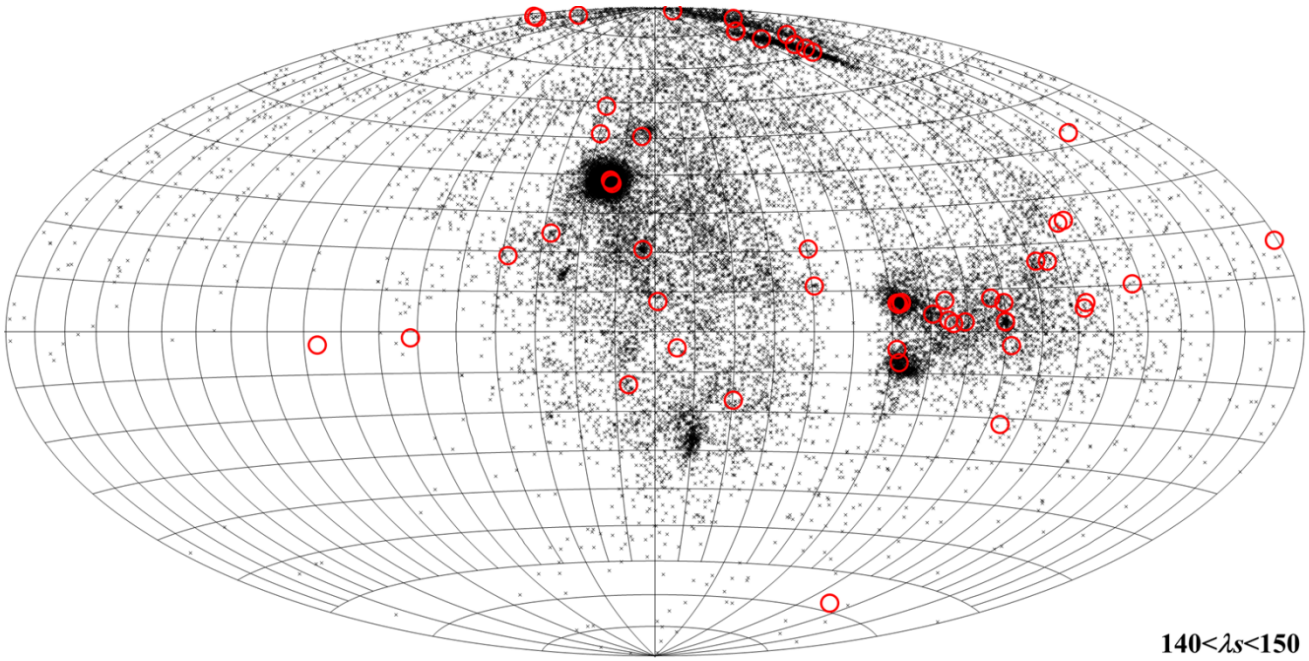

Figure 21 – Radiant distribution obtained by the Global Meteor Network during the interval 140° < $\lambda_\odot$ < 150°, the black crosses are the individual GMN radiants, the red circles the radiants according to the IAU shower database[11].

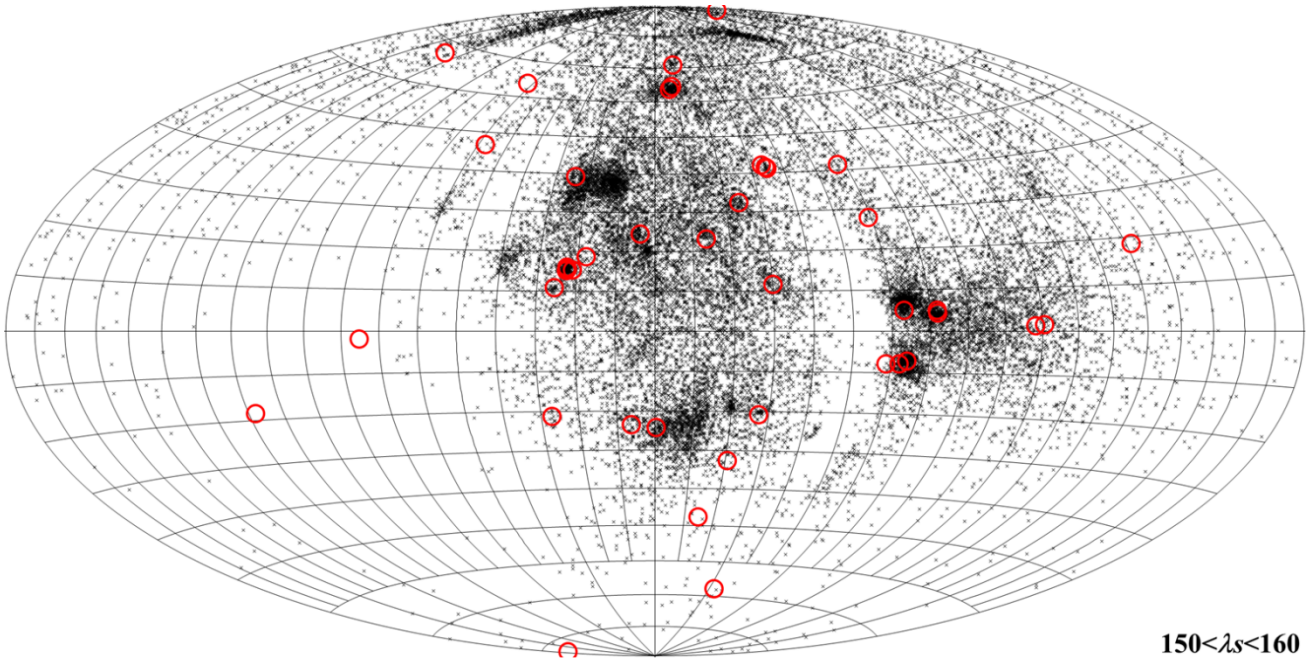

Figure 22 – Radiant distribution obtained by the Global Meteor Network during the interval 150° < $\lambda_\odot$ < 160°, the black crosses are the individual GMN radiants, the red circles the radiants according to the IAU shower database[11].

[11] https://www.ta3.sk/IAUC22DB/MDC2022/Roje/roje_lista.php?corobic_roje=0&sort_roje=0

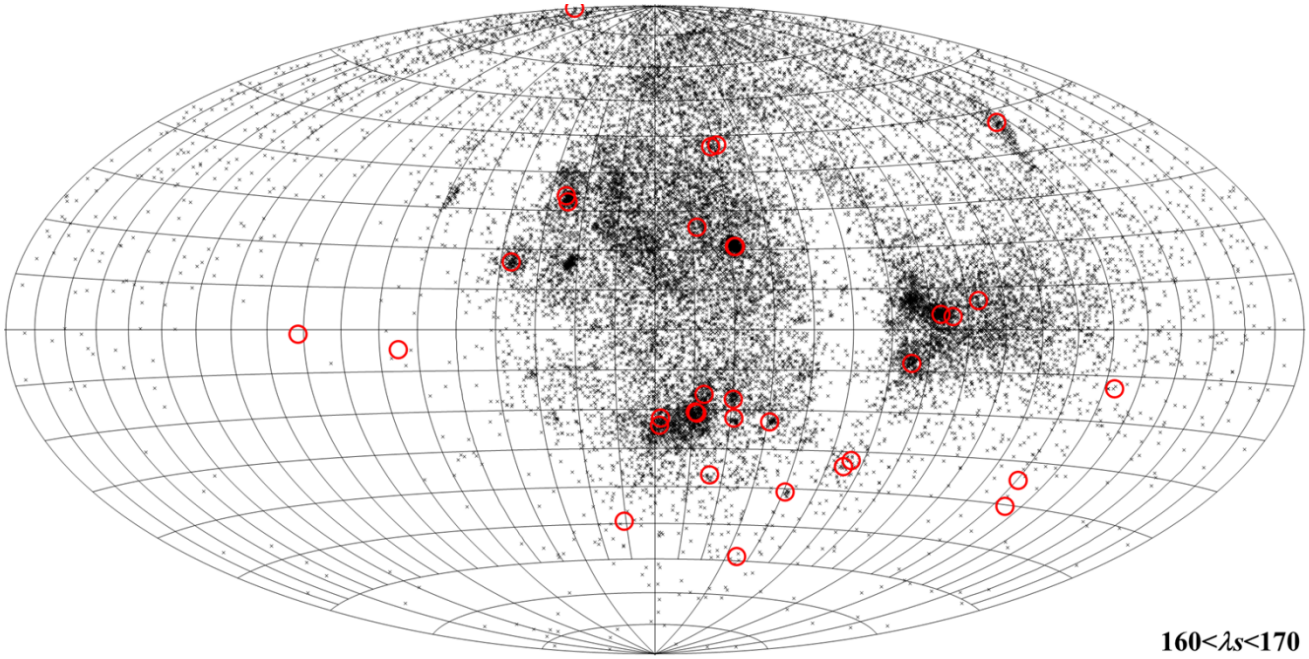

Figure 23 – Radiant distribution obtained by the Global Meteor Network during the interval 160° < $\lambda_\odot$ < 170°, the black crosses are the individual GMN radiants, the red circles the radiants according to the IAU shower database[12].

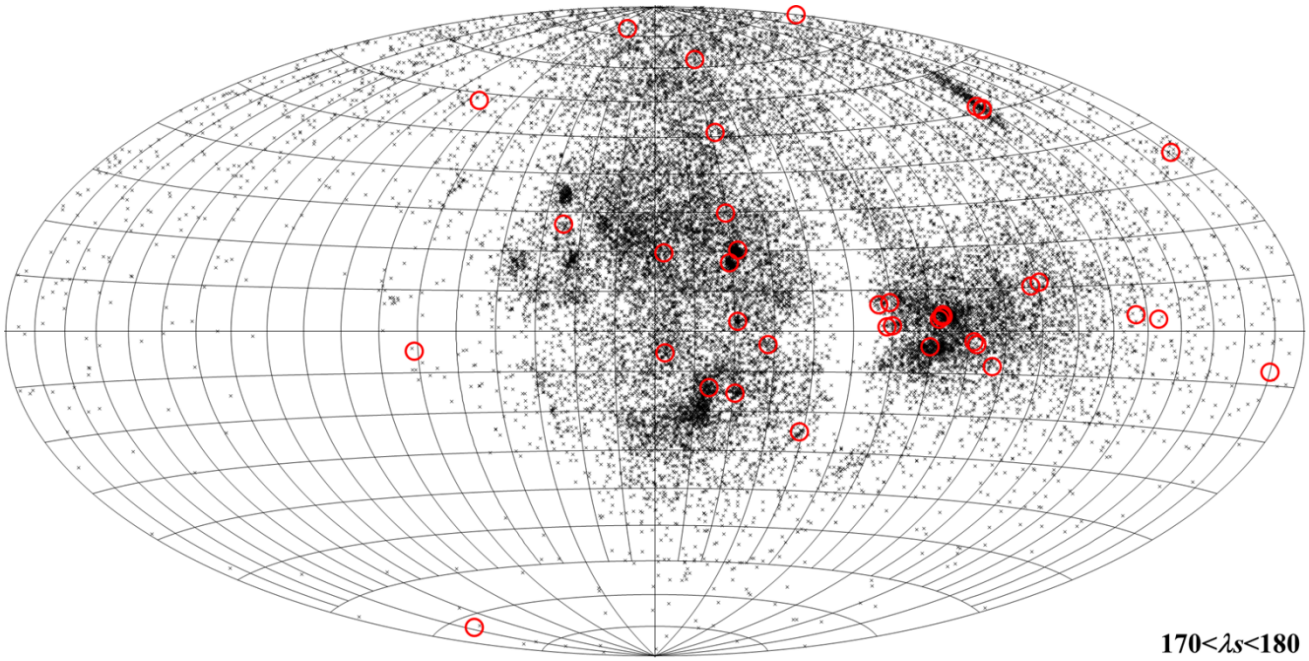

Figure 24 – Radiant distribution obtained by the Global Meteor Network during the interval 170° < $\lambda_\odot$ < 180°, the black crosses are the individual GMN radiants, the red circles the radiants according to the IAU shower database[12].

[12] https://www.ta3.sk/IAUC22DB/MDC2022/Roje/roje_lista.php?corobic_roje=0&sort_roje=0

 © eMeteorNews

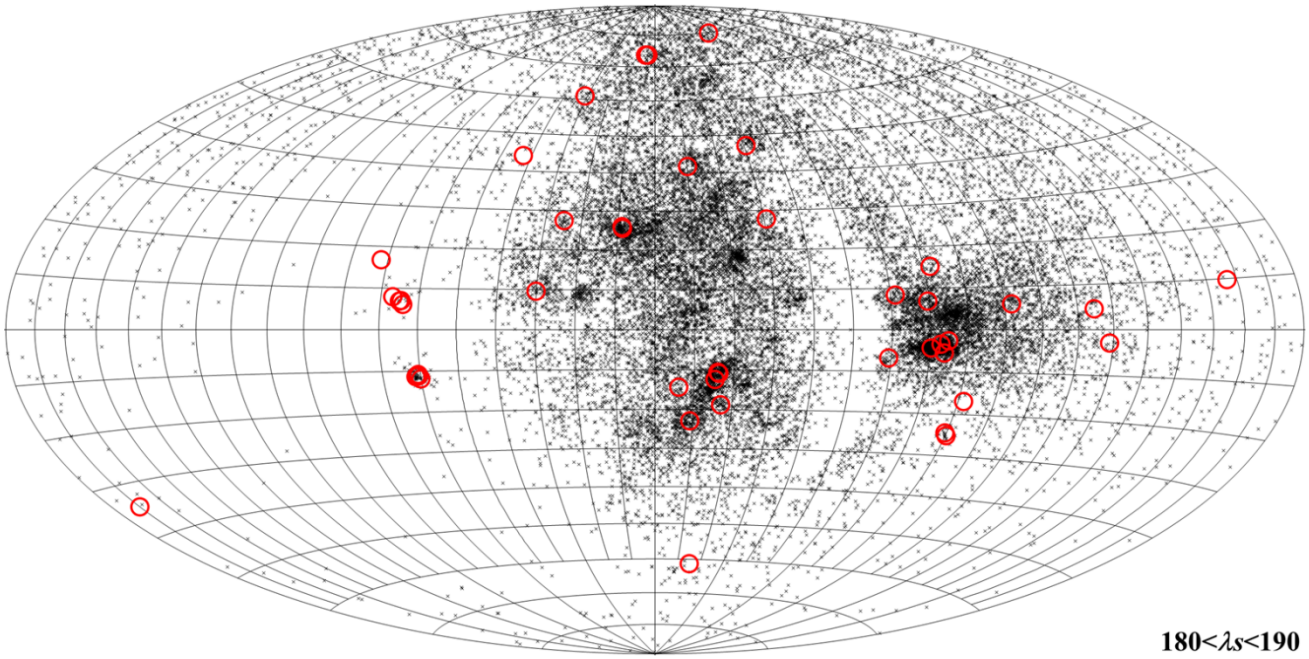

Figure 25 – Radiant distribution obtained by the Global Meteor Network during the interval 180° < $\lambda_\odot$ < 190°, the black crosses are the individual GMN radiants, the red circles the radiants according to the IAU shower database[13].

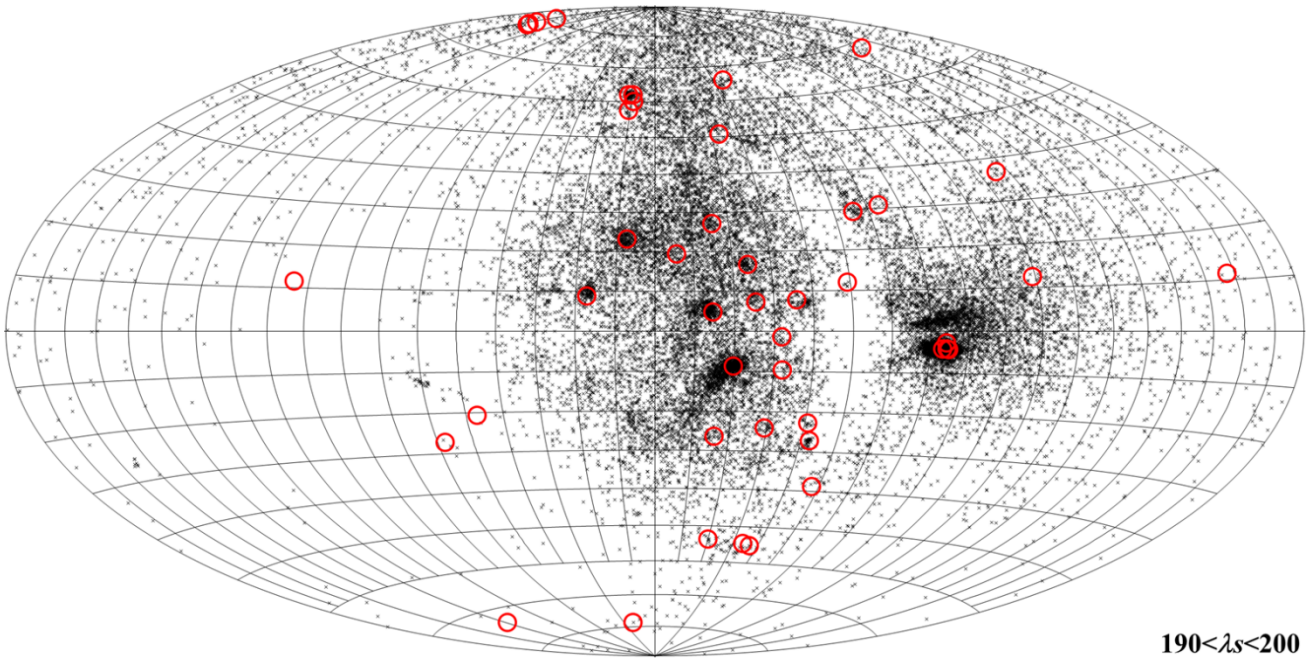

Figure 26 – Radiant distribution obtained by the Global Meteor Network during the interval 190° < $\lambda_\odot$ < 200°, the black crosses are the individual GMN radiants, the red circles the radiants according to the IAU shower database[13].

[13] https://www.ta3.sk/IAUC22DB/MDC2022/Roje/roje_lista.php?corobic_roje=0&sort_roje=0

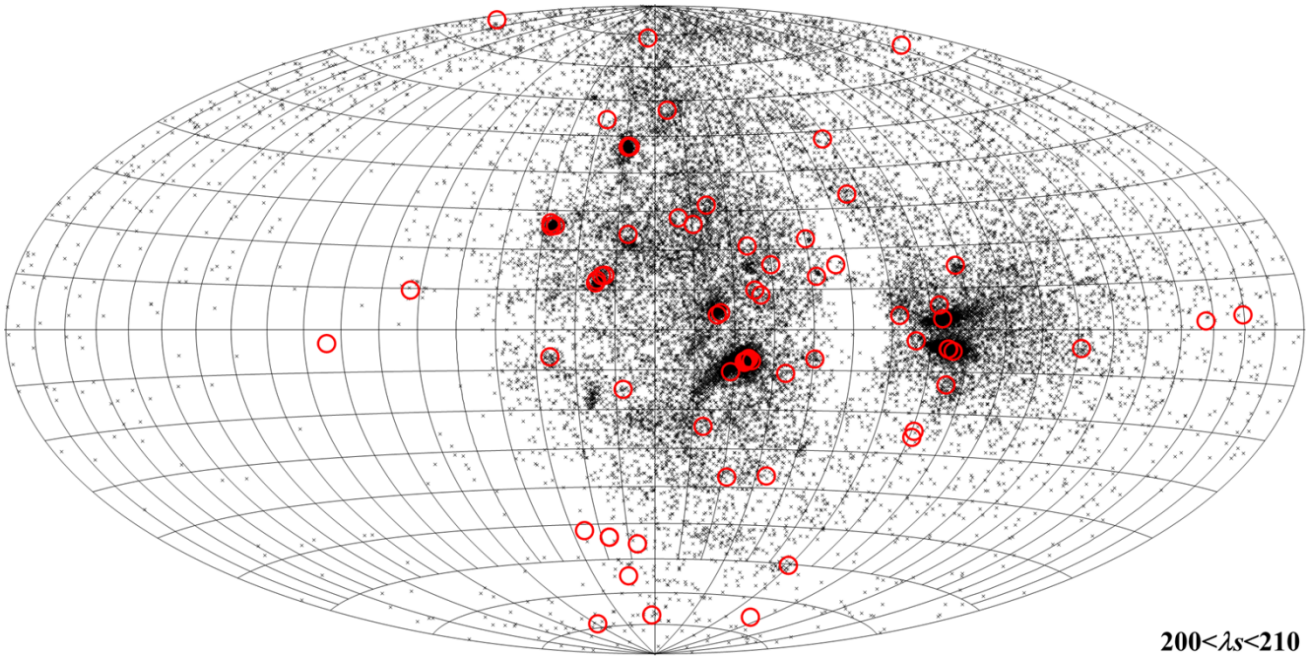

Figure 27 – Radiant distribution obtained by the Global Meteor Network during the interval 200° < $\lambda_\odot$ < 210°, the black crosses are the individual GMN radiants, the red circles the radiants according to the IAU shower database[14].

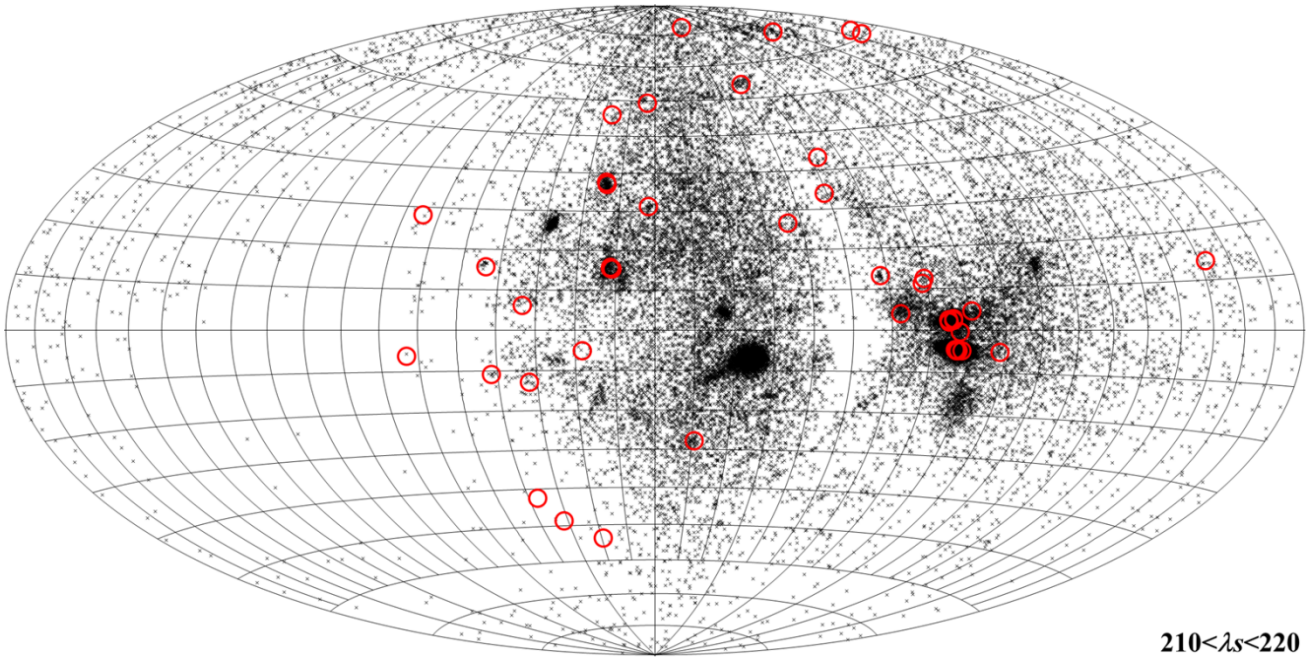

Figure 28 – Radiant distribution obtained by the Global Meteor Network during the interval 210° < $\lambda_\odot$ < 220°, the black crosses are the individual GMN radiants, the red circles the radiants according to the IAU shower database[14].

[14] https://www.ta3.sk/IAUC22DB/MDC2022/Roje/roje_lista.php?corobic_roje=0&sort_roje=0

 © eMeteorNews

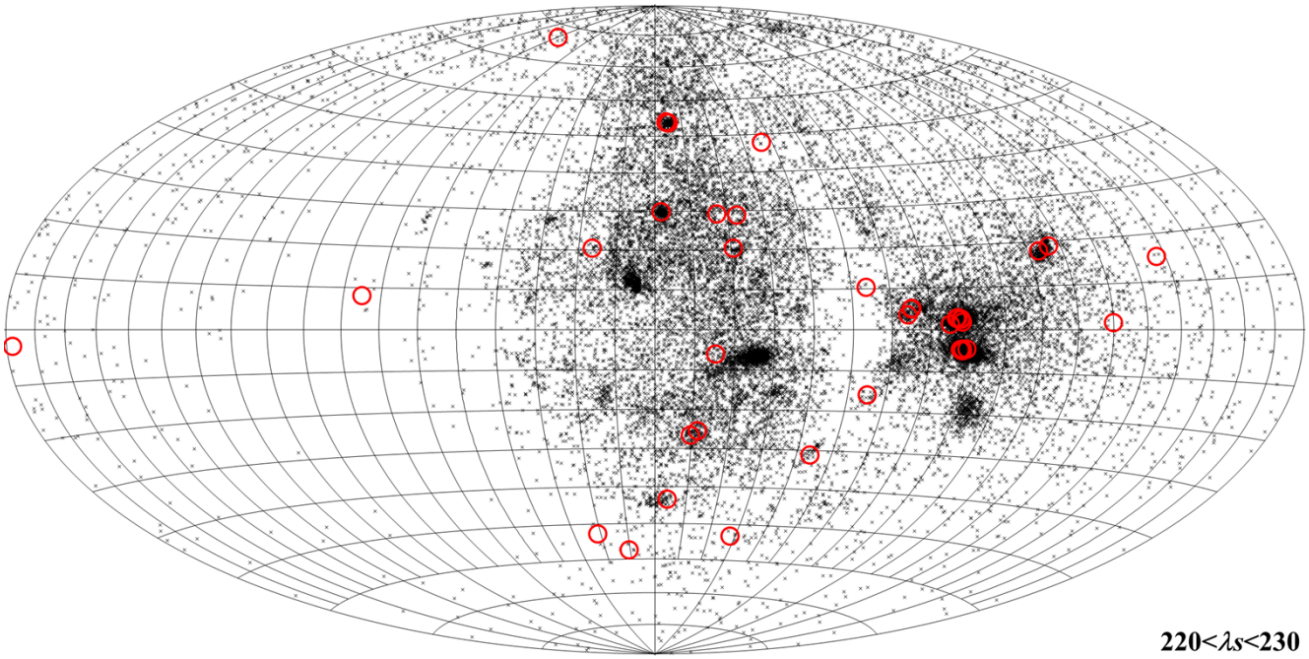

Figure 29 – Radiant distribution obtained by the Global Meteor Network during the interval 220° < $\lambda_\odot$ < 230°, the black crosses are the individual GMN radiants, the red circles the radiants according to the IAU shower database[15].

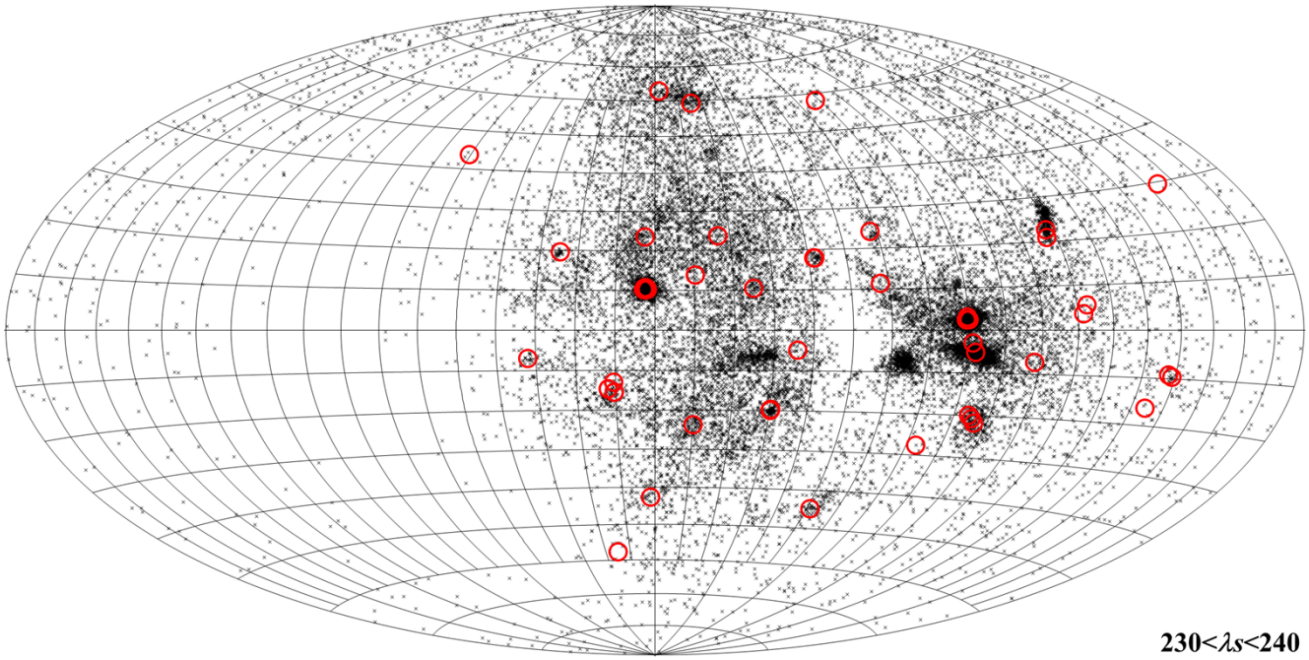

Figure 30 – Radiant distribution obtained by the Global Meteor Network during the interval 230° < $\lambda_\odot$ < 240°, the black crosses are the individual GMN radiants, the red circles the radiants according to the IAU shower database[15].

[15] https://www.ta3.sk/IAUC22DB/MDC2022/Roje/roje_lista.php?corobic_roje=0&sort_roje=0

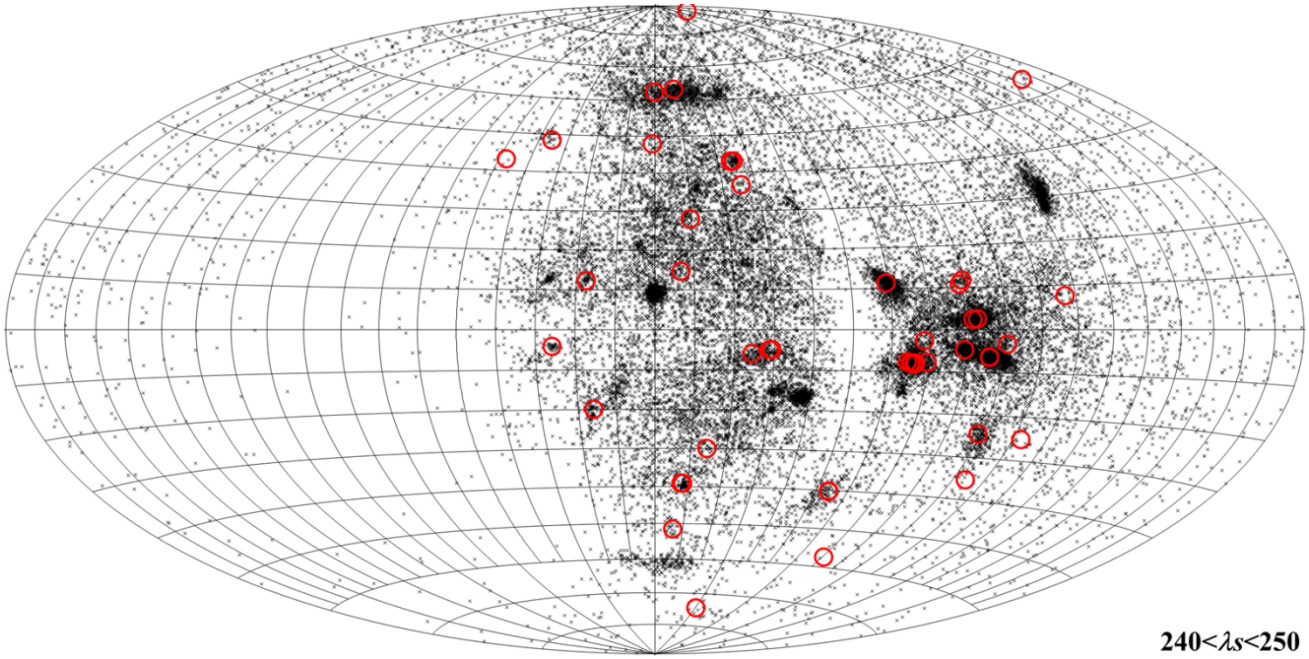

Figure 31 – Radiant distribution obtained by the Global Meteor Network during the interval 240° < $\lambda_\odot$ < 250°, the black crosses are the individual GMN radiants, the red circles the radiants according to the IAU shower database[16].

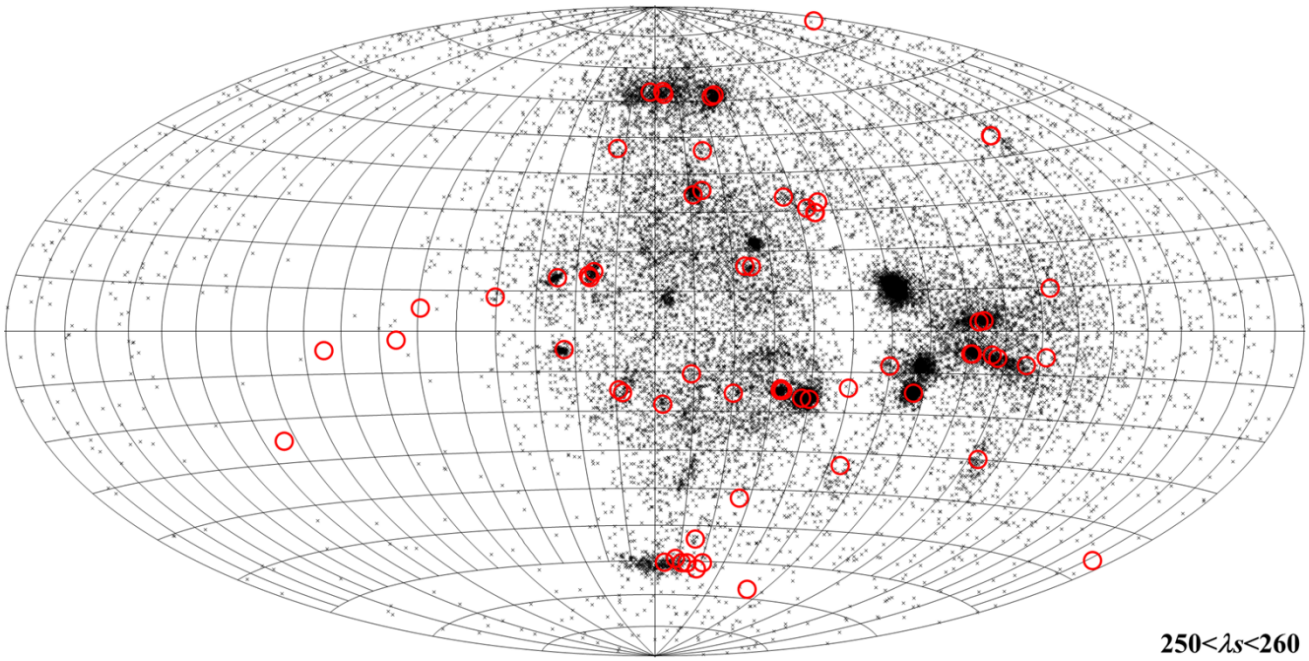

Figure 32 – Radiant distribution obtained by the Global Meteor Network during the interval 250° < $\lambda_\odot$ < 260°, the black crosses are the individual GMN radiants, the red circles the radiants according to the IAU shower database[16].

[16] https://www.ta3.sk/IAUC22DB/MDC2022/Roje/roje_lista.php?corobic_roje=0&sort_roje=0

 © eMeteorNews

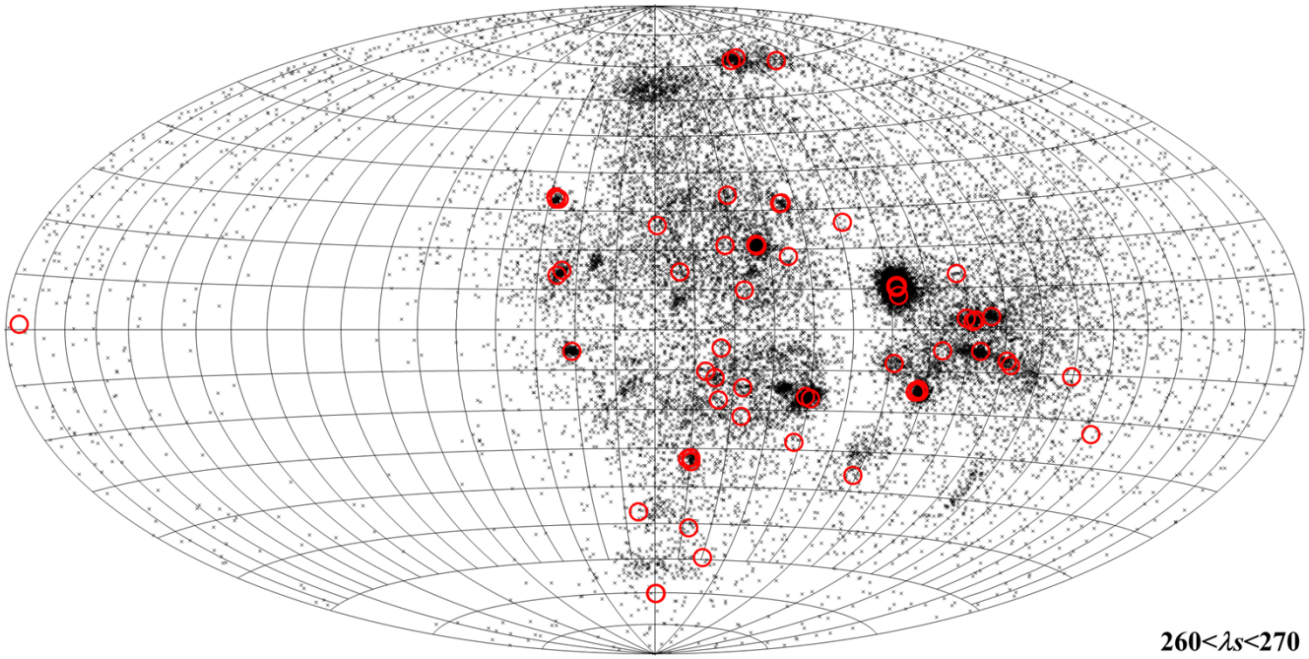

Figure 33 – Radiant distribution obtained by the Global Meteor Network during the interval 260° < $\lambda_\odot$ < 270°, the black crosses are the individual GMN radiants, the red circles the radiants according to the IAU shower database[17].

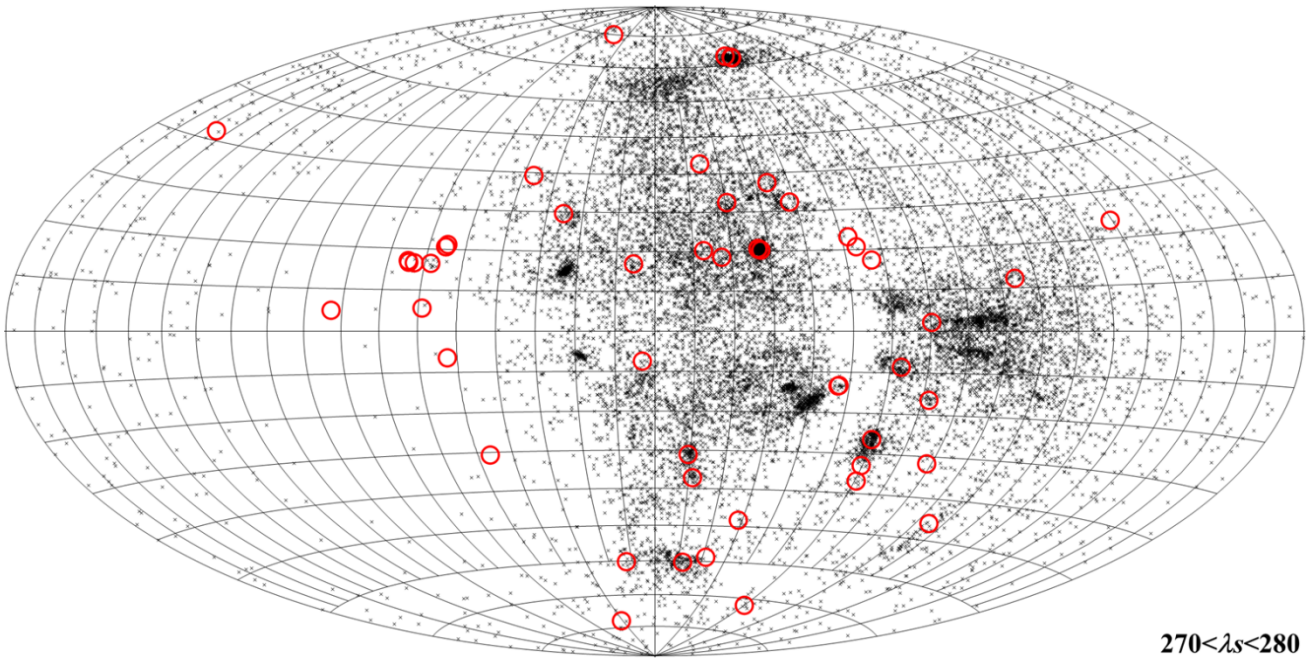

Figure 34 – Radiant distribution obtained by the Global Meteor Network during the interval 270° < $\lambda_\odot$ < 280°, the black crosses are the individual GMN radiants, the red circles the radiants according to the IAU shower database[17].

[17] https://www.ta3.sk/IAUC22DB/MDC2022/Roje/roje_lista.php?corobic_roje=0&sort_roje=0

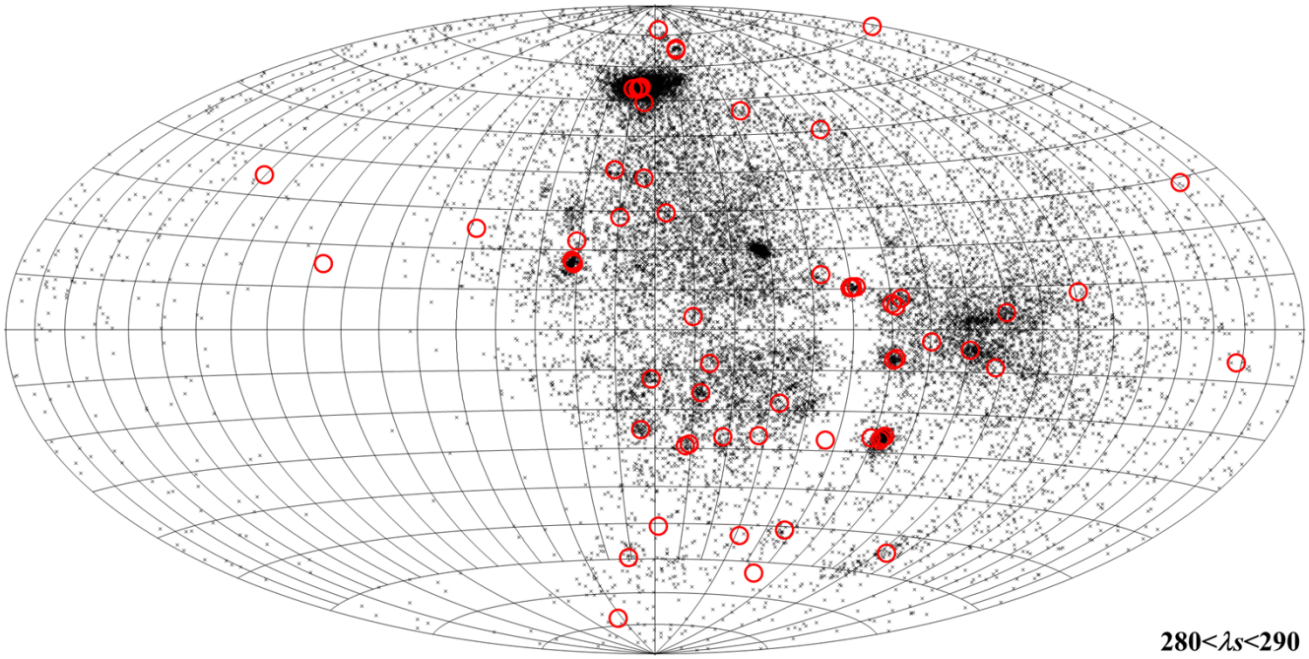

Figure 35 – Radiant distribution obtained by the Global Meteor Network during the interval 280° < $\lambda_\odot$ < 290°, the black crosses are the individual GMN radiants, the red circles the radiants according to the IAU shower database[18].

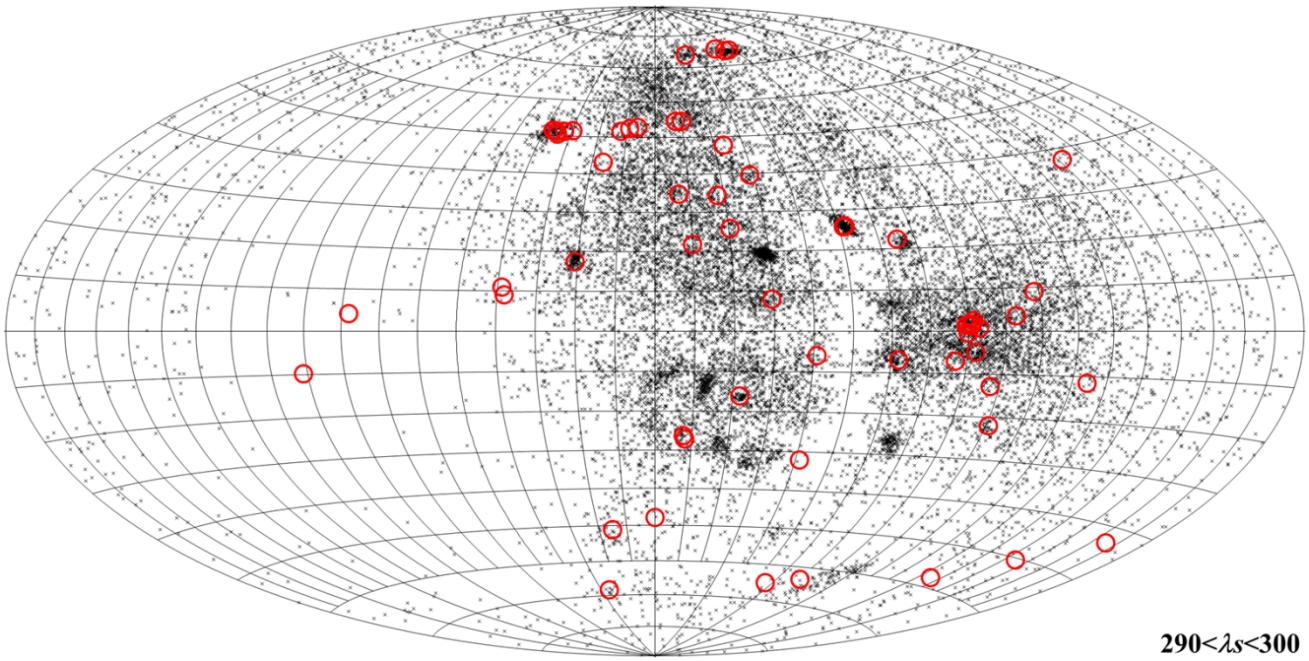

Figure 36 – Radiant distribution obtained by the Global Meteor Network during the interval 290° < $\lambda_\odot$ < 300°, the black crosses are the individual GMN radiants, the red circles the radiants according to the IAU shower database[18].

[18] https://www.ta3.sk/IAUC22DB/MDC2022/Roje/roje_lista.php?corobic_roje=0&sort_roje=0

 © eMeteorNews

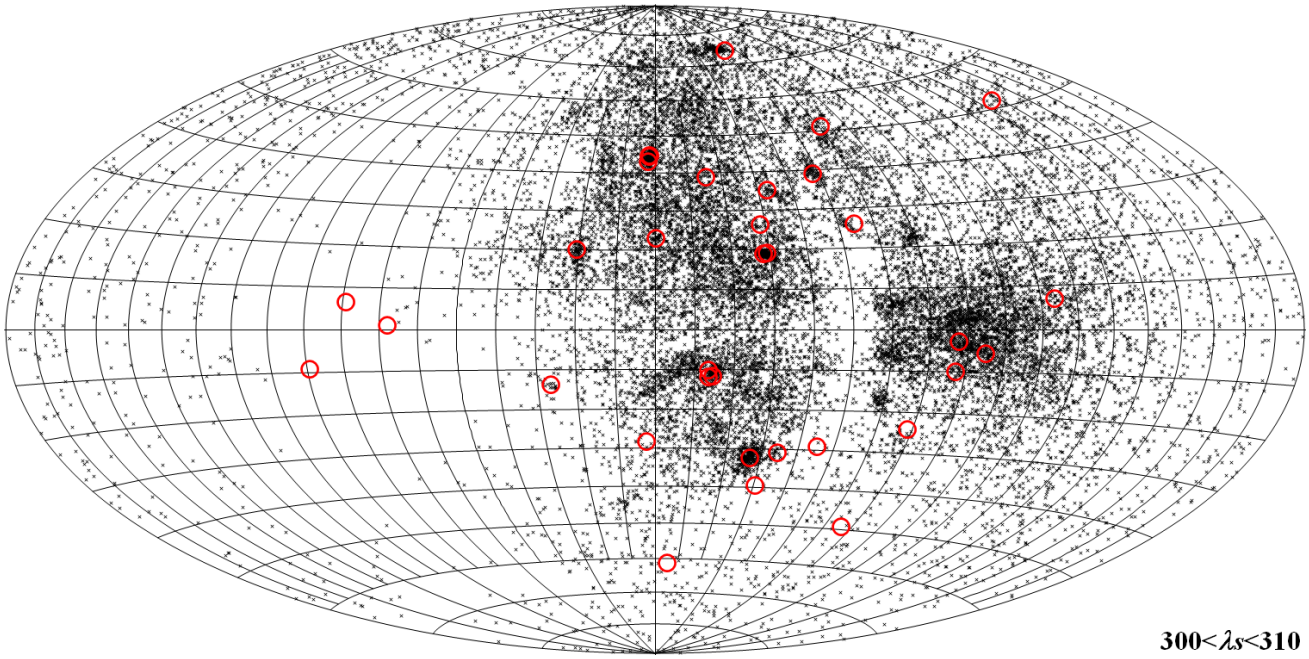

Figure 37 – Radiant distribution obtained by the Global Meteor Network during the interval 300° < $\lambda_\odot$ < 310°, the black crosses are the individual GMN radiants, the red circles the radiants according to the IAU shower database[19].

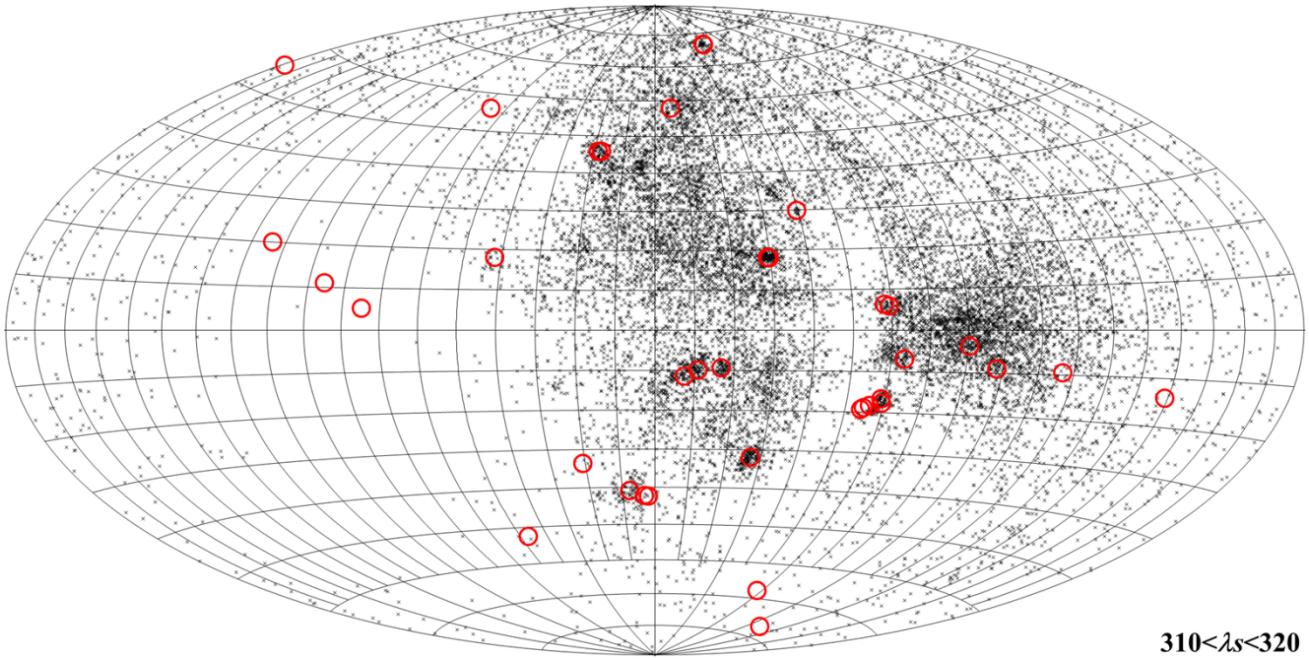

Figure 38 – Radiant distribution obtained by the Global Meteor Network during the interval 310° < $\lambda_\odot$ < 320°, the black crosses are the individual GMN radiants, the red circles the radiants according to the IAU shower database[19].

[19] https://www.ta3.sk/IAUC22DB/MDC2022/Roje/roje_lista.php?corobic_roje=0&sort_roje=0

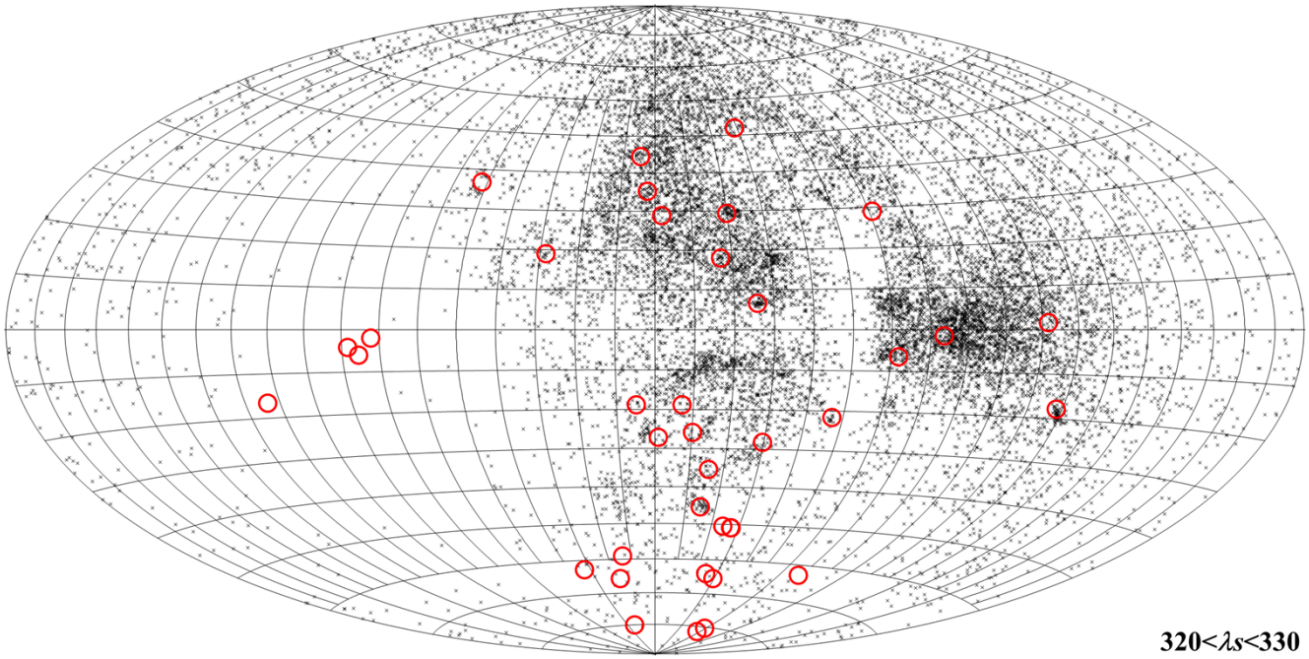

Figure 39 – Radiant distribution obtained by the Global Meteor Network during the interval 320° < $\lambda_{\odot}$ < 330°, the black crosses are the individual GMN radiants, the red circles the radiants according to the IAU shower database[20].

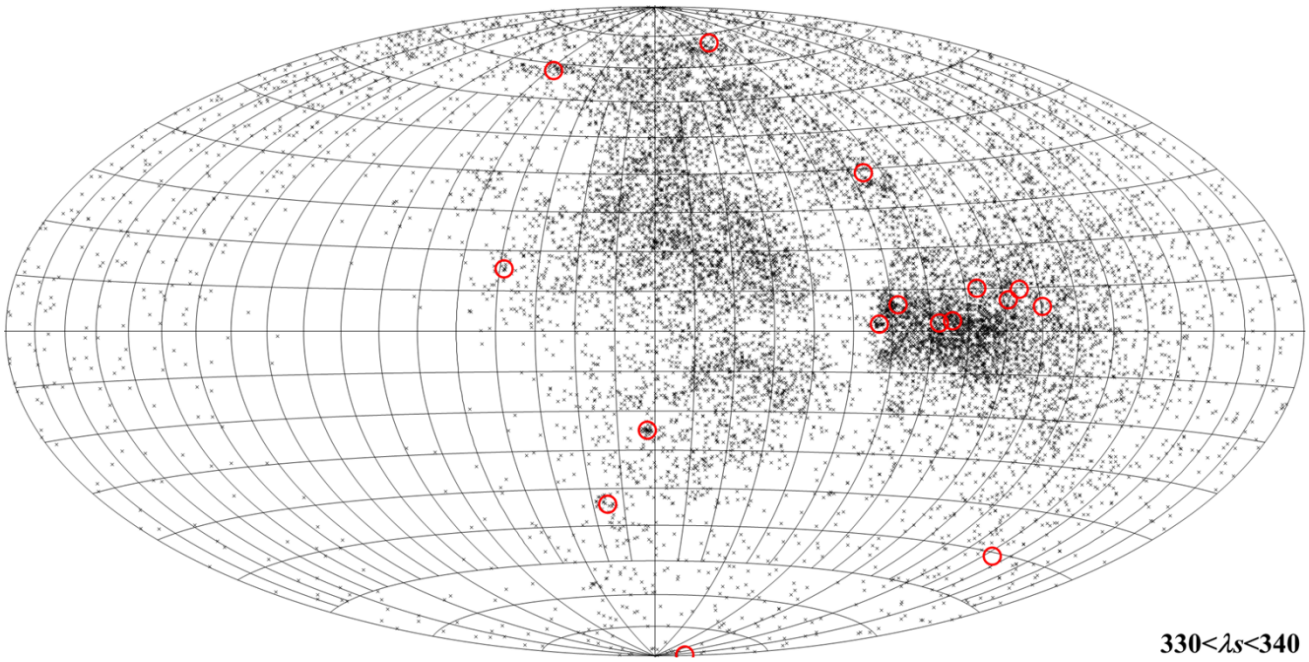

Figure 40 – Radiant distribution obtained by the Global Meteor Network during the interval 330° < $\lambda_{\odot}$ < 340°, the black crosses are the individual GMN radiants, the red circles the radiants according to the IAU shower database[20].

[20] https://www.ta3.sk/IAUC22DB/MDC2022/Roje/roje_lista.php?corobic_roje=0&sort_roje=0

 © eMeteorNews

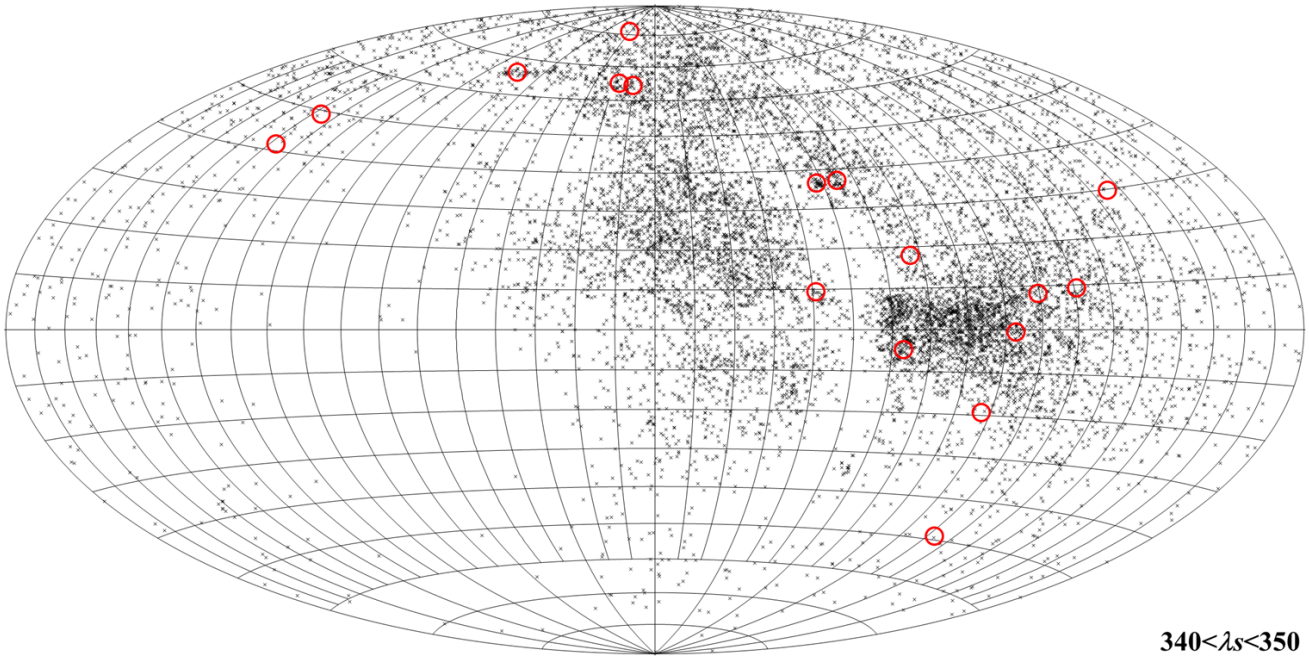

Figure 41 – Radiant distribution obtained by the Global Meteor Network during the interval 340° < $\lambda_\odot$ < 350°, the black crosses are the individual GMN radiants, the red circles the radiants according to the IAU shower database[21].

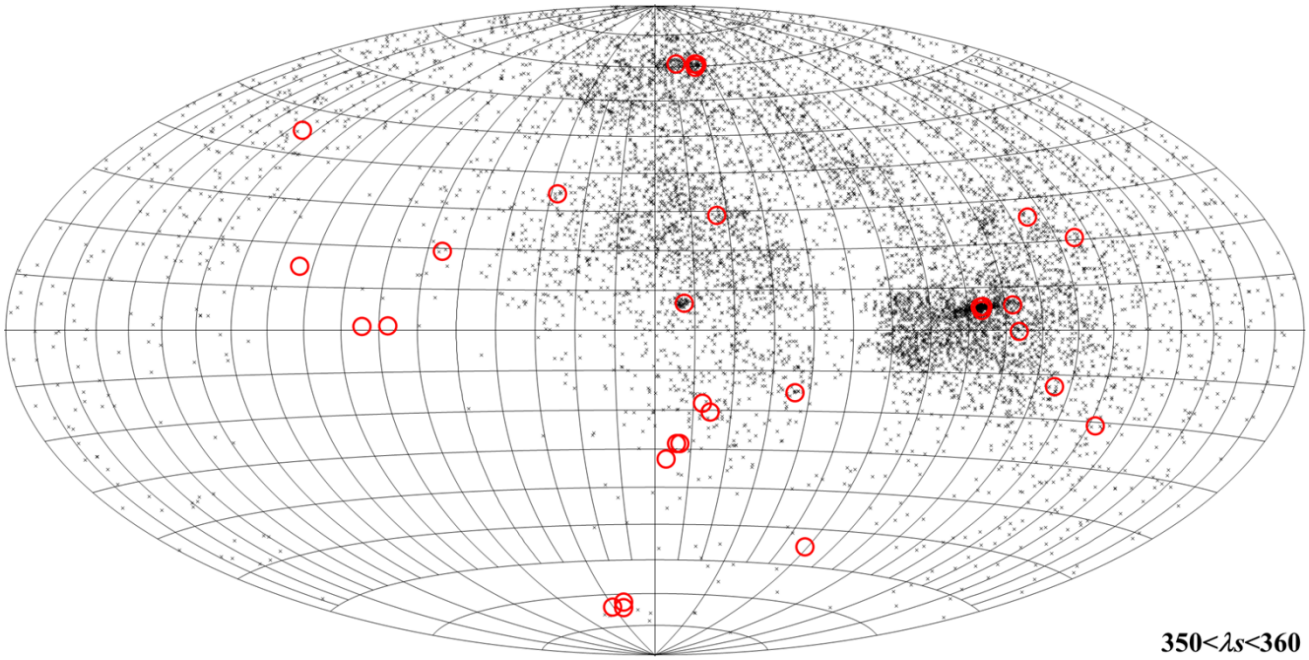

Figure 42 – Radiant distribution obtained by the Global Meteor Network during the interval 350° < $\lambda_\odot$ < 360°, the black crosses are the individual GMN radiants, the red circles the radiants according to the IAU shower database[21].

[21] https://www.ta3.sk/IAUC22DB/MDC2022/Roje/roje_lista.php?corobic_roje=0&sort_roje=0

Perseids in 2023: another outburst around $\lambda_\odot$ 141° and possibly dust trail activity from 68BC detected

Koen Miskotte

Dutch Meteor Society
k.miskotte@upcmail.nl

The visual observations analyzed by the author confirm the enhanced activity reported earlier by radio observers at at $\lambda_\odot = 140.82$. The observations by European observers show relatively many bright Perseids, especially between $\lambda_\odot = 140.57°$ and $\lambda_\odot = 140.77°$. This coincides with the expected activity of the old 68 BC dust trail between $\lambda_\odot = 140.70°$ and $\lambda_\odot = 140.77°$.

1 Introduction

Just as in previous years, 2018 (Miskotte, 2019a; 2019b), 2019 (Miskotte and Vandeputte, 2020a; 2020b), 2020 (Miskotte, 2020a; 2020b; 2020c; 2021) and 2021 (Jenniskens and Miskotte, 2021; Miskotte et al., 2021a; 2021b), an outburst of the Perseids has been observed this year, more than 24 hours after the annual maximum (Roggemans, 2023; Sugimoto and Ogawa, 2023). The IMO Meteor Shower Calendar 2023 also stated that in addition to the chance for a recurrence of the outburst from previous years, there was also a chance of some extra activity due to an old dust trail and a filament. On August 13, 2023 around 3^h UT ($\lambda_\odot = 139.83°$) the Earth would pass through a weak filament according to Peter Jenniskens. And on August 14, 2023 between 01^h00^m and 02^h45^m UT ($\lambda_\odot = 140.74$), Earth would pass through an old dust trail from comet 109P/Swift-Tuttle from 68 BC predicted by Jérémie. Vaubaillon. Forced by circumstances, the author decided to use a limited data set and do some preliminary calculations to see if the features mentioned in the Meteor Shower Calendar were effectively observed.

2 Perseid outburst?

The annual Perseid ZHR_r curve has again been published on the website of the Japanese radio observer Hirofumi Sugimoto. How these *ZHR* calculations are achieved is explained in Sugimoto (2017). The 2023 *ZHR* curve shows that there was an outburst around solar longitude 140.81° with a peak ZHR_r of 160. Radio observations have also been published in Sugimoto and Ogawa (2023). In the meantime, the author had also received a message from Pierre Martin from Canada who wrote: "*I had to drive nearly 1000km (!!!) to find clear skies on August 12–13 further south in Ontario, due to unstable weather. I was in a good position for the traditional maximum and it appears it was a normal level one, or maybe a bit below normal. On Sunday, my friend and I drove all the way back home. I then had clearing skies much closer to home in the evening of August 13–14 after a rainfall. I was aware of the possibility of a dust trail prediction, for the hours before midnight. So, I rushed to go to my dark sky site and setup soon after dark. Even though the radiant was still low I could see a good number of Perseids shooting in different directions without even trying to see them. Some long and bright! Unfortunately, clouds covered the sky and I had to wait until nearly midnight for it to clear again. Then I had only a few minor spells of thin patchy clouds in an otherwise very transparent sky. The meteor activity was very nice the rest of the night. The Perseids continued to do a good appearance with rates approaching one per minute I think and many bright long ones, with a few –3s and a –4. Also had a nice variety of other meteor sources… kappa Cygnids, Aquariids and eta Eridanids. The best meteor was a gorgeous very slow sporadic earth-grazer low in the north, moving from west to east, that reached –4 and lasted 7–8 seconds!! Then it fragmented in 3–4 pieces!!*".

This looks like there was significantly increased Perseid activity.

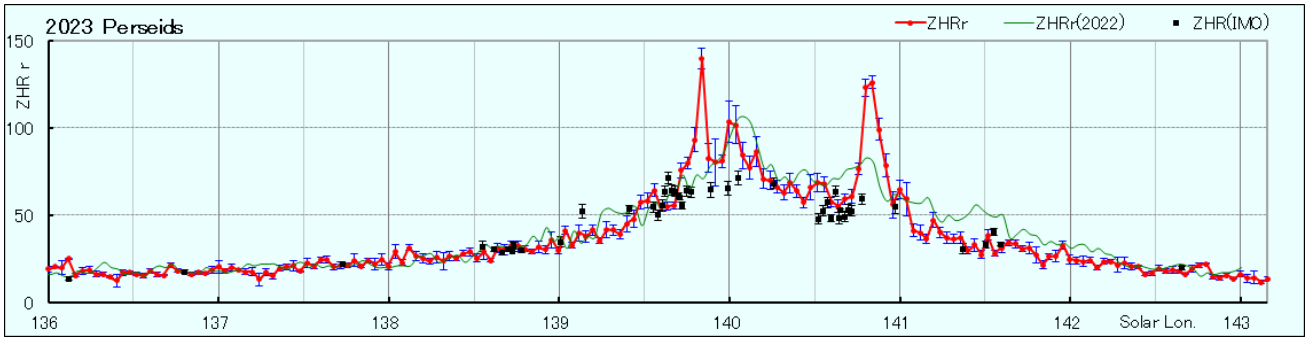

Figure 1 – The Perseid ZHR_r curve[22] from the website of Hirofumi Sugimoto.

[22] http://www5f.biglobe.ne.jp/~hro/Flash/2023/PER/index-e.htm

 © eMeteorNews

3 The used visual data

In the article by Sugimoto and Ogawa (2023) one of the conclusions states: "*The third peak had its maximum with AL(max) = 1.2 at $\lambda_\odot$ = 140.84° (August 14, 4^h30^m UT) (Comp.3). According to Vaubaillon as mentioned in the Meteor Shower Calendar published by IMO that a very old dust trail released in 68 BC may be encountered around $\lambda_\odot$ = 140.74° (between 01^h and 02^h45^m UT on August 14). Although the observed enhancement in activity was later than this prediction, it is possible that this activity was caused by this old trail. However, on the other hand, it is also possible that this third peak is related to the secondary peak around $\lambda_\odot$ = 140.5°–141.6° which was observed in previous years. It is very difficult to know whether or not an old dust trail and an unexpected peak activity are somehow related to the secondary peak observed in past years*".

In short: it is therefore unclear whether the observed radio peak is caused by the old dust trail from 68BC or whether it is the well-known "new" peak around solar longitude 141°. This was the reason to look into the available visual data. The time interval of Pierre Martin's meteor watch is from 03^h08^m to 08^h55^m UT. The IMO website has been checked to see if there were more observers active in Pierre Martin's interval, but unfortunately, he is the only observer active in that period. There is a small amount of overlap at the start of his observations with the observations of Michel Vandeputte and the author from Revest-du-Bion, France. And at the end of his session there is some overlap with observations from Terrence Ross from Texas, US. Because of lack of time the author made an analysis with the observations of Pierre Martin, supplemented with data from Michel Vandeputte (south of France), Koen Miskotte (south of France), Ina Rendtel (Germany), Javor Kac (Slovenia) and Kai Frode Gaarder (Crete, Greece).

The population index *r* was determined hourly based on two-hour periods. The *ZHR* was determined based on periods of 15 to 25 minutes, but some periods of Pierre Martin's data were shorter. A weighted average was used for the final *ZHR* determinations.

4 Another Perseid outburst

Table 1 and *Figure 2* could be created from Pierre Martin's data. This clearly shows that an outburst was going on at $\lambda_\odot$ = 140.82 (14 August 2023 at 04^h00^m UT). The highest *ZHR* is 167 ± 39. Added to this is the radio ZHR_r graph from Sugimoto and Ogawa (2023). This graph was created from radio observations collected by RMOB. Please note: the two observation techniques cannot be compared with each other, but it has only been used here to see if there are similarities. That is clearly the case because the radio observers had their highest activity exactly around Pierre Martin's highest *ZHR*. His observation is therefore a nice confirmation and valuable addition to the radio data.

The population index *r* at the time of the peak was $r[-2;5] = 2.13 \pm 0.26$. This is a fairly normal value for the Perseids and therefore does not indicate old material such as the old dust trail from 68BC should contain. We would expect relatively many bright meteors from an old dust trail and thus a lower population index *r*. It is therefore more likely that this was a new occurrence of the (now almost annual) second maximum around $\lambda_\odot$ = 141.0°. It is also striking that the Perseid activity appears to have increased during Pierre Martin's entire observational session. The high population index *r* at the end of its observation session is mainly due to the many +5 Perseids. *Table 2* provides a comparison between the peaks found in the period 2018–2023 in terms of *ZHR* and population index *r*.

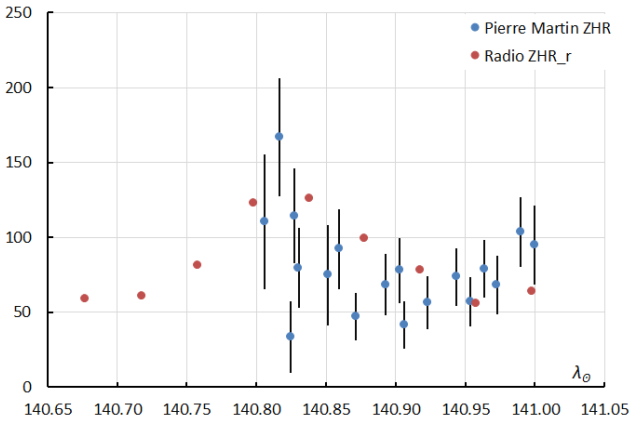

Figure 2 – Observed visual *ZHR* of Pierre Martin compared to the radio ZHR_r based on RMOB data for August 13–14, 2023.

Table 1 – Observed *ZHR* values by Pierre Martin from Canada, all on 2023 August 14.

Time UT	$\lambda_\odot$ (°)	ZHR	±
3.733	140.806	110	45
4.000	140.817	167	39
4.200	140.825	34	24
4.270	140.827	114	32
4.345	140.830	80	27
4.867	140.851	75	33
5.067	140.859	92	27
5.375	140.872	47	16
5.908	140.893	68	21
6.158	140.903	78	22
6.242	140.906	42	16
6.658	140.923	56	18
7.175	140.944	73	19
7.425	140.954	57	17
7.675	140.964	79	19
7.900	140.973	68	20
8.325	140.990	104	23
8.575	141.000	95	26

Table 2 – Comparing the outbursts at $\lambda_\odot = 141°$ during the years 2018, 2019,2020, 2021, 2022 and 2023.

Visual				Radio			
Year	$\lambda_\odot$	*ZHR*	Pop. Index *r*	Year	$\lambda_\odot$	ZHR_r	Remarks
2018	140.935	86 ± 6	r[-2;5] 2,06 ± 0,05	2018	~	~	No outburst in radio data
2019	~	~	~	2019	141.020	81 ± 4	No visual observations
2020	140.632	80 ± 15	r[-2;5] 2,31 ± 0,28	2020	140.612	84 ± 10	
	140.711	91 ± 16	r[-2;5] 2,49 ± 0,30		140.772	80 ± 6	
	140.765	91 ± 17	r[-2;5] 2,76 ± 0,28				
2021	141.489	195 ± 16	r[-1;5] 2,76 ± 0,22	2021	140.495	220 ± 20	
2022	~	~	~	2022	140.800	80 ± 15	Outburst?
2023	140.820	167 ± 39	r[-2:5] 2,13 ± 0,26	2023	140.82	126 ± 5	
			r[-1;5] 2,35 ± 0,27				

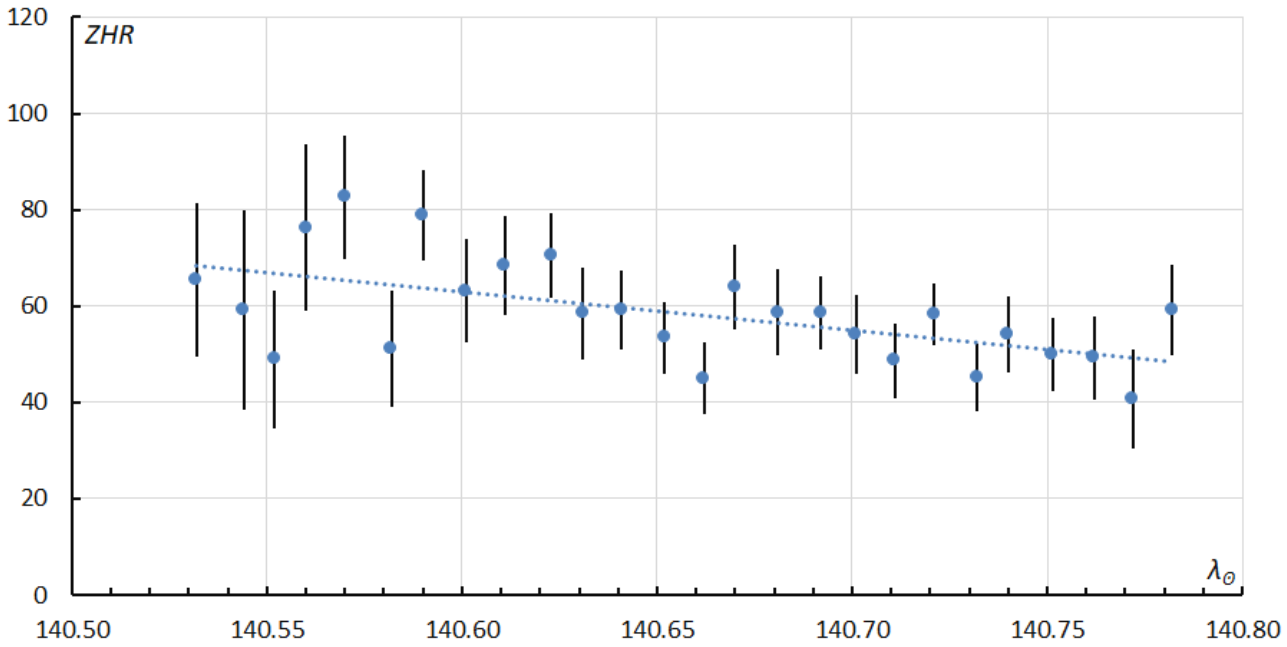

Figure 3 – Perseid activity as observed from Europe during the night of August 13–14, 2023.

Table 3 – Population index *r*[-2;5] Perseids during August 13–14, 2023.

Date	Time UT	$\lambda_\odot$ (°)	*r*[-2;5]	±
13/08/2023	21.25	140.547	2.05	0.14
13/08/2023	22.00	140.577	1.98	0.12
13/08/2023	23.01	140.617	1.93	0.11
14/08/2023	0.05	140.659	1.87	0.11
14/08/2023	1.10	140.701	1.88	0.1
14/08/2023	1.87	140.731	1.97	0.11
14/08/2023	2.75	140.767	2.04	0.23
14/08/2023	4.54	140.838	2.13	0.26
14/08/2023	5.54	140.878	2.24	0.28
14/08/2023	6.55	140.919	2.83	0.27
14/08/2023	7.50	140.957	3.00	0.22
14/08/2023	8.23	140.986	3.00	0.27

But the question remains, was there extra Perseid activity from the 68 BC dust trail of 109/P?

We assume that the peak at $\lambda_\odot = 140.82°$ (14 August 2023 at 04^h00^m UT) may have been caused by the same structure that was active in 2018, 2019 and 2021. The question then remains: was the dust trail from 68 BC active? According to J. Vaubaillon, the dust trail was expected on August 14, 2023 between 01^h00^m and 02^h45^m UT (between $\lambda_\odot = =140.70°$ and $\lambda_\odot = =140.77°$) and ideal for Europe. Calculations based on the data of the five European observers mentioned above resulted in *Table 3* and *Figure 3*. The *ZHR* plot shows a decreasing activity, see the trend line. This is something you would expect in a "normal" Perseid year. *ZHR*'s in de order of 60–80 slowly decreasing to 50–60. That seems "slightly" on the high side for this period.

What is striking is the low population index *r* (see *Table 3*) in the period from $\lambda_\odot = 140.57°$ to $\lambda_\odot = 140.77°$. This also covers the interval that Vaubaillon specifies for the 68BC dust trail between $\lambda_\odot = 140.70°$ and $\lambda_\odot = 140.77°$, see *Table 3*. The five observers also reported many bright Perseids on this night, especially in the second part. And four of the five also reported multiple Perseid fireballs in the –3 to –6 class.

© eMeteorNews

In *Figure 4* we see all *ZHR* values combined with the population index *r* in one graph. Both *ZHR* and population index as observed from Europe and US agree nicely with each other in terms of progression. With regard to the *ZHR*, it seems as if Europe may have just caught the start of the structure that has already been seen in 2018 and beyond (see the last data point in *Figure 2*). The orange points indicate the population index *r*[–2;5] based on *Table 3*. The conclusion of all this is that the dust trail of comet 109P/Swift-Tuttle from 68 BC appears to have been active before and during the predicted interval of J. Vaubaillon. Perhaps a slightly higher *ZHR* caused solely by the bright Perseids. This in combination with the annual activity gave a somewhat lower population index *r* than normal. And that is exactly what we would expect from such an old dust trail.

Table 4 – ZHR of the Perseids over Europe on the night of August 13–14, 2023 based on data from 5 visual observers.

Day	Time UT	$\lambda_\odot$ (°)	*ZHR*	±
13	20.63	140.522	36	16
13	20.88	140.532	65	21
13	21.18	140.544	59	14
13	21.38	140.552	49	17
13	21.59	140.560	76	13
13	21.83	140.570	83	12
13	22.13	140.582	51	9
13	22.31	140.590	79	11
13	22.61	140.601	63	10
13	22.87	140.611	69	9
13	23.15	140.623	70	10
14	23.35	140.631	59	8
14	23.62	140.641	59	8
14	23.88	140.652	53	7
14	0.13	140.662	45	9
14	0.33	140.670	64	9
14	0.61	140.681	59	8
14	0.88	140.692	59	8
14	1.10	140.701	54	8
14	1.35	140.711	49	6
14	1.62	140.721	58	7
14	1.88	140.732	45	8
14	2.09	140.740	54	8
14	2.36	140.751	50	9
14	2.63	140.762	49	10
14	2.88	140.772	41	9
14	3.13	140.782	59	12

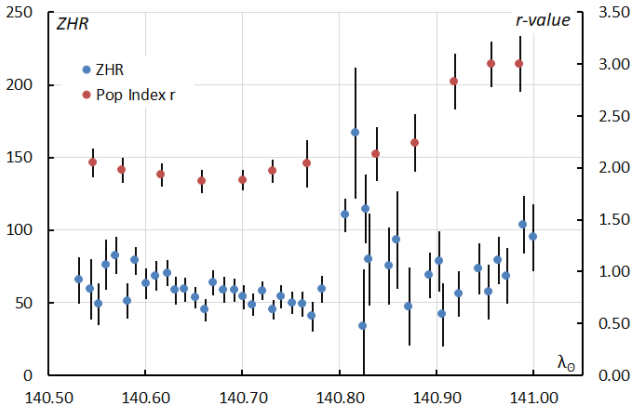

Figure 4 – Perseids *ZHR* and population index *r* between 13 August 20^h UT and 14 August 09^h UT.

5 Conclusion

The Perseid outburst observed by radio observers (Sugimoto and Ogawa, 2023) around $\lambda_\odot = 140.84°$ has also been confirmed by the visual observations of Pierre Martin. His data shows a maximum at $\lambda_\odot = 140.82°$ with a ZHR of 167 ± 39 and population index $r = 2.13$. This is in good agreement with the radio data. Most likely this was the occurrence of the new peak around $\lambda_\odot = 141°$ showing a similar or lower population index *r*.

The dust trail of comet 109P/Swift-Tuttle from 68 BC may also have been active. The observations of five European observers show relatively many bright Perseids, especially between $\lambda_\odot = 140.57°$ and $\lambda_\odot = 140.77°$. This coincides with the expected activity of the old 68 BC dust trail between $\lambda_\odot = 140.70°$ and $\lambda_\odot = 140.77°$. The strikingly high number of very faint Perseids at the end of Pierre Martin's session is also interesting enough for additional research.

Acknowledgment

Thanks to all observers who submitted data to the IMO website. This analysis used data from *Kai Frode Gaarder, Javor Kac, Pierre Martin, Koen Miskotte, Ina Rendtel* and *Michel Vandeputte*. A thank you for *Hiroshi Ogawa* and *Hirofumi Sugimoto* for providing the radio data, *Carl Johannink* and *Michel Vandeputte* for reading and commenting on this article.

References

Jenniskens P., Miskotte K. (2021). "Perseids meteor outburst 2021". *eMetN*, **6**, 260–261.

Miskotte K. (2019a). "Perseïden 2018: een analyse van de visuele waarneemdata". *Radiant*, **41**, 27–35.

Miskotte K. (2019b). "The Perseids in 2018 analysis of the visual data". *eMetN*, **4**, 135–142.

Miskotte K., Vandeputte M. (2020a). “Perseïden 2019 Opnieuw een piek in activiteit rond zonslengte 141,0?”. *Radiant*, **42**, 100–103.

Miskotte K., Vandeputte M. (2020b). “Perseids 2019: another peak in activity around solar longitude 141.0?”. *eMetN*, **5**, 25–29.

Miskotte K. (2020a). “Perseïden 2020: voor de derde keer een uitbarsting rond zonslengte 141° graden?”. *Radiant*, **42**, 87–89.

Miskotte K. (2020b). “Perseids 2020: again, enhanced Perseid activity around solar longitude 141?”. *eMetN*, **5**, 395–397.

Miskotte K. (2020c). “Perseids 2020 revisited”. *Radiant*, **42**, 162–163.

Miskotte K. (2021). “Perseids 2020 revisited”. *eMetN*, **6**, 29–30.

Miskotte K., Sugimoto H., Martin P. (2021a). “The big surprise: a late Perseid outburst!”. *eMetN*, **6**, 517–525.

Miskotte K., Sugimoto H., Martin P. (2021b). “De Perseïden uitbarsting van 14 augustus 2021”. *Radiant*, **43**, 51–58.

Roggemans P. (2023). “Unusual Perseid activity in 2023”. *eMetN*, **8**, 288–289.

Sugimoto H., Ogawa H. (2023). “Perseids 2023 by worldwide radio meteor observations”. *eMetN*, **8**, 285–287.

Sugimoto H. (2017). “The New Method of Estimating ZHR using Radio Meteor Observations”. *eMetN*, **2**, 109–110.

 © eMeteorNews

On “blue” trails of meteors

Alexandra Terentjeva[1] and Ilya Kurenya[2]

[1] **Institute of Astronomy of the Russian Academy of Sciences, Moscow, Russia**
ater@inasan.ru

[2] **Institute for the Humanities and IT, Moscow, Russia**
luisito@inbox.ru

During observations of meteors in high-altitude conditions in 1947 I.S. Astapovich discovered “blue” trails of meteors (Astapovich, 1947; 1951). This phenomenon remained, unfortunately, unknown in meteor astronomy for 76 years. The article acquaints meteor researchers with this phenomenon and sets objectives for its study.

1 Introduction

Our article aims to draw attention to the phenomenon of “blue” trails of meteors in meteor astronomy. It was discovered by I.S. Astapovich 76 years ago (Astapovich, 1947, 1951) and remained unknown in the scientific world.

2 Detection of “blue” meteor trails

In September 1947, I.S. Astapovich made visual observations of meteors from the site of the High-Altitude Station of the Astrophysical Laboratory of the Turkmen Branch of the USSR Academy of Sciences in the Central Kopet Dagh, Kheirabad plateau at H = 2234m, 52km from Ashkhabad. The dust atmosphere lies here beneath the feet on average 1.3km lower, with the transparency coefficient of 0.957, and at zenith distance of $Z \leq 50°$ usually visible stars are of 7.0m–7.2m (Astapovich, 1947).

Under these conditions, I.S. Astapovich was able to discover a new phenomenon, which he describes as follows (Astapovich, 1951): “*sometimes in the pre-dawn hours, the usual appearance of meteors was preceded by a faint bluish glow. The phenomenon resembled the flight of a meteor making a very pale ionization trail. The meteor itself remained invisible and appeared in its usual form only a few degrees later, after the disappearance of the “blue” trail. This “blue” trail was brighter than the sky background by 30–50% or more, being quite wide (up to 1°–2° at zenith); it seemed delicately radiant, as if “furry”,*

Figure 1 – The International Conference “Physics and Dynamics of Small Bodies of the Solar System”, dedicated to the 90th anniversary of the birth of the outstanding astronomer and founder of Soviet meteor astronomy Prof. I.S. Astapovich. The conference was organised by the Astronomical Observatory of the Kiev National University on December 17–19, 1998, and was held at this observatory (Photo from the personal archive of A.K. Terentjeva).

and disappeared within 1–2 seconds, turning into a pale solid line. Under plain (valley) conditions, despite repeated attempts in 1948–1951, we never managed to see such "blue" trails, whereas in Kheirabad in 1948 they were again seen with some meteors. Probably, the emission of "blue" trails is rich in short waves which are absorbed in the lower atmosphere. With the height of the appearance of meteors with "blue" trails taken as H_1 = 110km and their disappearance height taken as H_2 = 75km, the localization area of "blue" trails appears to be within H = 160–120km. Their linear width is calculated as 2–5km. In 1947–1948 we provided basic observations of meteors with binoculars and astronomical binoculars. Several good observations are given among 57 meteors for a group of very high (H = 160–120km) but weak meteors which are of a somewhat unusual appearance. One of them was observed on August 4, 1948, from 4 (!) locations, and all observations were consistent. Summarizing these data, supplemented by observations from 1949–1950 (trigonometric determinations of 350 meteor heights on bases of 22.1km, 24.0km, 38.0km, 46.2km), carried out at altitudes of up to 2700m, we must conclude that in some cases conditions may arise, conducive to the formation of the "blue" trails described above. The latter may probably occur mainly as a result of ionization of air by short-wave emission from a meteor or (to a much lesser extent) by the impact of ejected air particles. The third type of meteor ionization, thermal, is yet irrelevant here.

For the sake of brevity, we suggest the name of "blue" trail of meteor for this phenomenon".

Figure 2 – The International Conference "Physics and Dynamics of Small Bodies of the Solar System", dedicated to the 90th anniversary of the birth of the outstanding astronomer and founder of Soviet meteor astronomy Prof. I.S. Astapovich. The conference was organised by the Astronomical Observatory of the Kiev National University on December 17–19, 1998, and was held at this observatory (Photo from the personal archive of A.K. Terentjeva).

Further, I.S. Astapovich (1947) reports that observations of meteors carried out under the above-mentioned high-altitude conditions gave in fact somewhat unexpected results. For example, the path lengths of λ of ordinary 2m–5m meteors are 80–100% longer than those observed under "plain" conditions. The relative number of weak meteors is very high, which makes their distribution curve significantly different from usual. These meteors belong to a multitude of tertiary radiants, totaling several dozens, acting simultaneously. Weak meteors strongly increase the absolute hourly number *nh*. For example, on September 22, 1947, between 0^h00^m–0^h30^m UT $nh = 40$ versus normal $nh = 18$–20 in Ashkhabad. The number of telescopic meteors up to 10m seems to be almost double.

3 Conclusion

What problems can be put forward for study of the "blue" trails of meteors? First of all, basic photographic observations alongside visual observations are needed to determine the exact heights of the appearance and disappearance of "blue" trails and a number of other characteristics. It is necessary to find out the dependence of the appearance of "blue" trails on stellar magnitude, velocity, etc. Of course, it would be good to understand what conditions may arise in some cases in the atmosphere, contributing to the formation of "blue" trails.

Further, it is also necessary to know the diurnal and annual variations for "blue" trails of meteors. As for the diurnal and annual variations for ordinary gas trails of meteors, this question is studied well enough (Astapovich, 1966). The following data can be provided according to I.S. Astapovich (1958): "*It follows from the Ashkhabad series of observations, that in spring and in the morning, trails occur "less willingly", and those which occur keep intact less and their trail is less lasting. Before and after midnight, trails are twice as rare, with the optimum falling between 11 p.m. and 3 a.m. During the year, the largest number of trails falls in August, and the smallest number in February-March. This is the influence of large showers. Taking them into account, we still find the annual maximum in autumn and the minimum in spring. It is not only the number of trails that experiences diurnal and annual variations, but also their duration of their radiance, drift velocity, and other characteristics*".

Figure 3 – The International Conference "Physics and Dynamics of Small Bodies of the Solar System", dedicated to the 90th anniversary of the birth of the outstanding astronomer and founder of Soviet meteor astronomy Prof. I.S. Astapovich. The conference was organised by the Astronomical Observatory of the Kiev National University on December 17–19, 1998, and was held at this observatory (Photo from the personal archive of A.K. Terentjeva).

© eMeteorNews

In conclusion, we would like to express the hope that the "blue" trails will find their enthusiastic observers of meteors under high-altitude conditions and that the mere fact that they will see them will be a step towards their study.

Acknowledgment

This paper was translated into English by *I. Kurenya*.

The authors thank *Paul Roggemans* for his efforts enabling the preparation and publication of this paper.

References

Astapovich I. S. (1947). "Some results of meteor observations in high-altitude conditions". *Astron. Tsirk. AN SSSR*, **No. 67**, 4–5. (In Russian).

Astapovich I. S. (1951). "On "blue" trails of meteors". *Astron. Tsirk. AN SSSR*, **No. 121**, 4–5. (In Russian).

Astapovich I. S. (1958). "Meteor phenomena in the Earth's atmosphere". Fizmatgiz. (In Russian).

Astapovich I. S. (1966). "Some results of visual observations of meteor trails". Results of researches of international geophysical projects: Meteor Investigations. No. 1. Publishing House "Nauka", Moscow, pages 7–61. (In Russian).

Figure 4 – The International Conference "Physics and Dynamics of Small Bodies of the Solar System", dedicated to the 90th anniversary of the birth of the outstanding astronomer and founder of Soviet meteor astronomy Prof. I.S. Astapovich. The conference was organised by the Astronomical Observatory of the Kiev National University on December 17–19, 1998, and was held at this observatory (Photo from the personal archive of A.K. Terentjeva).

Fireball of 22 December 2022 over North Italy

Enrico Stomeo and Stefano Crivello

IMG/UAI-Sezione Meteore, IMO Video Meteor Network, Italy
stom@iol.it

A brilliant meteor, captured by 4 video cameras, was observed in northern Italy on 22 December 2022 at 03^h39^m UT. The trajectory of the meteoroid was determined together with its orbit in the Solar System.

1 Introduction

This meteoroid entered the atmosphere on 22 December 2022 at $03^h39^m46^s$ UT between the Adamello and Stelvio national parks with a trajectory roughly from SSE to NNW (mean azimuth N_154°E), producing a spectacular bolide of video magnitude –8 or so. The event was observed from all surrounding regions that had no haze or cloud cover at the time.

The brilliant meteor showed a progressive increase in brightness, revealing a persistent trail even before halfway, as well as two almost consecutive explosions.

2 Observational data

Four stations filmed the event[23], one from our monitoring network Italian Meteor Group/ UAI-Sezione Meteore[24], two from the SAT Società Astronomica Ticinese and a webcam from the Alleghe cableway station at Piani di Pezzé (*Figures 1 to 4*).

Figure 1 – © Maurizio Carli – Italian Meteor Group – UAIsm / IMO Video Meteor Network.

Figure 2 – © Stefano Sposetti – Beobachtungsstation Locarno (Switzerland).

Figure 3 – © Stefano Sposetti – Astronomical Observatory of Gnosca (Switzerland).

[23] Video station BMH2, Obs: Maurizio Carli (mt Baldo, VR). Video station GNO, Obs: Stefano Sposetti (Gnosca, Switzerland). Video station LOC, Obs: Stefano Sposetti (Locarno, Switzerland). Webcam Alleghe cableways at Piani di Pezzé (BL).

[24] Italian Meteor Group – UAI Sezione Meteore http://meteore.uai.it.

 © eMeteorNews

Figure 4 – © Webcam of Alleghe cableways at the Pezzè plateau (courtesy of Giuseppe De Donà).

3 The triangulation results

The image in *Figure 5* shows the ground projection of the atmospheric path of the fireball between the two yellow dots as well as the viewing directions of the individual stations. A dotted line shows the possible continuation of the trajectory, after the meteor's luminosity had ended.

An evaluation of the available data shows that the meteoroid was observed entering the atmosphere with an average speed of 14.6 km/s, an average inclination of 30.5°, and that the meteor became visible at an altitude of 84. 4 km above the mountains 12.6 km north of Rovereto (46.01°N, 11.04°E), ending at a height of about 28.6 km above the mountains 1.4 km west of Lago della Muta (46.75°N, 10.51°E), covering a trajectory length of about 128 km.

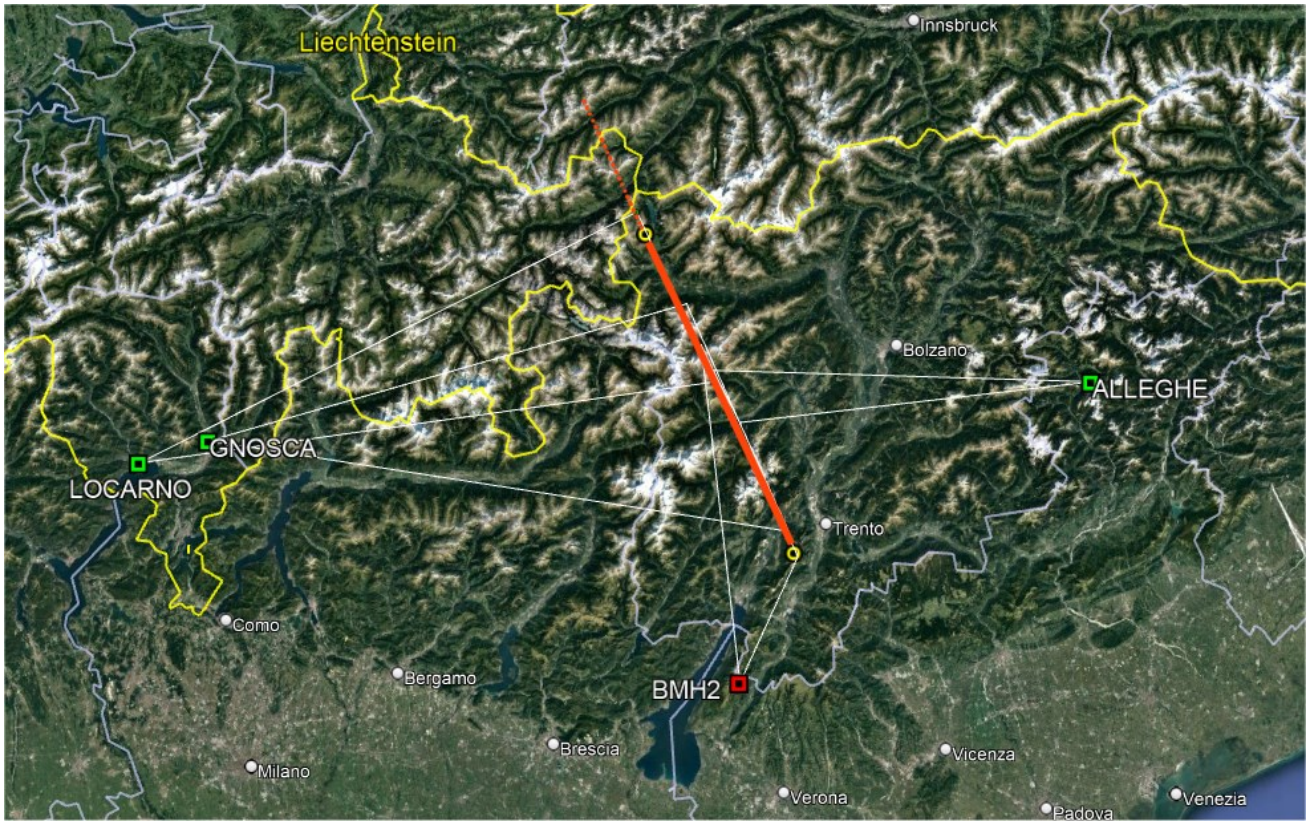

Figure 5 – Ground projection of the bolide's atmospheric path.

It can be seen in *Figure 5* that none of the four stations filmed the entire trail. BMH2 captured the first part of the atmospheric trajectory up to about halfway for 4.28 seconds. Being close, it saw the persisting trail begin at about 79 km height and the gradual increase in brightness culminating in two almost consecutive flares at about 60 and 59 km height. At an altitude of about 51 km, the fireball exited the camera field after having moved over a distance of 64 km.

A decisive contribution to the analysis of this bolide was made by the two Swiss stations, as their video data provided information on the final phase of the meteor, but unfortunately not on the frame-by-frame values of the velocity. Thus, only the deceleration (about 2 km/s) deduced from BMH2 up to about 52 km above the ground was evaluated, but not the lower part of the final atmospheric path. GNOSCA saw the fireball start a few moments after BMH2, following the path for 4.88 seconds until it left the field of view, when the meteor was about 46 km high. LOCARNO, on the other hand, filmed the bolide for 5.02 seconds from about halfway, i.e., from entering the field of view, to the end of the meteor at a height of 28.6 km. The ALLEGHE cableway webcam filmed the bolide from the east, only in its central part for about 18 km.

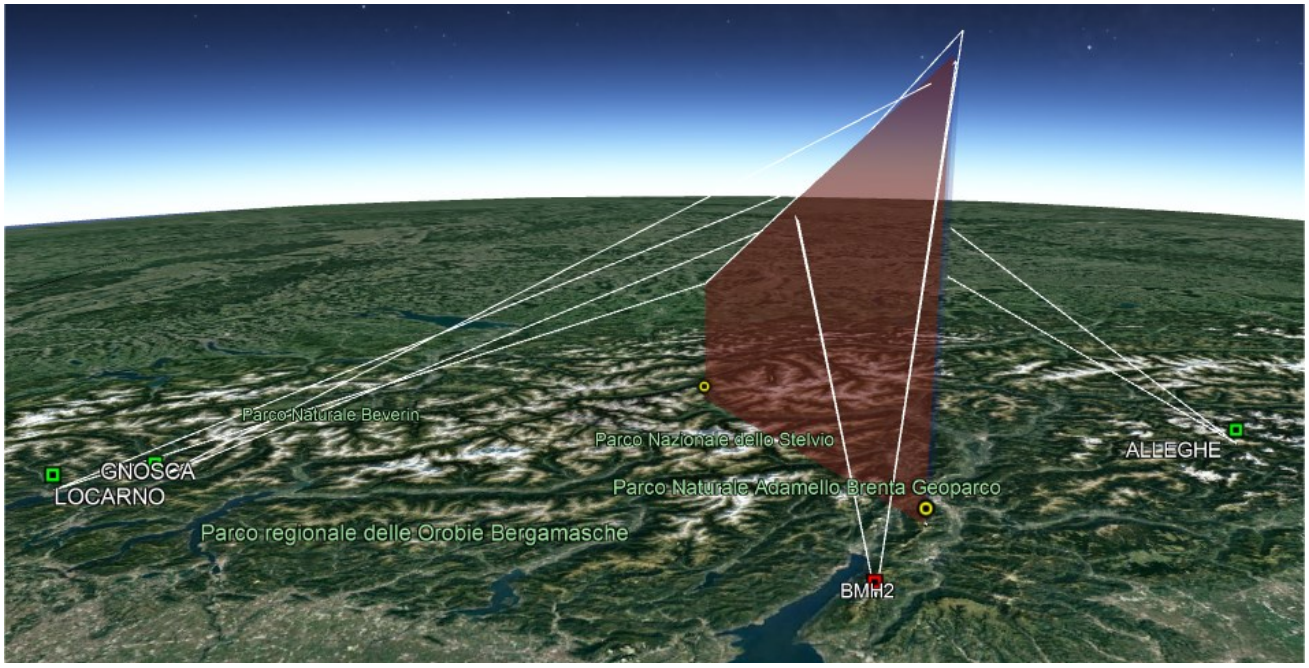

Figure 6 – Geometry of the bolide's trajectory as seen from the south.

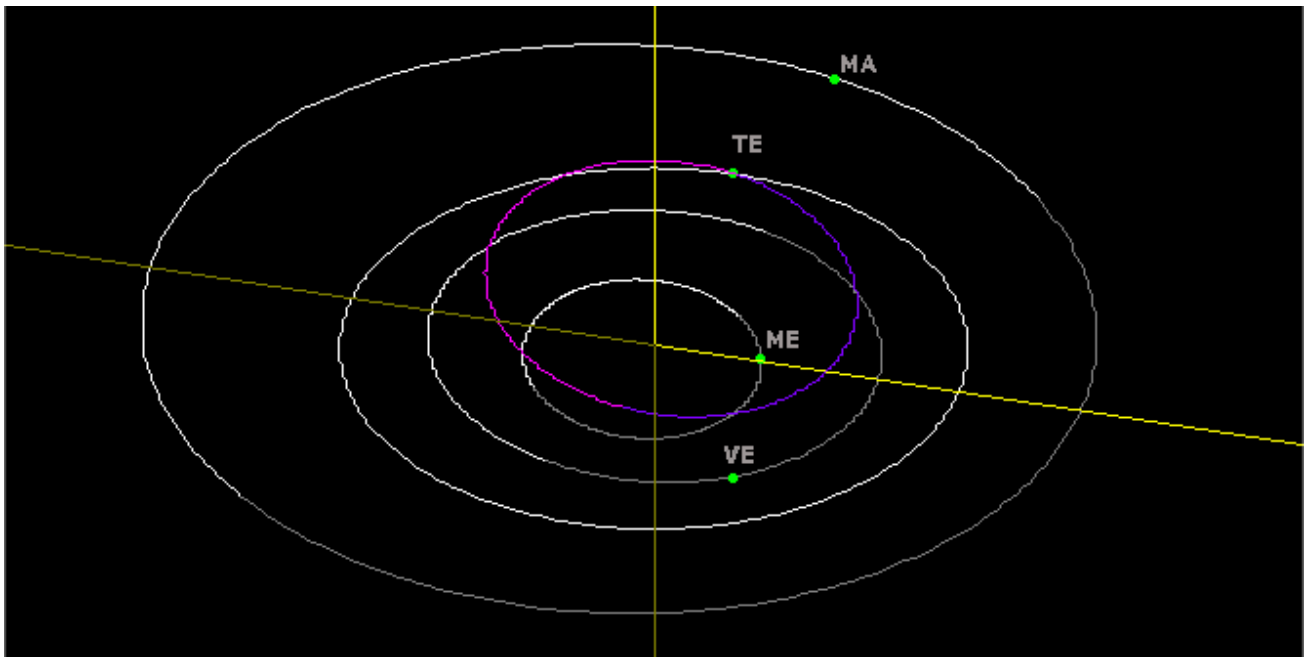

Figure 7 – The most probable orbit of the meteoroid resulting from the best triangulation.

4 Orbital elements

The best solution indicates the radiant at $\alpha = 178.3°$ and $\delta = –10.2°$ (eq.2000) between the constellations of Virgo and Crater. No association with known meteor showers could be established. The other most relevant values describing the orbit of the meteoroid are summarized below, based on the available data: geocentric radiant and velocity: $\alpha_g = 181.6°$ $\delta_g = –22.6°$ and $v_g = 9.2$ km/s, radiant heliocentric radiant and velocity $\alpha_h = 355.8°$ $\delta_h = –8.2°$ and $v_h = 22.1$ km/s. Orbital elements (*Figure 7*): $a = 0.673$ AU, $q = 0.361$ AU, $e = 0.465$, $\omega = 185.01°$, $\Omega = 89.96°$, $i = 8.28°$ (eq.2000). A comparison of the orbit found with that of known cometary and asteroidal objects indicates a possibility ($D_{SH} = 0.13$, Southworth and Hawkins (1963)) of similarity with the orbit of asteroid 348306 (2005 AY28).

Acknowledgements

Special thanks to *Giuseppe De Donà* for providing the Alleghe webcam image and to *Alberto Latini* for contacting the stations across the border.

References

Ceplecha Z. (1987). "Geometric, dynamic, orbital and photometric data on meteoroids from photographic fireball networks". *Bull. Astron. Inst. Cz.*, **38**, 222–234.

Southworth R. B. and Hawkins G. S. (1963). "Statistics of meteor streams". *Smithsonian Contributions to Astrophysics*, **7**, 261–285.

 © eMeteorNews

A successful Perseid campaign from Revest-du-Bion, Provence, Southern France

Koen Miskotte and Michel Vandeputte

Dutch Meteor Society
k.miskotte@upcmail.nl

The authors present a report on their 2023 observing campaign in Southern France.

1 Introduction

On August 14, 2016, just after 03^h UT, the two authors shaked hands at Revest-du-Bion to congratulate each other on the fantastic observing results for the Perseids that year (Miskotte and Vandeputte, 2016). The August 11–12 Perseid outburst was successfully observed with a maximum ZHR of 330. But almost all other nights had very good observing conditions. The expectation was that we would soon observe again in Revest-du-Bion in the following years. However, in 2018 it became Aubenas-les-Alps (Miskotte, 2018), where the Perseids were observed by both authors, together with Jos Nijland, Carl Johannink and Casper ter Kuile. In the following years, only Michel stayed in Revest with varying degrees of success. Koen was unable to participate in those years due to various circumstances, including Covid restrictions.

By the way, this year marks exactly ten years since the first Perseid campaign was organized at Revest-du-Bion. In 2013 the team consisted of Casper ter Kuile, Sietse Dijkstra, Peter van Leuteren and the first author. Simultaneous video observations were made with Klaas Jobse using 2 × 2 CAMS systems that filmed more than 600 meteors simultaneously.

2 Perseids 2023: to go or not to go?

This year too, it was far from certain whether there would be an observing campaign in Revest-du-Bion during the Perseids. Fortunately, Michel confirmed at the end of June that they would go. For Koen this meant figuring out how to get there. That was not easy, it now turned out to be difficult to book something between the train stations of Brussels Midi and Marseille St Charles via the Thalys (only on Saturdays) or the French TGV. Via Paris is not an option because of the hassle between Gare du Nord and Gare de Lyon. After some deliberation, a plane was booked to Marseille Airport and from there by train via Marseille St Charles to Manosque. Although the flight takes just less than two hours, the entire journey takes just as long as the TGV. Checking in, collecting luggage, waiting, transferring to the train: in total it is also 12 hours of travel time. There were also works on the railway around Amsterdam, so the author decided at the last minute to travel to Amsterdam on Monday evening and book a hotel at Schiphol. The flight to Marseille Airport was on Tuesday.

3 Perseids 2023

And so, the first author got off the train in Manosque on Tuesday, August 8 around 6 p.m. local time, where he was met by Michel, Inneke, Laurien and Boris. An hour's drive took us to familiar terrain: Domain Pierre Rousse near Revest-du-Bion.

The house has been considerably renovated, the shower facility upstairs was renovated and even included a room with an in-suite shower. And there was also a new built swimming pool at the house, which was used eagerly from the first day on! The first night was canceled, the Moon was still quite disturbing in the second part of the night and we wanted to get some rest before the observational marathon would start.

The weather in Provence was very stable during this period, sometimes (a lot) of cirrus during the day, but dissolving in the evening. So many clear nights, but just not the top-notch Provencal skies. But we have absolutely no complaints about limiting magnitudes of 6.6! The stable weather up to and including the Perseid maximum was due to an extension of the continental high-pressure area over the extreme southeast of France. The recurring pattern during the night was: a calm start, a weak northerly wind halfway through the night and then changing further to the east at dawn and then the best SQMs were achieved. This is due to an increasingly drier air supply during the night. This was also the dominant pattern at night in 2021, in case no Mistral was present.

So, the first observations were done in the night of August 9–10.

© eMeteorNews

Figure 1 – The Pierre Rousse domain, 3 km south of Revest du Bion with the large field where we carried out the meteor observations. Good views in all directions, except in the northern direction because of a group of high poplars.

2023, August 9–10

We took it easy the first night. In the evening the all-sky camera was set. This is a new all-sky system that is equipped the same way as the all-sky camera EN908 at home of Koen in Ermelo: a Canon 6D with a Sigma 8 mm F2.8 fish-eye lens with built in Liquid Crystal Shutter. But this one does not run on mains power but on an Omegon GP09 battery. The controller of the LC shutter, camera and lens heating can operate for more than 12 hours on a full battery, as has been extensively tested in Ermelo. But the test in the field failed: when I checked the all-sky later that night at 22^h30^m UT, it appeared not to be working. The first shot went well, but as soon as the new recording started, the camera and shutter failed to work (working on the USB connections of the battery), but the lens heating on a cigarette lighter connection continued to work. Koen could not and did not want to solve this in the field, so only visual observations were made this night. That is the biggest priority for both authors.

The authors are always observing 15 meters apart, so that they cannot disturb each other. Communication at night remains very limited to: "*did you see that fireball?*" or we can talk during a short break. Observations were done between 20^h48^m and 01^h02^m UT. After that time the Moon became too disturbing. The limiting magnitude slowly decreased from 6.6 to 6.4. Thanks to the strong contrast of the night sky, meteors remained easily visible. There were also some bright meteors, at 21^h18^m UT a beautiful green-blue –2 Capricornid flashed through Aquila and at 23^h18^m UT a –2 Perseid in Pisces. Both observers also saw a short flash of light in the sky. This appeared to come from a Perseid fireball that was coincidentally seen by the domain administrator Jerome and was also recorded by the FRIPON network.

It was a restless night, the domain owner's two dogs, Pepsi and Maxi, barked almost continuously all night. Besides that, also sounds of owls, pigs and deer (burring) were heard. Koen and Michel counted a total of 148 meteors. In addition to the Perseids, some Southern delta Aquariids (SDA) and Capricornids (CAP) were also seen.

2023, August 10–11

After a day with some cirrus clouds, these clouds dissolved in the evening, a situation that often occurred in Provence this year. The all-sky was now connected to the battery slightly differently and the daytime tests seemed to be going well. Unfortunately, the same problem happened again in the evening, a power failure on the USB connections. So, again no all-sky camera this night. We started a little later and continued a little longer, namely from 22^h03^m to 02^h10^m UT, because the Moon is now interfering a little later and a little less. It is a warm and especially humid night. Lavender scents can be smelled and in addition to the usual sounds (but Pepsi and Maxi were quiet that night), bats could also be seen and heard. The sky is a bit hazy, but a weak mistral later blows the haze away and the sky became rich in contrast. It yielded increasing SQM values up to 21.4 even with a rising Moon. The *Lm* dropped from 6.7 to 6.4 that night. Koen and Michel counted a total of 184 meteors. Again, some bright meteors were seen: the session started well with a –3 Perseíd with three flares in the famous square of Pegasus. At 00^h41^m UT a beautiful –2 sporadic meteor appeared leaving a bright blue persistent train of 3 seconds. No Capricornids were seen, until within a few seconds two Capricornids appeared in line with each other of +3 and 0. The latter was green-blue and had a long wake. All in all, a nice meteor watch!

2023, August 11–12

Expectations weren't high for this night. The Perseid maximum would occur during the day on August 13th, so the numbers would still be limited. The all-sky camera finally worked fine all night after a new intervention. The camera was connected separately to a second battery and the problem seemed to be solved. Once again, the start of the visual observations was at 22^h00^m UT and continued until dusk around 03^h15^m UT. The Moon was still a bit disturbing in the last two hours. The night started nicely

 © eMeteorNews

with within a few minutes a beautiful white –1 SDA earth-grazer (00^h01^m UT) in the south and a little later a 0 Capricornid (00^h07^m UT). The numbers of Perseids were not too bad, the hourly counts increased from 13 to 57. A striking number of bright meteors: relatively many Perseids from 0 to –6 were seen. It was a bit like 2008 when many bright Perseids were spotted in the nights of August 10–11 and 12–13. And this was also the case in 1980. The Perseid fireball of magnitude –6 appeared at $00^h13^m05^s$ UT (*Figure 2*) in the constellation Aquila and left an 8-second persistent train. The all-sky camera captured this fireball beautifully. At 01^h37^m a –5 Perseid appeared low in the south and a little later at 01^h49^m UT a –2 to –3 Perseid. Michel and Koen counted 413 meteors in total. During the last two hours the small crescent Moon was above the horizon, but it did not disturb the observations anymore.

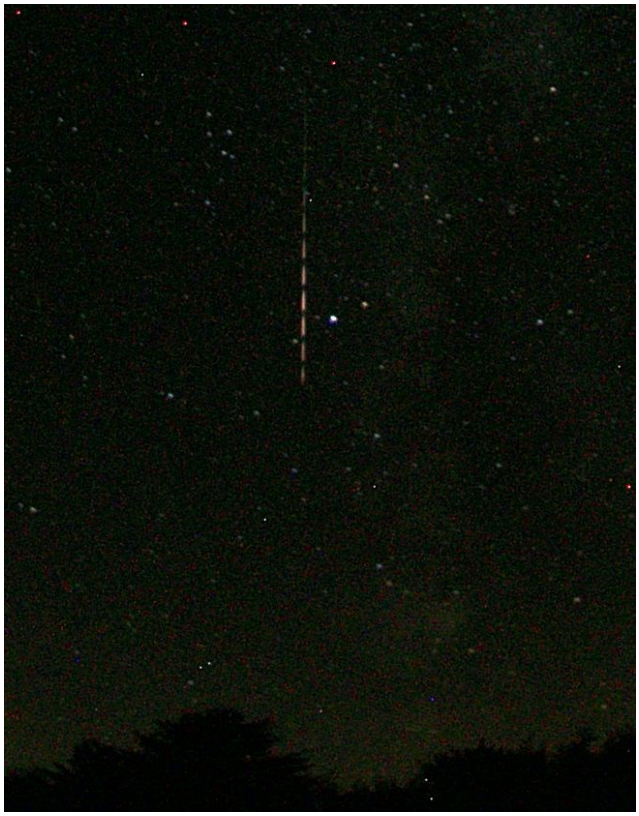

Figure 2 – The Perseid fireball of August 12, 2023 at $00^h13^m05^s$ UT in the constellation of Aquila. Camera and lens: Canon 6D with Sigma 8mm F3.5 EX DG Circular Fisheye lens with built in Liquid Crystal Shutter, set at 16 breaks per second.

2023, August 12–13

According to the IMO Meteor Shower Calendar 2023, the Perseid maximum was expected to occur on August 13 between 07^h and 14^h UT. Extra attention this night around 3^h00^m UT as a weak filament could cause some extra activity. We used the entire night from evening to dawn to do observations. In addition to the all-sky camera, Koen also used a Sony Alpha A7sII with a Sigma 20 mm F 1.4 lens. This to shoot video images of earth-grazing Perseids. Just before the start of the visual observations, Koen put his glasseson, oops, a glass dropped out. A tiny screw had come loose. Fortunately, Koen found the screw, but fixing it immediately was too late. So, he did his observations with double focus glasses. Ultimately, it seemed to have had some negative influence on the observed numbers of meteors. Calculating a separate C_p for this night will be necessary.

The authors signed on at 20^h00^m UT under a still slightly twilight sky. Immediately we saw a Starlink train (referred by us as “annoying Mosquitoes”) disappearing into the shadow of the Earth. It gave a twofold feeling: it was a nice sight, but in the end, there are far too many… Again, the sky is not perfect, but with a limiting magnitude of 6.6 we were absolutely not complaining.

The activity this night was excellent: hourly counts increased from 20 to 65. Again, a lot of bright meteors were seen: 6 Perseids of –3, a –4, a –6 and even a –7! At 01^h22^m UT a –4 Perseid appeared in Cassiopeia and a beautiful –7 Perseid low at the southwestern horizon briefly lit up the sky at 01^h47^m UT (*Figure 4*). A Perseid of –6 was observed in Capricornus (*Figure 3*). All these bright meteors were captured with the all-sky camera.

Figure 3 – This Perseid fireball of magnitude –6 appeared on August 12, 2023 at 23^h00^m UT in the constellation of Capricornus. Camera and lens: Canon 6D with Sigma 8mm F3.5 EX DG Circular Fisheye lens with built in Liquid Crystal Shutter, set at 16 breaks per second.

Figure 4 – The Perseid fireball of magnitude –7 very low at the southwestern horizon. August 13, 2023 at 01^h47^m UT. Camera and lens: Canon 6D with Sigma 8mm F3.5 EX DG Circular Fisheye lens with built in Liquid Crystal Shutter, set at 16 breaks per second.

Around 3h UT we didn't really notice any increase in activity. But the expected additional activity was not much and only a thorough analysis will perhaps reveal something. In total, we counted 741 meteors.

2023, August 13–14

In addition to the maximum night, this night was also important to monitor. Since 2018 (and with the exception of 2022), a second peak in activity has been observed around solar longitude 141 (24–30 hours after the annual maximum). The ZHR increased to 190 in 2021 (Miskotte and Vandeputte, 2019; Miskotte, 2020; Miskotte et al., 2021). The 2023 IMO Meteor Shower Calendar also highlighted an old dust trail of Comet 109P/Swift-Tuttle from 68BC, which could cause increased Perseid activity between 01h00m and 02h45m UT. Predicting the ZHR for this very old dust trail was not possible according to Jérémie Vaubaillon.

Figure 5 – The photographic equipment in front of our rented house.

Figure 6 – The travel all-sky camera and the Sony Alpha A7SII on a small tripod, set up on a heavy garden table that we placed in the middle of the field for this campaign. In the background three stretchers are ready for the kids and Inneke.

During the evening of the 13th the authors are accompanied by Laurien, Boris and Inneke. We were hoping for some nice bright earth-grazers. Just before 20h UT we all see the new Starlink train diving into the Earth's shadow again. We all started around 20h UT. The whole night we had serious lightning in eastern direction, this weakened a bit later on in the night. And Koen observed for the first time in his life a reddish jellyfish like sprite (but without the tentacles) low in eastern direction during a short break.

Activity was not as high as hoped this evening, but there were plenty of events to see, including some earth-grazers. The number of bright meteors was somewhat disappointing. Just after 22h UT the casual observers called it a day. Laurien (10 years old) has excellent eyes, she counted more than 50 meteors in those two hours. That is about as many as those two "old" meteor observers. We hope she will be an excellent meteor observer in the future!

After 22h UT, more bright Perseids started to appear. An increase that continued and especially after 23h UT there were many bright Perseids, mostly in the range of +1 to –3. Two Perseid fireballs were seen: at 02h06m UT to the right of Jupiter in Cetus a –5/–6 Perseid with a 10 second persistent train. And at 02h30m UT a beautiful –6 Perseid with three short flares flashed from Pisces to Cetus with a 10 second persistent train. The hourly counts were not too shabby this night: they increased from 15 to 50+. Perhaps this is a bit higher than what we normally would expect at this solar longitude. Also worth mentioning was a beautiful blue-green –3 sporadic meteor at the end of the night with a bright blue persistent train. In total, the authors counted 685 meteors, slightly fewer than the previous night.

Figure 7 – Composite image of two Perseid fireballs that appeared in quick succession at 02h06m UT (–5 Perseid in Cetus) and 02h30m UT (–6 Perseid in Pisces). These Perseids appeared in the interval of the predicted dust trail passage of comet 109P/Swift-Tuttle of 68 BC. Camera and lens: Canon 6D with Sigma 8mm F3.5 EX DG Circular Fisheye lens with built in Liquid Crystal Shutter set at 16 breaks per second.

Figure 8 – This Perseid fireball appeared on August 14, 2023 at 23h22m UT. The "flare" in the last part of the fireball is a star: Markab (alpha Pegasi). Camera and lens: Canon 6D with Sigma 8mm F3.5 EX DG Circular Fisheye lens with built in Liquid Crystal Shutter set at 16 breaks per second.

© eMeteorNews

2023, August 14–15

From this night on we started at a later time, starting around 23^h UT. Soon a beautiful Perseid fireball of –6 appeared. The star alpha Pegasi (Markab) was "shot" out of the sky… The persistent train was visible for 12 seconds. In addition to the –6 Perseid, a few Perseids of –2 and –3 were seen. The Perseids hourly counts were initially up to 31 meteors, but halved in the last two hours of the night. In total, the authors counted 387 meteors.

2023, August 15–16: a falling DCF clock and a very bright Perseid…

For this night, Koen planned a session between 23^h15^m and 03^h15^m UT. Michel would start a little later. However, Koen was startled awake by a falling alarm DCF clock on the tiled floor in his room, around 22^h15^m UT. He tried to sleep again, but is fully awake… So, then decided to go outside! He first checked the all-sky camera: it appeared not to be working due to an empty battery. When he replaced it with a full battery the camera worked flawlessly.

Then Koen shifted the focus to the Sony Alpha A7sII with the Sigma 20 mm F 1.4 lens. The plan was to aim the camera to the house together with the nice starry sky above it. However, the milky way in the south now also looks beautiful and he decided to photograph in that direction for the first 30 minutes. The camera started at 22^h30^m UT. Then it was time to prepare for the visual watch. Start was at 22^h47^m UT which was more than 25 minutes earlier than planned. After only two minutes, to be precise at $22^h49^m58^s$ UT (timing of FRIPON station Marseille[25]), one of the most beautiful Perseids Koen has seen appeared! With a brightness of at least magnitude –8, this bright green meteor moved from Cygnus through Aquila to slightly left of the "starcloud" of Scutum! Wow: what a beast and the bright green persistent train (magnitude +1) was phenomenal! To Koen's surprise, a big part of the persistent train remained easily visible. At 22^h55^m UT the persistent train was still as bright as the Andromeda nebula, only at 22^h57^m UT it became a bit faint, at 22^h58^m UT you really had to look closely to see it and at 22^h59^m it was finally too weak to see it. This meant that the persistent train remained visible for the naked eye for as long as 9 minutes! It was from the Leonids of 2001 that Koen had seen such long-lasting lingering persistent trains.

However, immediately after the fireball appeared there were concerns about the all-sky camera. There was a shutter click just after the fireball. This could be the closing shutter (no problem), but also an opening shutter (a problem…)! Fortunately, I also realized that the fireball had also appeared in the field of view of the Sony Alpha A7. Indeed, after the session it turned out that the all-sky camera was closed during the fireball: $22^h49^m57^s$ UT camera closed, fireball at $22^h49^m58^s$ UT, camera open $22^h50^m00^s$ UT… The persistent train is visible on 6 consecutive images (6 minutes in total).

Fortunately, the image from the Sony Alpha A7sII was of great beauty, the fireball was largely depicted with a beautiful Milky Way (*Figures 9 and 10*). With the persistent train in mind, Koen let the camera run a little longer than planned. Until 23^h34^m UT, after that the camera was aimed at the house and the sky above it. And even this was still too early, because the persistent train is still faintly visible until that last image! This means that the persistent train was photographically visible for at least 45 minutes on the images!

Figure 9 – The Super-Perseid of August 15, 2023 at $22^h49^m58^s$ UT. Camera: Sony Alpha A7sII. Lens: Sigma ART 20mm F 1.4 lens.

[25] https://fireball.fripon.org/displaymultiple.php?id=20974

Figure 10 – The first image taken after that the fireball appeared, a beautiful bright persistent train is visible. A spectaculair animated GIF of the fireball was published of the website of the Dutch Meteor Society[26].

Figure 11 – These two fireballs were captured right after each other on August 18, 2023 at 01^h54^m UT (left, low east-southeast in Orion) and 02^h12^m UT (low west), respectively. Camera and lens: Canon 6D with Sigma 8mm F3.5 EX DG Circular Fisheye lens with built in Liquid Crystal Shutter set at 16 breaks per second.

What a way to start your observing session, WOW! If that DCF clock had not fallen, this session would have started around 23^h15^m UT and the fireball would not have been photographed or visually seen! Murphy rules, but not this time….

This night was shortened because of incoming clouds from the southwest around 02^h30^m UT. Perseid hourly counts were between 10–17 this night. A total of 184 meteors were counted during this night. The night of August 16–17, 2023 we had to skip because of too many cirrus clouds. We didn't mind this, we were longing for some extra sleep after 7 cloudless nights in a row!

2023, August 17–18

Observations were done between 22^h45^m and 03^h15^m UT. The hourly counts of the Perseids were now between 6 and 11. Not many bright meteors: a few Perseids of –1 and –2, but at 01^h54^m UT a slow sporadic fireball appeared low east in Orion with several flares up to –6. This was seen by both authors. And 18 minutes later at 02^h12^m UT another –6 sporadic fireball appeared low in the west; this one was only seen by Michel (*Figure 11*). Both fireballs were captured with the all-sky camera. In total, the authors counted 184 meteors.

2023, August 18–19

The last night in Revest-du-Bion in 2023! This night would be largely full of cirrus, with a chance of clearings after 23^h UT. Alarm was set by Koen at 23^h30^m UT: unfortunately,

[26] https://www.dutch-meteor-society.nl/DMS/Perseid_fireball.mp4

© eMeteorNews

the sky was still full of cirrus. Michel had also set an alarm clock and looked outside around 1^h UT: sky was clear with the last cirrus visible low in the south. Koen was thrown out of bed (…) and at 01^h15^m UT the observations started and lasted until 03^h15^m UT. Perseid hourly counts between 6 and 10. A total of 101 meteors were counted. Best meteors were a pair of Perseids of –1 and –2. The all sky and the Sony Alpha A7SII were no longer used due to Koen's early departure to Manosque and flight back to Amsterdam that morning.

4 Conclusion

Another successful campaign in the Provence this year! In total, both observers counted more than 3000 meteors. We didn't really get top quality skies (apart from some shorter good periods), but we're certainly not complaining. We had sometimes luck with bad weather just at a short distance. The All-Sky has captured quite a few fireballs, the most beautiful ones are included in this article. In addition, seeing each other again was also very pleasant. And the tradition of the previous campaigns in the Provence were also honored: eating local delicious goat cheeses with tomato and baguette during the setting Sun! Hopefully next year we'll be again in the Provence!

References

Miskotte K., Vandeputte M. (2016). "Perseid observing expedition at Revest du Bion, Provence, Southern France". *eMetN*, **1**, 83–87.

Miskotte K. (2018). "Preview: Perseid observations from Aubenas Les Alps, Southern France". *eMetN*, **3**, 77–79.

Miskotte K. and Vandeputte M. (2020). "Perseids 2019: another peak in activity around solar longitude 141.0?". *eMetN*, **5**, 25–29.

Miskotte K. (2020). "Perseids 2020: again, enhanced Perseid activity around solar longitude 141?". *eMetN*, **5**, 395–397.

Miskotte K., Sugimoto H. and Martin P. (2021). "The big surprise: a late Perseid outburst on August 14, 2021!". *eMetN*, **6**, 517–525.

© eMeteorNews

August 2023 report CAMS-BeNeLux

Carl Johannink

Am Ollenkamp 4, 48599 Gronau, Germany
c.johannink@t-online.de

A summary of the activity of the CAMS-BeNeLux network during the month of August 2023 is presented. This month was good for 43080 multi-station meteors resulting in 12074 orbits.

1 Introduction

In August, of course, all attention goes to the Perseid meteor shower. Little moonlight this year during the maximum and in the post-maximum period offered potentially good conditions.

2 August 2023 statistics

The period without moonlight interference this year coincided with mostly good weather between August 8 and 24. Before and after, the weather was very unsettled. Like in July, also this month was very rainy, mostly in the form of rain showers. However, that did not prevent us from capturing meteors in every single night this month.

In terms of results, we found the worst nights at the beginning, and at the end of the month. On the night of August 2–3, 95 cameras captured only 99 meteors, resulting in three orbits. The night August 31 – September 1 wasn't much better: 101 active cameras during this night, captured only 105 meteors, resulting in 8 orbits. But these nights were the exceptions. More than 100 orbits were recorded in 24 nights, a result nearly as good as in August 2022.

CAMS-BeNeLux recorded data of 43080 meteors from all stations this month, resulting in 12074 orbits. This is the second-best result for this month (*Figure 1*). Under cloudless circumstances in the whole of our region, as many as 2189 orbits were recorded during August 13–14. That is a new one-night-record since the start of our network in March 2012. Until now, December 12–13, 2022 with 1946 orbits was the most productive night. It is remarkable that, although it is possible to capture meteors during this night twice as long as in August, the number of orbits is even higher during this August night. Both nights had clear conditions in all parts of the BeNeLux. In my opinion, an explanation for this difference, is not only the slightly increased number of cameras available now.

On December 12–13 a waning moon, still 80% illuminated, was above the horizon in the constellation of Cancer for nearly the whole night. On August 13–14 there was no moonlight at all. One could wonder what the number of orbits could be during clear skies, and no moonlight, throughout the BeNeLux during a long winter night.

60.1% of all orbits were captured from more than two stations. A result compatible with the percentages during most of the last months.

Table 1 – Number of orbits and active cameras in the BeNeLux during the month of August in the period 2012–2023.

Year	Nights	Orbits	Stations	Max. Cams	Min. Cams	Mean Cams
2012	21	283	5	6		3.2
2013	27	1960	13	25		15.3
2014	28	2102	14	32		20.8
2015	25	2821	15	45		30.4
2016	30	5102	20	54	15	46.2
2017	28	8738	21	82	45	69.9
2018	30	5403	19	72	56	62.4
2019	29	9916	23	87	65	79.0
2020	31	8845	24	90	59	80.6
2021	29	7496	27	89	65	80.2
2022	31	14807	31	104	90	98.1
2023	31	12074	37	115	92	107.3
Total	340	79547				

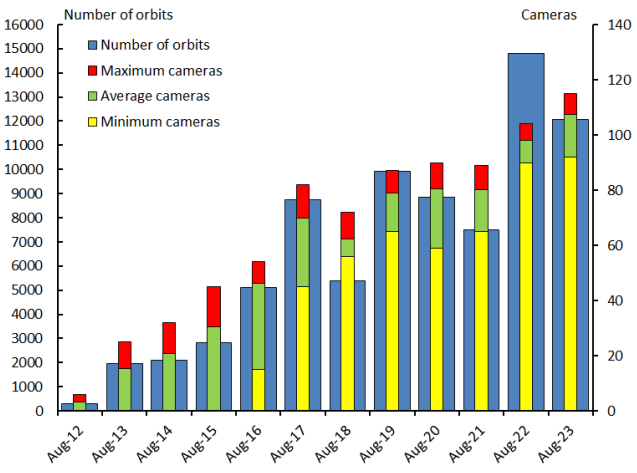

Figure 1 – Comparing August 2023 to previous months of August in the CAMS-BeNeLux history. The blue bars represent the number of orbits, the red bars the maximum number of cameras capturing in a single night, the green bars the average number of cameras capturing per night and the yellow bars the minimum number of cameras.

© eMeteorNews

We could welcome two new stations this month. At Colombey-Les-Belles in France, *Stéphane Barré* contributes now to our network with his RMS-camera FR000F (CAMS -number 3907). From Alphen aan de Rijn in the Netherlands, *Roel Gloudemans* contributes now to our network with his RMS-camera NL000N (CAMS-number 3197). Both stations are a valuable addition to our network.

On average there were 107 cameras active on every night in August, which is a fairly high number, although some operators faced minor technical problems again. At least 92 cameras, and at most 115 cameras recorded meteors in every night (*Figure 1*).

3 Perseids

The huge number of data we could collect between July 29 and August 20 was used to look at the radiant drift of the Perseids during this time. Therefore, we used data from July 29–30 (313 orbits), August 4–5 (327 orbits), August 7–8 (522 orbits), August 9–10 (760 orbits), August 13–14 (2189 orbits) and August 19–20 (444 orbits). From these data, we used the D-criterium of Drummond to distillate the Perseids from this dataset. We found $\Delta\alpha = 1.31$ degrees/day and $\Delta\delta = 0.28$ degrees/day. Both values are in good agreement with the literature (Jenniskens, 2011; 2016a; 2016b).

4 Conclusion

Good conditions during most time of this month, resulted in the second-best score of orbits for this month.

Acknowledgement

Many thanks to all participants in the CAMS-BeNeLux network for their dedicated efforts. The CAMS-BeNeLux team was operated by the following volunteers during the month of August 2023:

Stéphane Barré (Colombey-Les-Belles, France, RMS 3907), *Hans Betlem* (Woold, Netherlands, Watec 3071, 3072, 3073, 3074, 3075, 3076, 3077 and 3078), *Felix Bettonvil* (Utrecht, Netherlands, Watec 376), *Jean-Marie Biets* (Wilderen, Belgium, Watec 379, 380 and 381), *Ludger Boergerding* (Holdorf, Germany, RMS 3801), *Günther Boerjan* (Assenede, Belgium, RMS 3823), *Martin Breukers* (Hengelo, Netherlands, Watec 320, 321, 322, 323, 324, 325, 326 and 327, RMS 319, 328 and 329), *Seppe Canonaco* (Genk, RMS 3818 and 3819), *Pierre de Ponthiere* (Lesve, Belgium, RMS 3816 and 3826), *Bart Dessoy* (Zoersel, Belgium, Watec 397, 398, 804, 805, 806, 3888 and RMS 3827), *Tammo Jan Dijkema* (Dwingeloo, Netherlands, RMS 3199), *Isabelle Ansseau, Jean-Paul Dumoulin, Dominique Guiot* and *Christian Wanlin* (Grapfontaine, Belgium, Watec 815, RMS 3814 and 3817), *Uwe Glässner* (Langenfeld, Germany, RMS 3800), *Roel Gloudemans* (Alphen aan de Rijn, Netherlands, RMS 3197), *Luc Gobin* (Mechelen, Belgium, Watec 3890, 3891, 3892 and 3893), *Tioga Gulon* (Nancy, France, Watec 3900 and 3901), *Robert Haas* (Alphen aan de Rijn, Netherlands, Watec 3160, 3161, 3162, 3163, 3164, 3165, 3166 and 3167), *Robert Haas* (Texel, Netherlands, Watec 811 and 812), *Kees Habraken* (Kattendijke, Netherlands, RMS 3780, 3781, 3782 and 3783), *Klaas Jobse* (Oostkapelle, Netherlands, Watec 3030, 3031, 3032, 3033, 3034, 3035, 3036 and 3037), *Carl Johannink* (Gronau, Germany, Watec 3100, 3101, 3102), *Reinhard Kühn* (Flatzby, Germany, RMS 3802), *Hervé Lamy* (Dourbes, Belgium, Watec 394 and 395, RMS 3825 and 3841), *Hervé Lamy* (Humain, Belgium, RMS 3821 and 3828), *Hervé Lamy* (Ukkel, Belgium, Watec 393 and 817), *Hartmut Leiting* (Solingen, Germany, RMS 3806), *Horst Meyerdierks* (Osterholz-Scharmbeck, Germany, RMS 3807), *Koen Miskotte* (Ermelo, Netherlands, Watec 3051, 3052, 3053 and 3054), *Pierre-Yves Péchart* (Hagnicourt, France, RMS 3902, 3903, 3904 and 3905), *Eduardo Fernandez del Peloso* (Ludwigshafen, Germany, RMS 3805), *Tim Polfliet* (Gent, Belgium, Watec 396, RMS 3820 and 3840), *Steve Rau* (Oostende, Belgium, RMS 3822), *Steve Rau* (Zillebeke, Belgium, Watec 3850 and 3852, RMS 3851 and 3853), *Paul and Adriana Roggemans* (Mechelen, Belgium, RMS 3830 and 3831, Watec 3832, 3833, 3834, 3835, 3836 and 3837), *Jim Rowe* (Eastbourne, Great Britain, RMS 3829), *Philippe Schaack* (Roodt-sur-Syre, Luxemburg, RMS 3952), *Hans Schremmer* (Niederkruechten, Germany, Watec 803), *Erwin van Ballegoij* (Heesh, Netherlands Watec 3148 and 3149), *Andy Washington* (Clapton, England, RMS 3702).

References

Jenniskens P., Gural P. S., Dynneson L., Grigsby B. J., Newman K. E., Borden M., Koop M., Holman D. (2011). "CAMS: Cameras for Allsky Meteor Surveillance to establish minor meteor showers". *Icarus*, **216**, 40–61.

Jenniskens P., Nénon Q., Albers J., Gural P. S., Haberman B., Holman D., Morales R., Grigsby B. J., Samuels D. and Johannink C. (2016). "The established meteor showers as observed by CAMS". *Icarus*, **266**, 331–354.

Jenniskens P., Nénon Q., Gural P. S., Albers J., Haberman B., Johnson B., Holman D., Morales R., Grigsby B. J., Samuels D., Johannink C. (2016). "CAMS confirmation of previously reported meteor showers". *Icarus*, **266**, 355–370.

September 2023 report CAMS-BeNeLux

Carl Johannink

Am Ollenkamp 4, 48599 Gronau, Germany
c.johannink@t-online.de

A summary of the activity of the CAMS-BeNeLux network during the month of September 2023 is presented. This month was good for 42968 multi-station meteors resulting in 11331 orbits.

1 Introduction

In September, sporadic meteor activity is already quite high, and as nights get longer in this time of the year, this is always a prelude to fascinating nights, even if there are no major streams active.

2 September 2023 statistics

September got off with very sunny and warm weather. The first ten nights yielded a very rich harvest of 5191 simultaneous meteors. In the nights between September 4 and 10, more orbits were collected each night than on any other September night in the past 11 years.

Although the weather got less sunny after the middle of the month, we could collect orbits in every single September night. In just 5 nights during this month, less than 100 orbits were obtained, a very special situation.

The least productive night was September 28–29 with 17 orbits collected by 95 cameras. The highest number on September 6–7 was 747 orbits.

CAMS-BeNeLux collected data of 42968 multi-station meteors this month, resulting in a total of 11331 orbits. By far the best result for a September month in the history of our network (*Figure 1*). 61.1% of all orbits were collected from more than 2 stations. This is more or less the same percentage as in recent months.

We could welcome *Stef Vancampenhout* as a new participant in our network. He operates his RMS-camera (CAMS number 3842) from Vorselaar in the northern parts of Belgium. His data gives a better coverage for the northwestern parts of the BeNeLux.

On average 104 cameras were active every night, at least 89 cameras on September 19–20. The highest number was 115 cameras on September 14–15.

Table 1 – Number of orbits and active cameras in the BeNeLux during the month of September in the period 2012–2023.

Year	Nights	Orbits	Stations	Max. Cams	Min. Cams	Mean Cams
2012	18	209	5	5		3.4
2013	19	712	9	20		13.7
2014	27	1293	14	32		22.0
2015	29	2763	15	46		30.0
2016	30	3982	19	54	32	46.5
2017	29	4839	22	83	47	70.2
2018	28	5606	20	80	57	65.4
2019	29	4609	20	79	64	72.3
2020	26	6132	24	90	52	76.2
2021	30	7457	26	93	64	82.0
2022	30	5446	30	95	66	82.8
2023	30	11331	37	115	89	104.1
Total	325	54379				

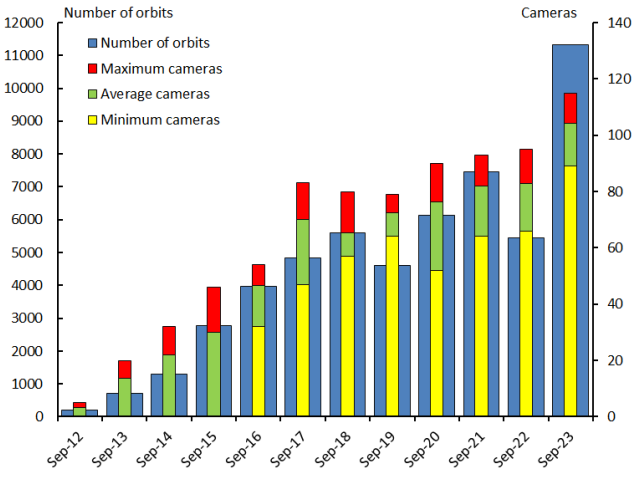

Figure 1 – Comparing September 2023 to previous months of September in the CAMS-BeNeLux history. The blue bars represent the number of orbits, the red bars the maximum number of cameras capturing in a single night, the green bars the average number of cameras capturing per night and the yellow bars the minimum number of cameras.

 © eMeteorNews

3 Conclusion

In September our network collected a record number of orbits since the start of our network in 2012. This result is nearly as good as last August. But September has no major meteor showers like the Perseids, what emphasizes how special this result is.

Acknowledgement

Many thanks to all participants in the CAMS-BeNeLux network for their dedicated efforts. The CAMS-BeNeLux team was operated by the following volunteers during the month of September 2023:

Stéphane Barré (Colombey-Les-Belles, France, RMS 3907), *Hans Betlem* (Woold, Netherlands, Watec 3071, 3072, 3073, 3074, 3075, 3076, 3077 and 3078), *Felix Bettonvil* (Utrecht, Netherlands, Watec 376), *Jean-Marie Biets* (Wilderen, Belgium, Watec 379, 380 and 381), *Ludger Boergerding* (Holdorf, Germany, RMS 3801), *Günther Boerjan* (Assenede, Belgium, RMS 3823), *Martin Breukers* (Hengelo, Netherlands, Watec 320, 321, 322, 323, 324, 325, 326 and 327, RMS 319, 328 and 329), *Seppe Canonaco* (Genk, RMS 3818 and 3819), *Pierre de Ponthiere* (Lesve, Belgium, RMS 3816 and 3826), *Bart Dessoy* (Zoersel, Belgium, Watec 397, 398, 804, 805, 806, 3888 and RMS 3827), *Tammo Jan Dijkema* (Dwingeloo, Netherlands, RMS 3199), *Isabelle Ansseau, Jean-Paul Dumoulin, Dominique Guiot* and *Christian Wanlin* (Grapfontaine, Belgium, Watec 815, RMS 3814 and 3817), *Uwe Glässner* (Langenfeld, Germany, RMS 3800), *Roel Gloudemans* (Alphen aan de Rijn, Netherlands, RMS 3197), *Luc Gobin* (Mechelen, Belgium, Watec 3890, 3891, 3892 and 3893), *Tioga Gulon* (Nancy, France, Watec 3900 and 3901), *Robert Haas* (Alphen aan de Rijn, Netherlands, Watec 3160, 3161, 3162, 3163, 3164, 3165, 3166 and 3167), *Robert Haas* (Texel, Netherlands, Watec 811 and 812), *Kees Habraken* (Kattendijke, Netherlands, RMS 3780, 3781, 3782 and 3783), *Klaas Jobse* (Oostkapelle, Netherlands, Watec 3030, 3031, 3032, 3033, 3034, 3035, 3036 and 3037), *Carl Johannink* (Gronau, Germany, Watec 3100, 3101, 3102), *Reinhard Kühn* (Flatzby, Germany, RMS 3802), *Hervé Lamy* (Dourbes, Belgium, Watec 394 and 395, RMS 3825 and 3841), *Hervé Lamy* (Humain, Belgium, RMS 3821 and 3828), *Hervé Lamy* (Ukkel, Belgium, Watec 393 and 817), *Hartmut Leiting* (Solingen, Germany, RMS 3806), *Horst Meyerdierks* (Osterholz-Scharmbeck, Germany, RMS 3807), *Koen Miskotte* (Ermelo, Netherlands, Watec 3051, 3052, 3053 and 3054), *Pierre-Yves Péchart* (Hagnicourt, France, RMS 3902, 3903, 3904 and 3905), *Eduardo Fernandez del Peloso* (Ludwigshafen, Germany, RMS 3805), *Tim Polfliet* (Gent, Belgium, Watec 396, RMS 3820 and 3840), *Steve Rau* (Oostende, Belgium, RMS 3822), *Steve Rau* (Zillebeke, Belgium, Watec 3850 and 3852, RMS 3851 and 3853), *Paul and Adriana Roggemans* (Mechelen, Belgium, RMS 3830 and 3831, Watec 3832, 3833, 3834, 3835, 3836 and 3837), *Philippe Schaack* (Roodt-sur-Syre, Luxemburg, RMS 3952), *Hans Schremmer* (Niederkruechten, Germany, Watec 803), *Erwin van Ballegoij* (Heesh, Netherlands Watec 3148 and 3149), *Stef Vancampenhout* (Vorselaar, Belgium, RMS 3842), *Andy Washington* (Clapton, England, RMS 3702).

Radio meteors August 2023

Felix Verbelen

Vereniging voor Sterrenkunde & Volkssterrenwacht MIRA, Grimbergen, Belgium
felix.verbelen@skynet.be

An overview of the radio observations during August 2023 is given.

1 Introduction

The graphs show both the daily totals (*Figure 1 and 2*) and the hourly numbers (*Figure 3 and 4*) of "all" reflections counted automatically, and of manually counted "overdense" reflections, overdense reflections longer than 10 seconds and longer than 1 minute, as observed here at Kampenhout (BE) on the frequency of our VVS-beacon (49.99 MHz) during the month of August 2023.

The hourly numbers, for echoes shorter than 1 minute, are weighted averages derived from:

$$N(h) = \frac{n(h-1)}{4} + \frac{n(h)}{2} + \frac{n(h+1)}{4}$$

Due to mechanical damage to its transmitting antenna the beacon was out of order between August 24th at 17h40m UT and August 25th at 13h49m UT. Therefore, observations for this period are left out of the counts, especially because on these days also strong lightning activity made things worse. On 5 other days weak to moderate lightning activity was also observed, but over the month local or unidentified noise remained moderate to low. Quite strong solar bursts happened almost every day, but in general these were weaker than the previous month.

Eye-catchers were of cause the Perseids, reaching their maximum on both 13th and 14th of August, having been quite active as from the beginning of the month. After their maximum the number dropped rapidly, but on August 27th and the following days a moderate increase of overdense reflections longer than 10 seconds showed up.

Over the entire month, 67 reflections longer than 1 minute were observed. A small selection of these, along with some other interesting reflections is included (*Figures 5 to 28*). Many more of these are available on request.

In addition to the usual graphs, you will also find the raw counts in cvs-format[27] from which the graphs are derived. The table contains the following columns: day of the month, hour of the day, day + decimals, solar longitude (epoch J2000), counts of "all" reflections, overdense reflections, reflections longer than 10 seconds and reflections longer than 1 minute, the numbers being the observed reflections of the past hour.

[27] https://www.meteornews.net/wp-content/uploads/2023/09/202308_49990_FV_rawcounts.csv

 © eMeteorNews

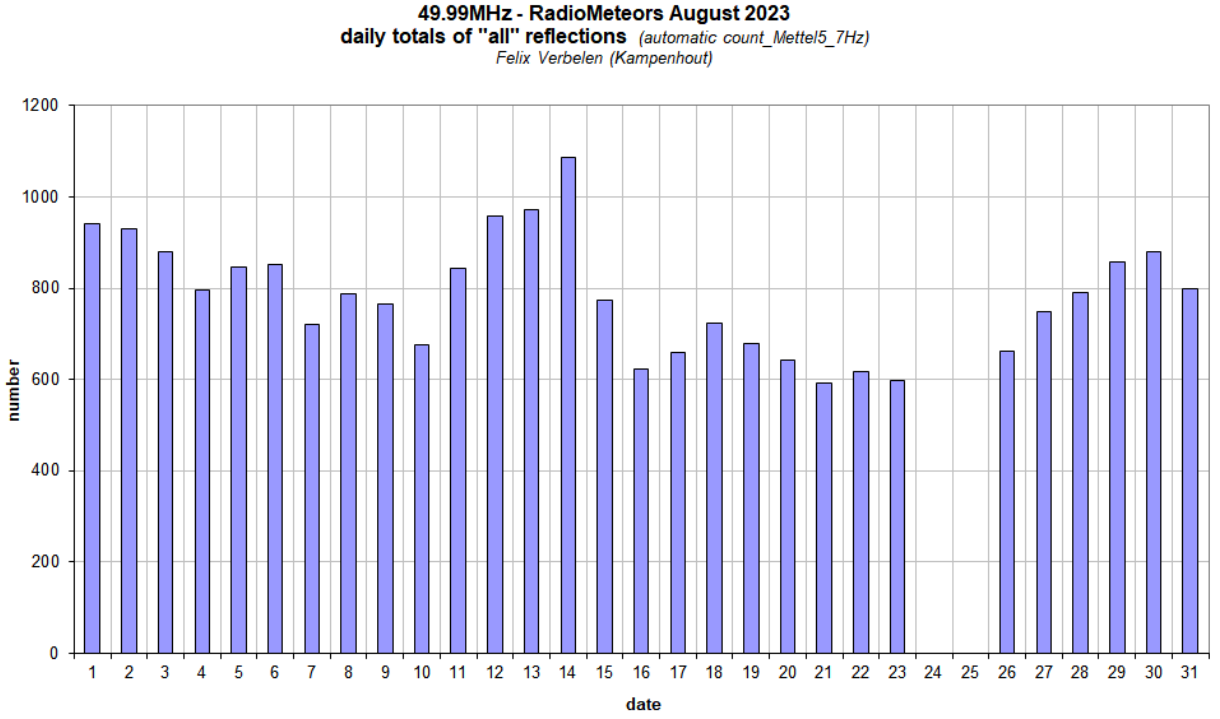

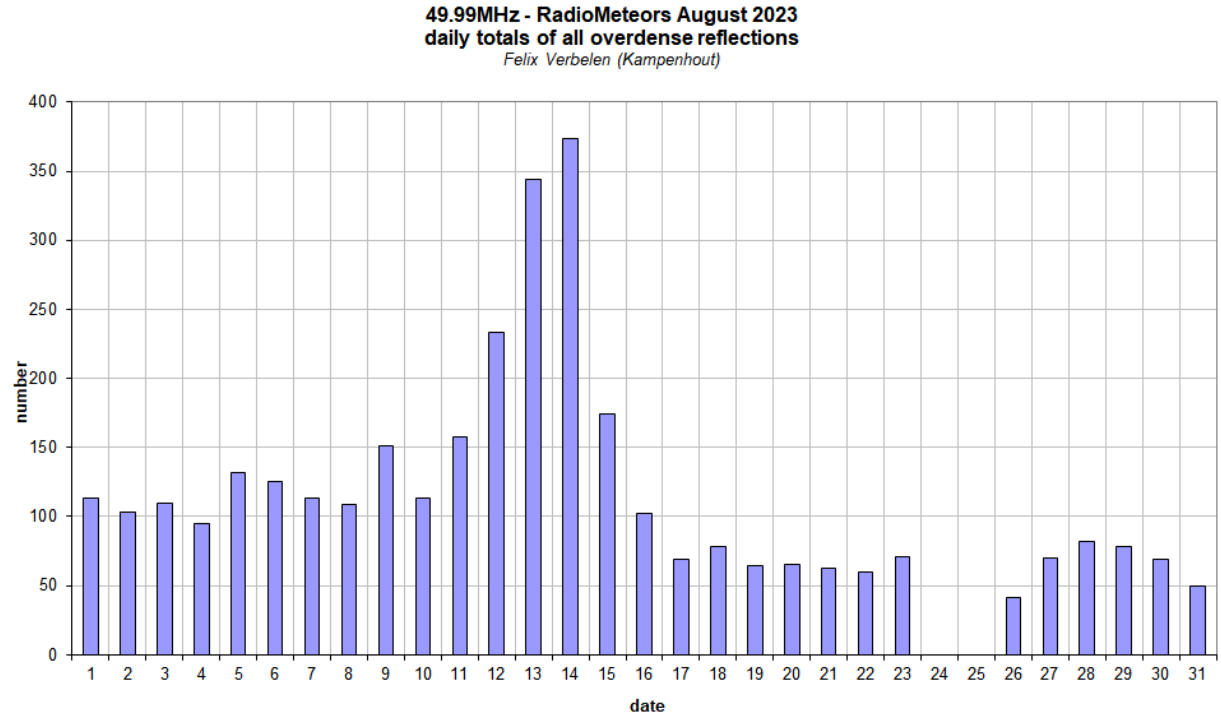

Figure 1 – The daily totals of "all" reflections counted automatically, and of manually counted "overdense" reflections, as observed here at Kampenhout (BE) on the frequency of our VVS-beacon (49.99 MHz) during August 2023.

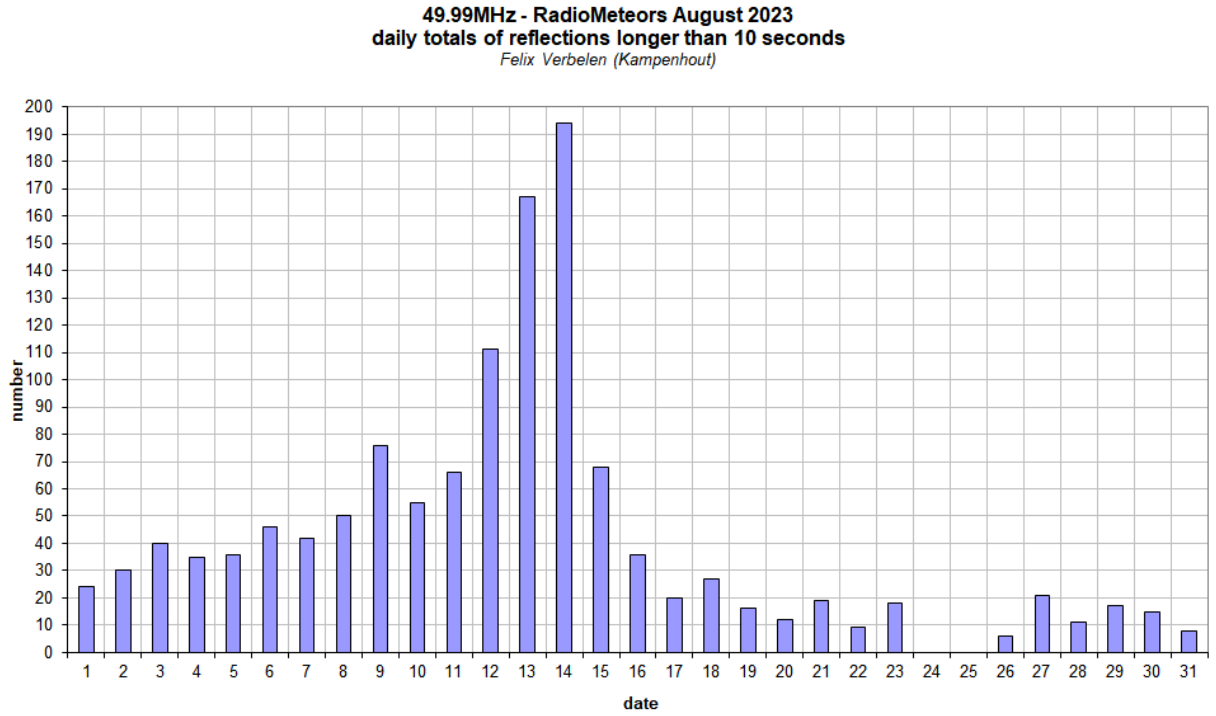

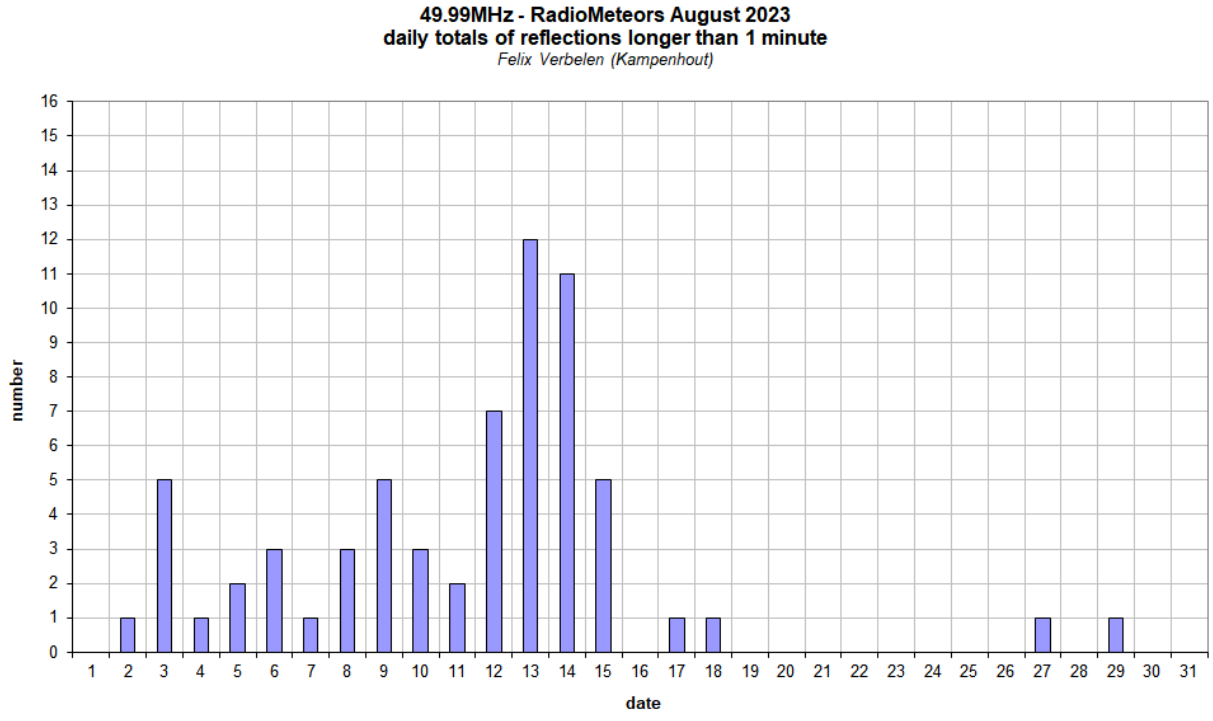

Figure 2 – The daily totals of overdense reflections longer than 10 seconds and longer than 1 minute, as observed here at Kampenhout (BE) on the frequency of our VVS-beacon (49.99 MHz) during August 2023.

 © eMeteorNews

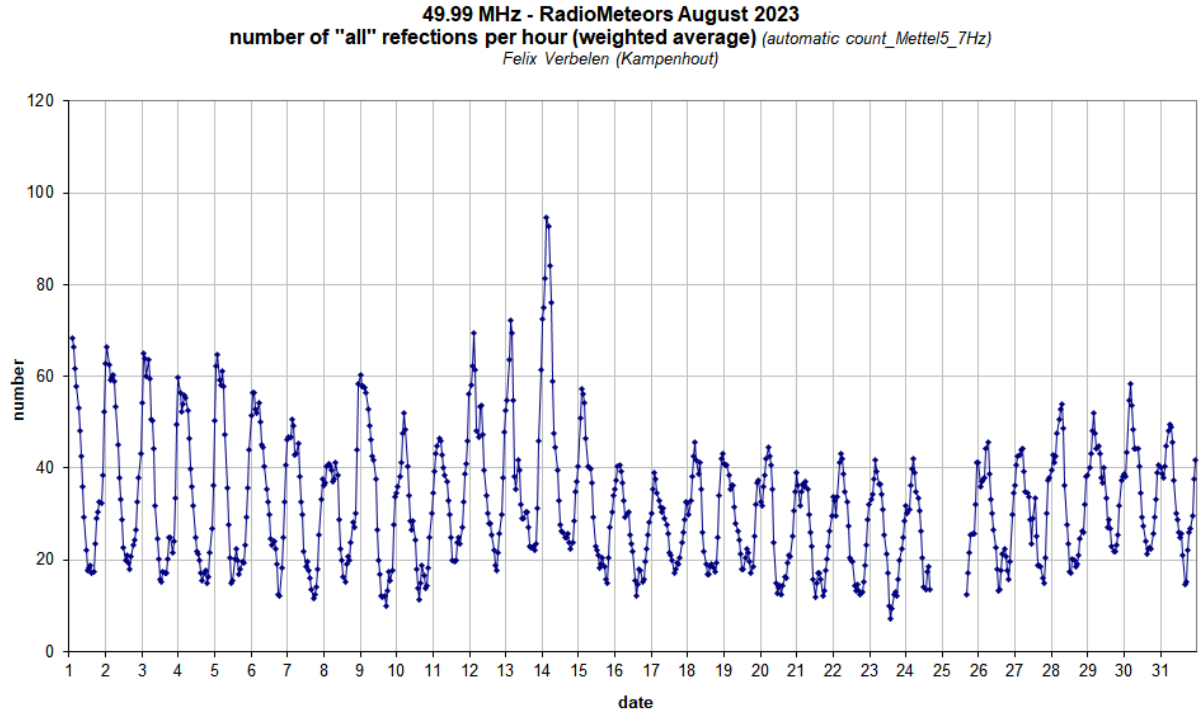

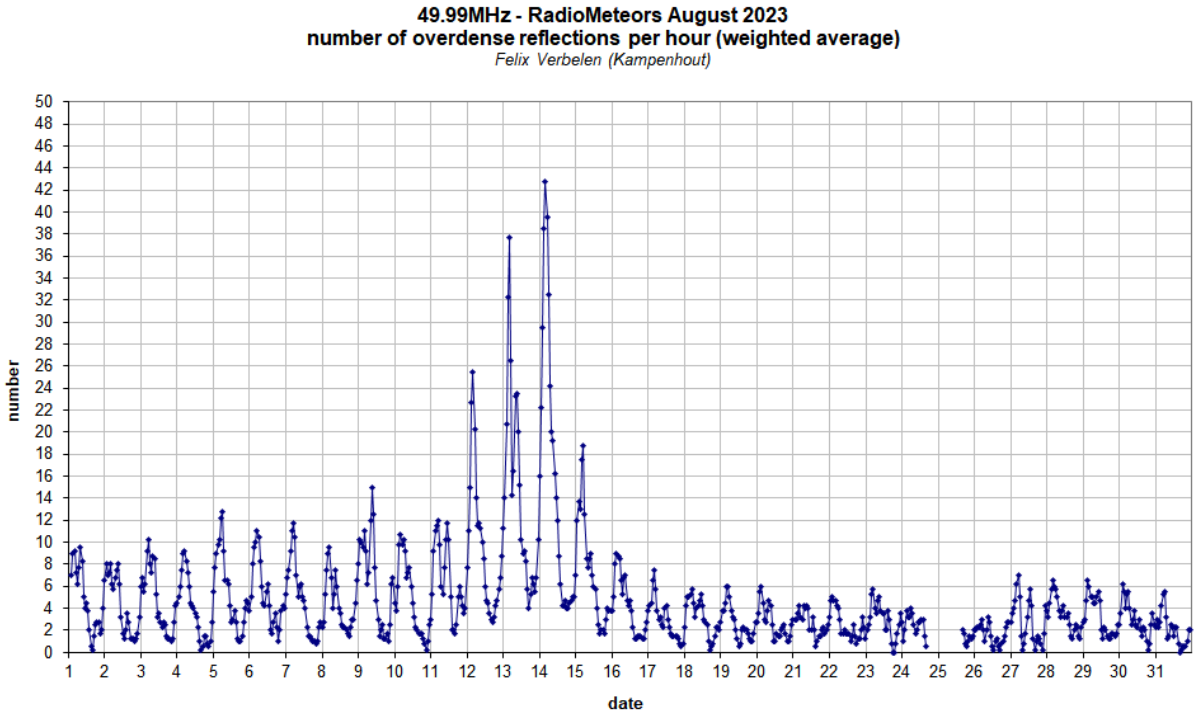

Figure 3 – The hourly numbers of "all" reflections counted automatically, and of manually counted "overdense" reflections, as observed here at Kampenhout (BE) on the frequency of our VVS-beacon (49.99 MHz) during August 2023.

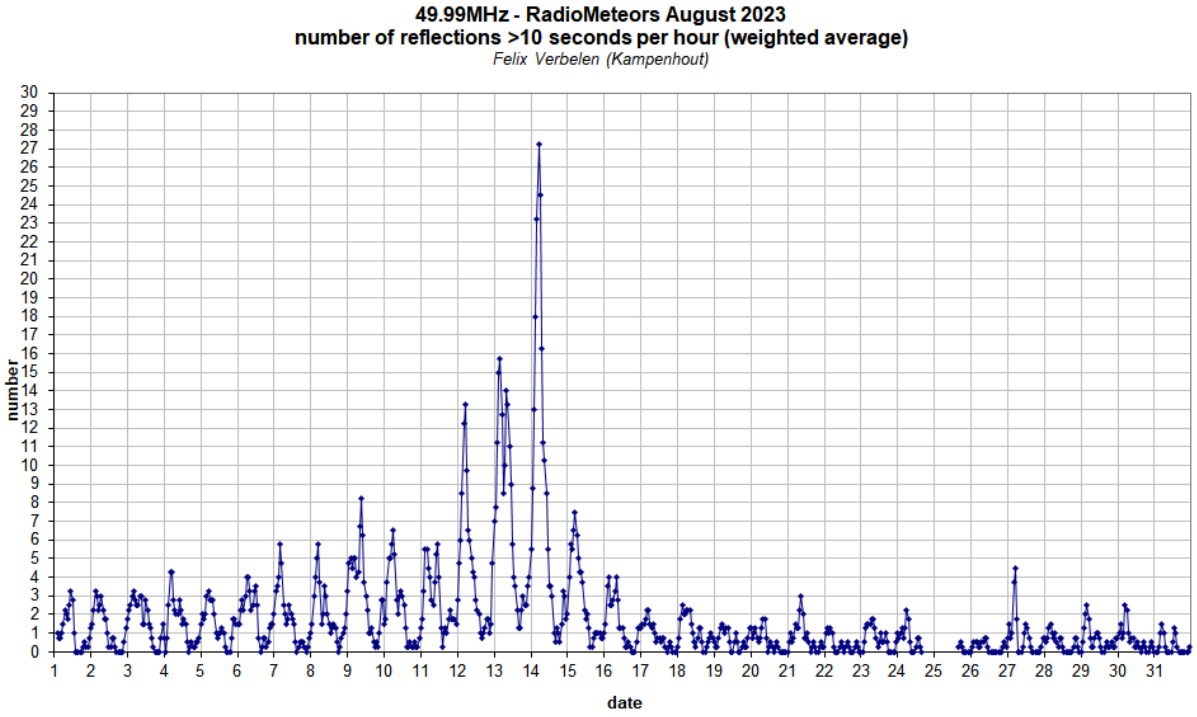

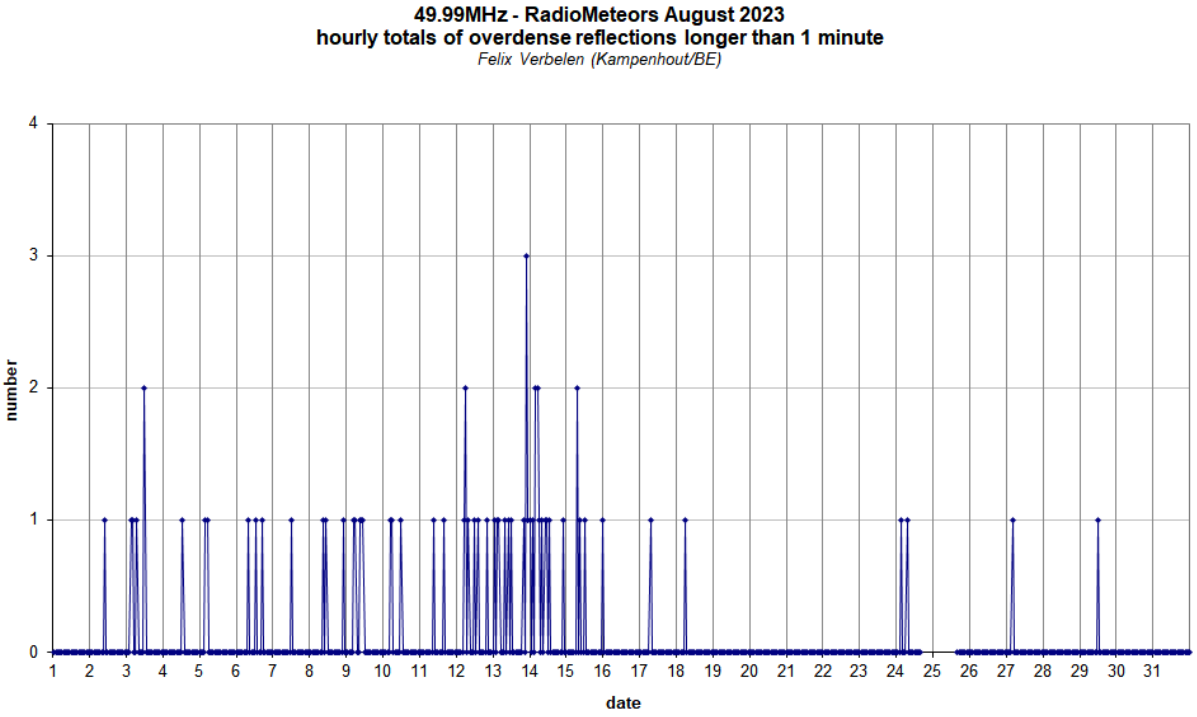

Figure 4 – The hourly numbers of overdense reflections longer than 10 seconds and longer than 1 minute, as observed here at Kampenhout (BE) on the frequency of our VVS-beacon (49.99 MHz) during August 2023.

 © eMeteorNews

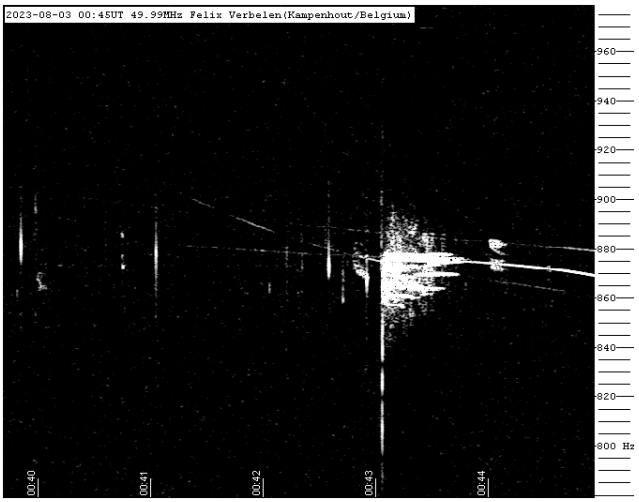

Figure 5 – Meteor echo 3 August 2023, 0^h45^m UT.

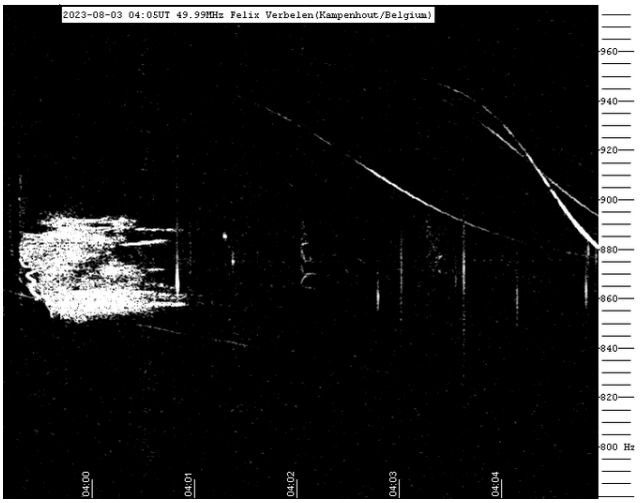

Figure 6 – Meteor echo 3 August 2023, 4^h05^m UT.

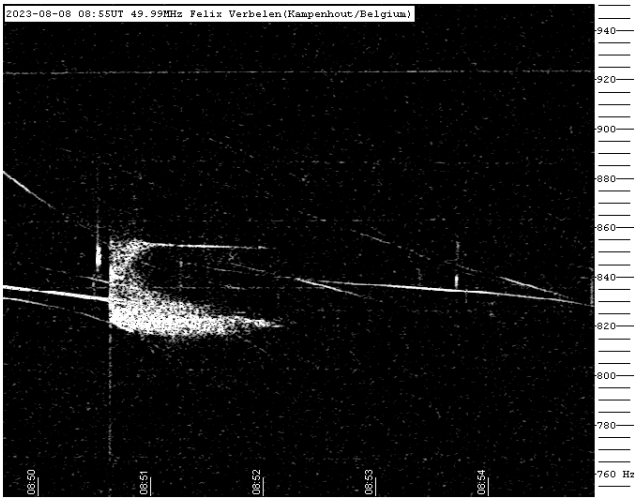

Figure 7 – Meteor echo 8 August 2023, 8^h55^m UT.

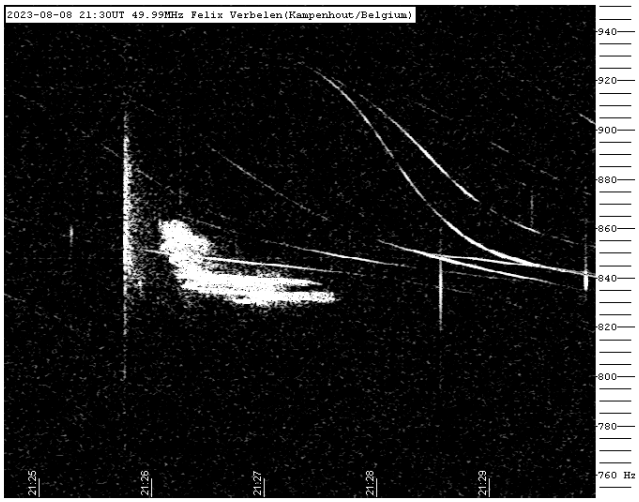

Figure 8 – Meteor echo 8 August 2023, 21^h30^m UT.

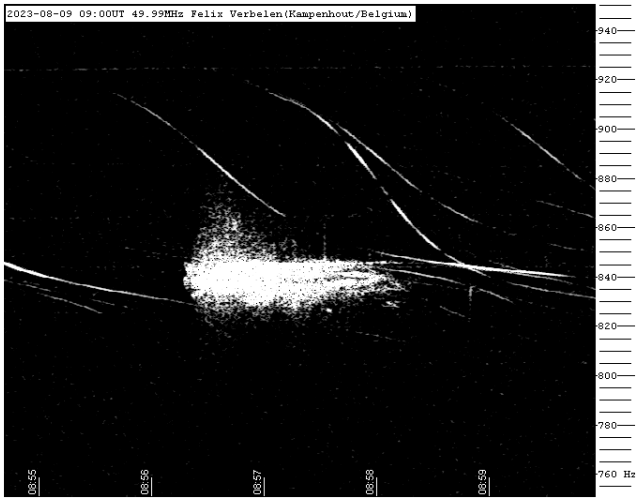

Figure 9 – Meteor echo 9 August 2023, 9^h00^m UT.

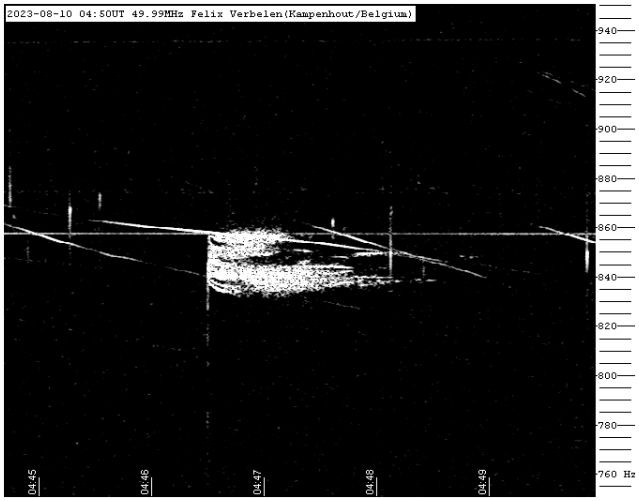

Figure 10 – Meteor echo 10 August 2023, 4^h50^m UT.

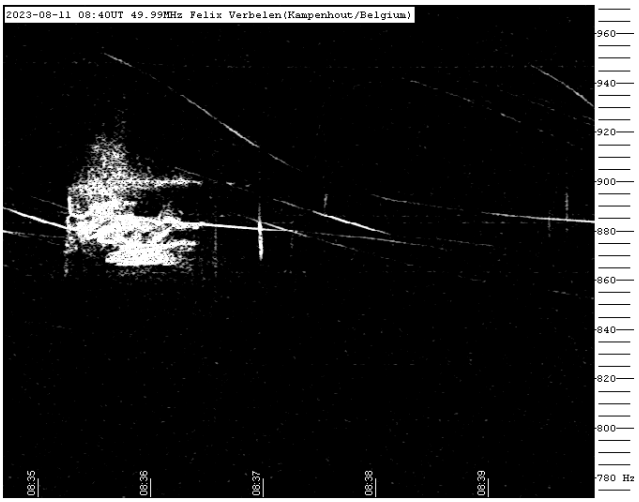

Figure 11 – Meteor echo 11 August 2023, 8^h40^m UT.

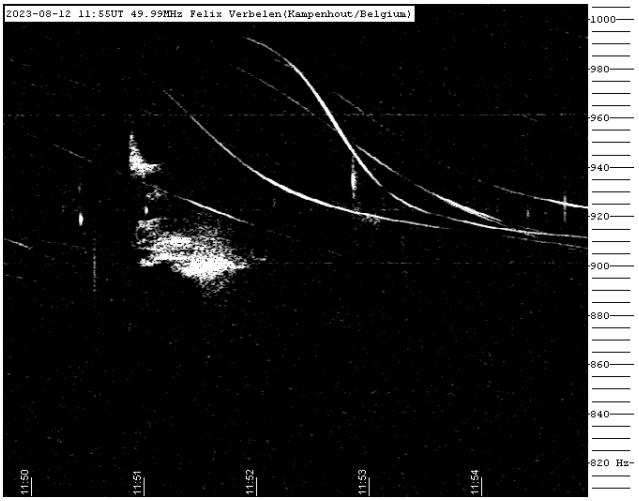

Figure 12 – Meteor echo 12 August 2023, 11^h55^m UT.

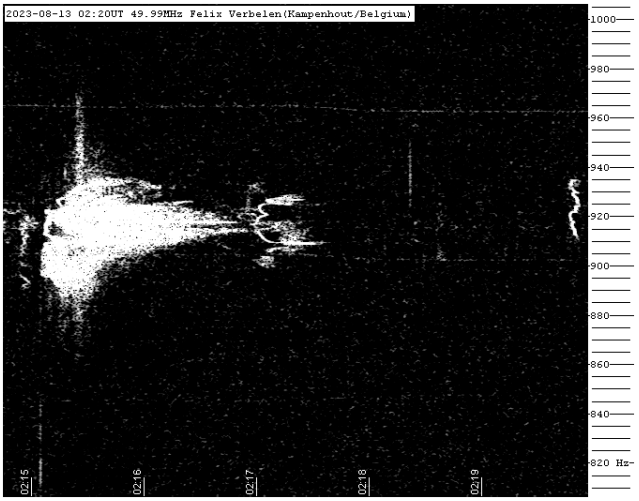

Figure 13 – Meteor echo 13 August 2023, 2^h20^m UT.

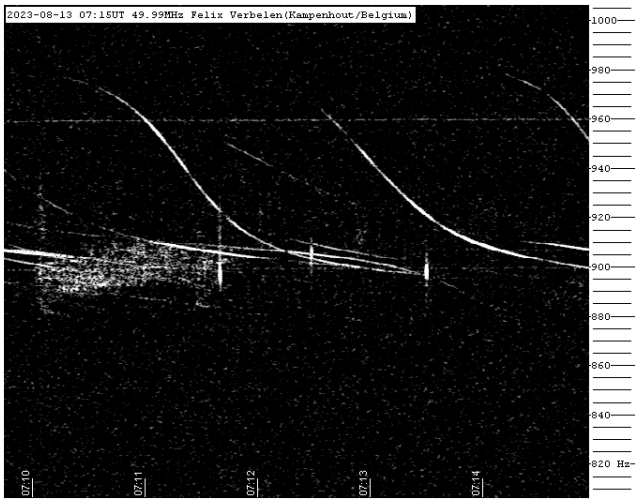

Figure 14 – Meteor echo 13 August 2023, 7^h15^m UT.

Figure 15 – Meteor echo 13 August 2023, 10^h30^m UT.

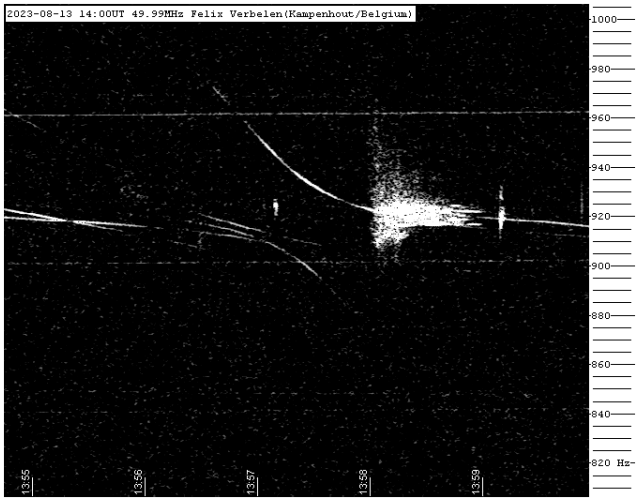

Figure 16 – Meteor echo 13 August 2023, 14^h00^m UT.

© eMeteorNews

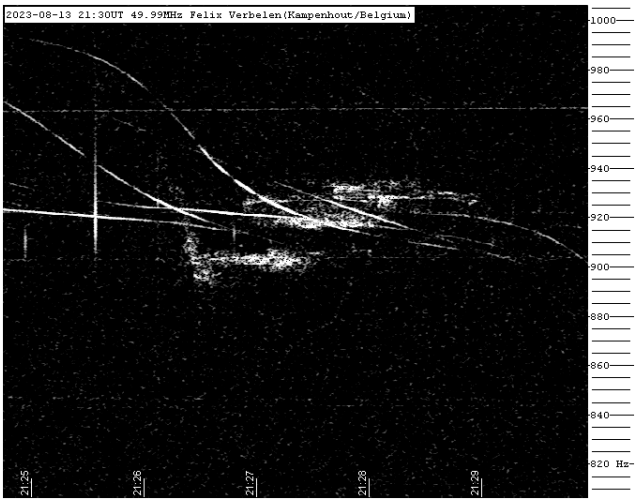

Figure 17 – Meteor echo 13 August 2023, 21^{h}30^{m} UT.

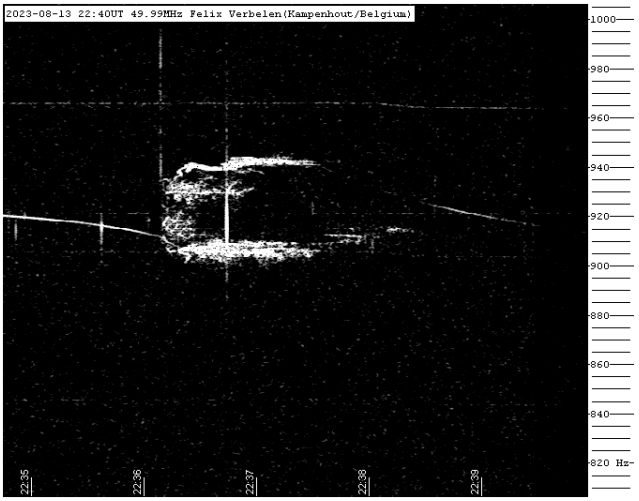

Figure 18 – Meteor echo 13 August 2023, 22^{h}40^{m} UT.

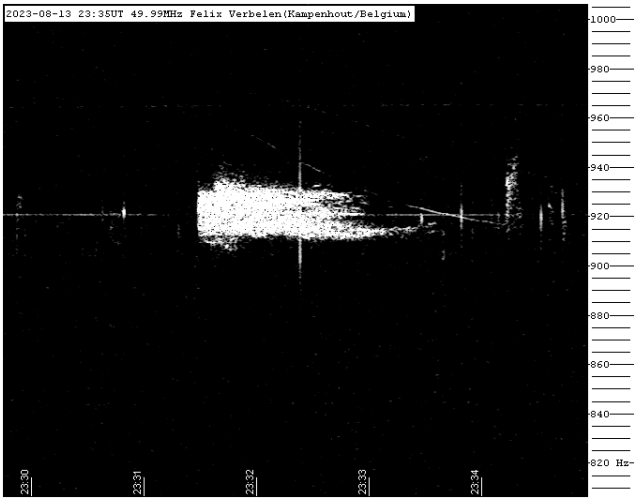

Figure 19 – Meteor echo 13 August 2023, 23^{h}35^{m} UT.

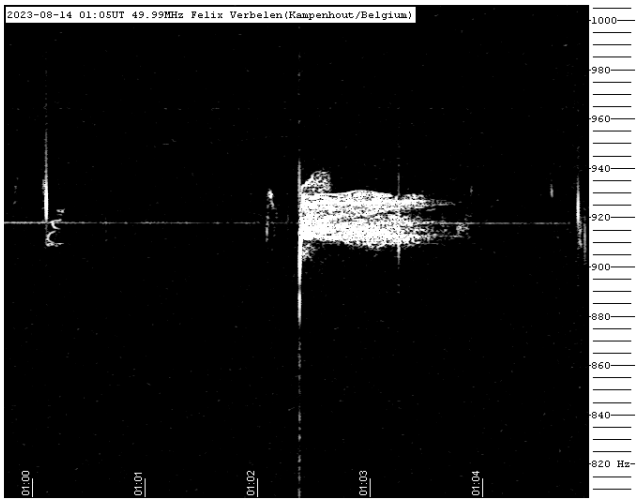

Figure 20 – Meteor echo 14 August 2023, 01^{h}05^{m} UT.

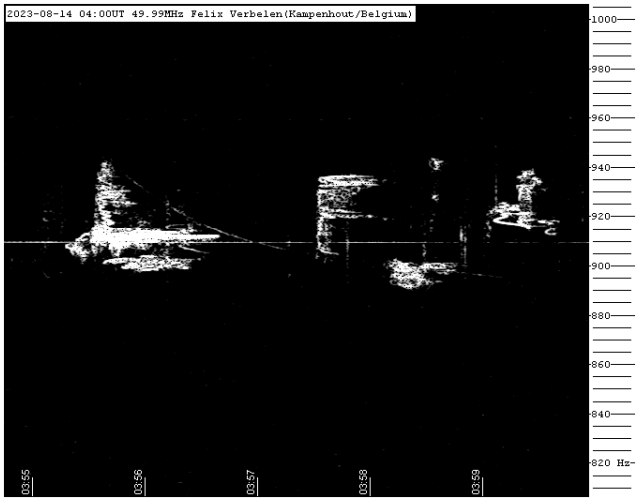

Figure 21 – Meteor echo 14 August 2023, 04^{h}00^{m} UT.

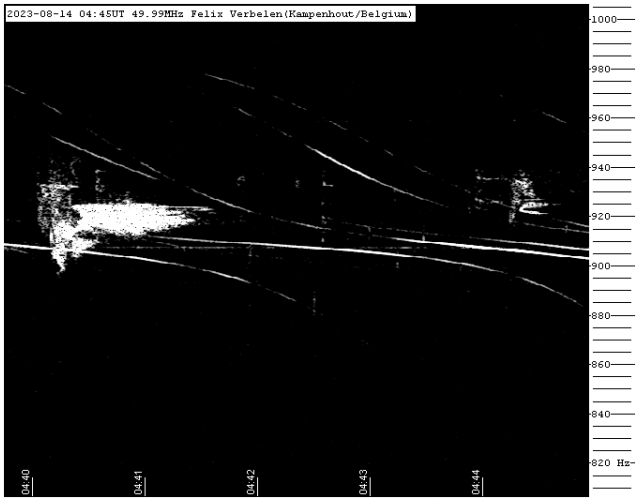

Figure 22 – Meteor echo 14 August 2023, 04^{h}45^{m} UT.

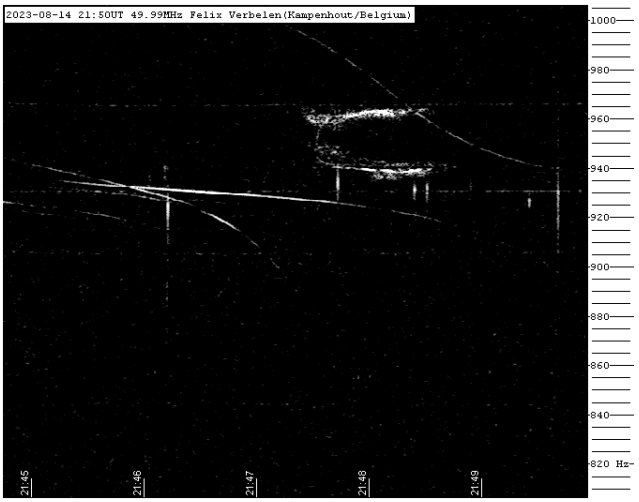

Figure 23 – Meteor echo 14 August 2023, 21^h50^m UT.

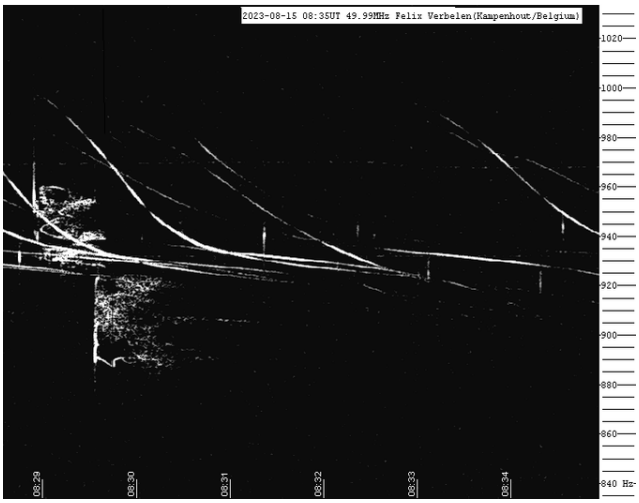

Figure 26 – Meteor echo 15 August 2023, 8^h35^m UT.

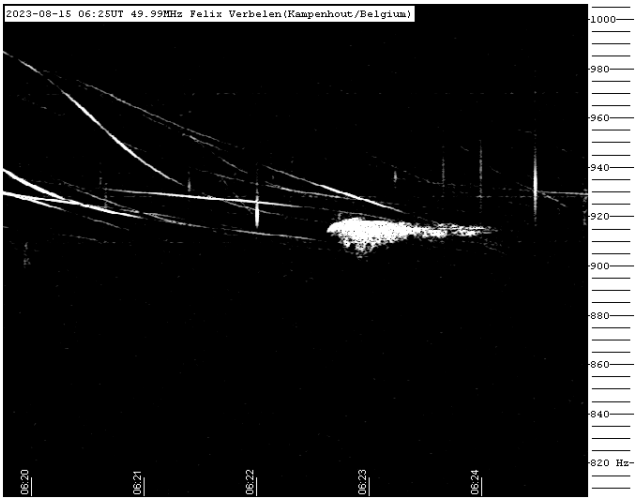

Figure 24 – Meteor echo 15 August 2023, 6^h25^m UT.

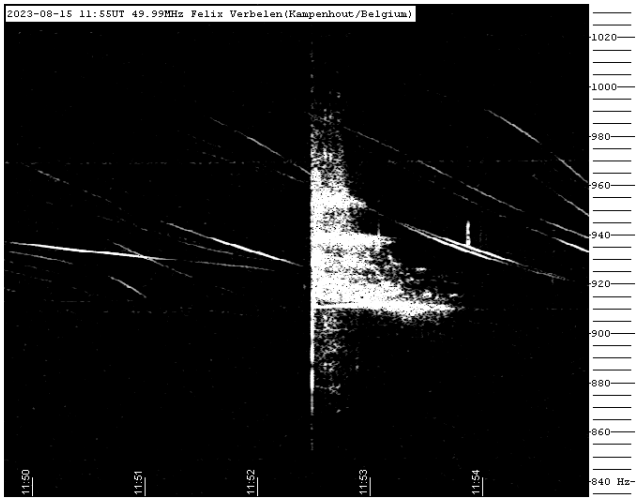

Figure 27 – Meteor echo 15 August 2023, 11^h55^m UT.

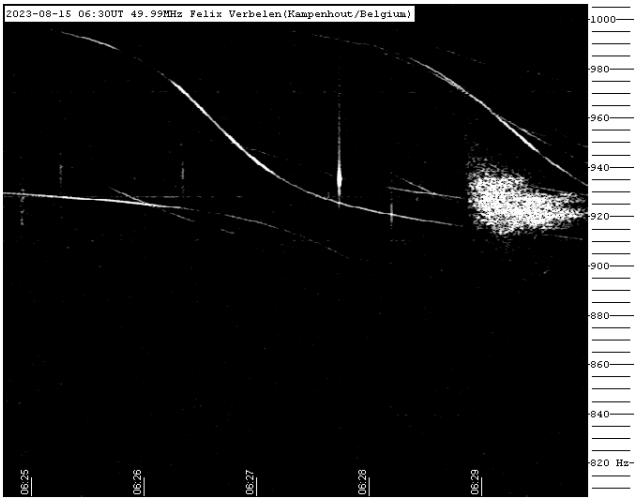

Figure 25 – Meteor echo 15 August 2023, 6^h30^m UT.

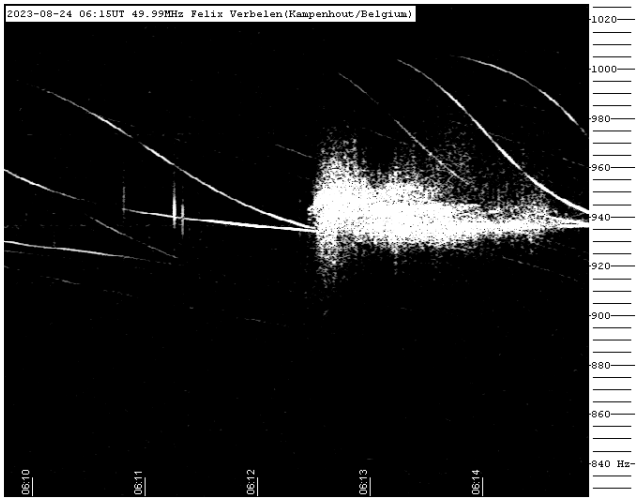

Figure 28 – Meteor echo 24 August 2023, 6^h15^m UT.

© eMeteorNews

Radio meteors September 2023

Felix Verbelen

Vereniging voor Sterrenkunde & Volkssterrenwacht MIRA, Grimbergen, Belgium
felix.verbelen@skynet.be

An overview of the radio observations during September 2023 is given.

1 Introduction

The graphs show both the daily totals (*Figure 1 and 2*) and the hourly numbers (*Figure 3 and 4*) of "all" reflections counted automatically, and of manually counted "overdense" reflections, overdense reflections longer than 10 seconds and longer than 1 minute, as observed here at Kampenhout (BE) on the frequency of our VVS-beacon (49.99 MHz) during the month of September 2023.

The hourly numbers, for echoes shorter than 1 minute, are weighted averages derived from:

$$N(h) = \frac{n(h-1)}{4} + \frac{n(h)}{2} + \frac{n(h+1)}{4}$$

Due to problems with the transmitting antenna, the beacon signal was unstable and weakened on many days during the month, especially in the period September 15 to 18. Therefore, observations for this period have been excluded from the counts and the automatic counts of "all" reflections for the other days are given with reservations.

During the month, local or unidentified noise remained rather low, but moderate to strong solar outbursts occurred almost every day. Some examples are attached (*Figures 5 to 10*). There was lightning activity on 4 days, which was quite intense on September 11 and 22.

Overall meteor activity was moderate, with a clear increase in overdense reflections during the first half of the month and daytime activity during the last days. Throughout the month, 12 reflections longer than 1 minute were observed, the most spectacular occurring during the last days of the month. A small selection of these, along with some other interesting reflections is included (*Figures 11 to 18*). Many more of these are available on request.

In addition to the usual graphs, you will also find the raw counts in cvs-format[28] from which the graphs are derived. The table contains the following columns: day of the month, hour of the day, day + decimals, solar longitude (epoch J2000), counts of "all" reflections, overdense reflections, reflections longer than 10 seconds and reflections longer than 1 minute, the numbers being the observed reflections of the past hour.

[28] https://www.meteornews.net/wp-content/uploads/2023/10/202309_49990_FV_rawcounts.csv

© eMeteorNews

Figure 1 – The daily totals of "all" reflections counted automatically, and of manually counted "overdense" reflections, as observed here at Kampenhout (BE) on the frequency of our VVS-beacon (49.99 MHz) during September 2023.

 © eMeteorNews

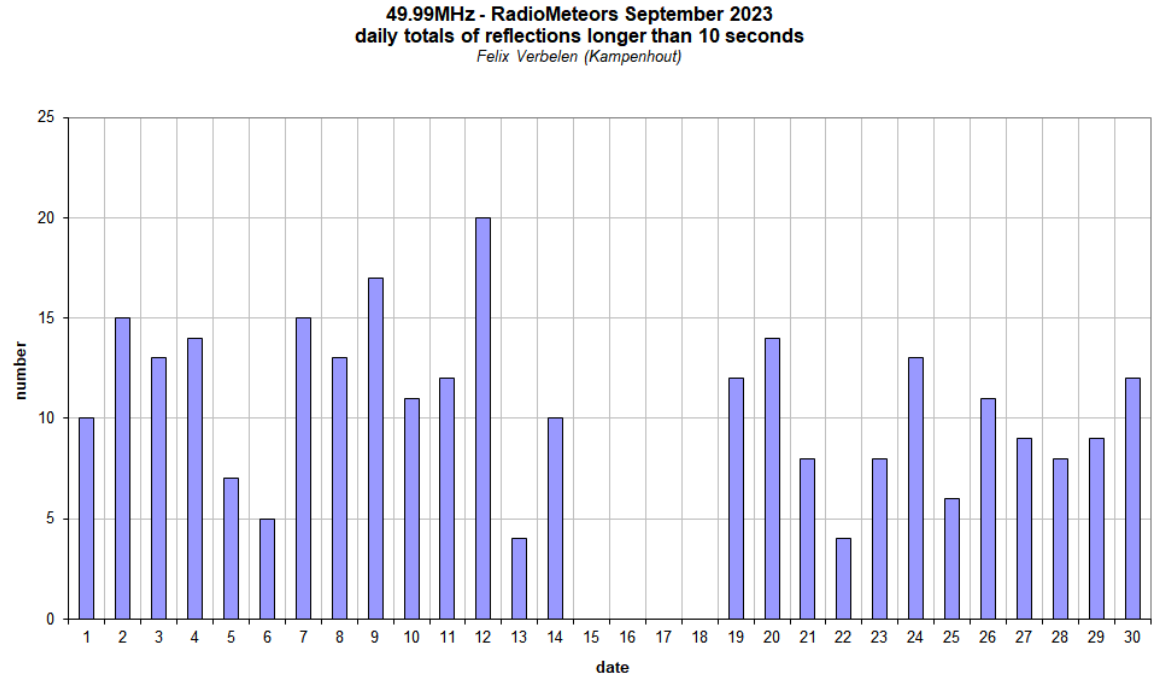

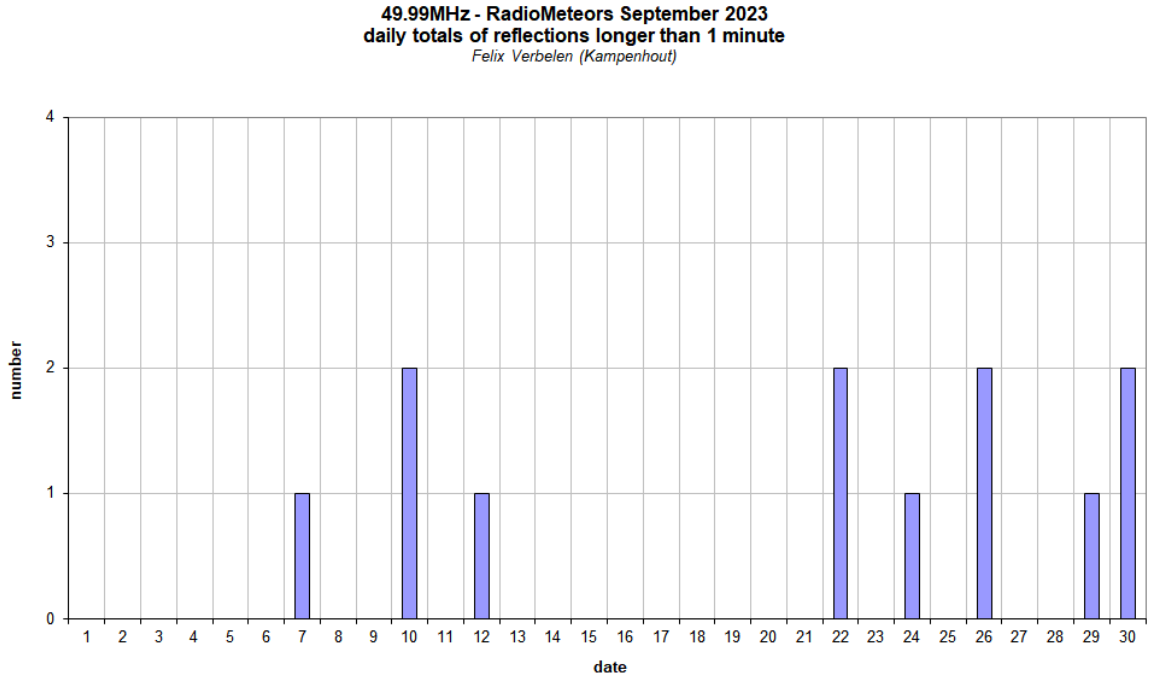

Figure 2 – The daily totals of overdense reflections longer than 10 seconds and longer than 1 minute, as observed here at Kampenhout (BE) on the frequency of our VVS-beacon (49.99 MHz) during September 2023.

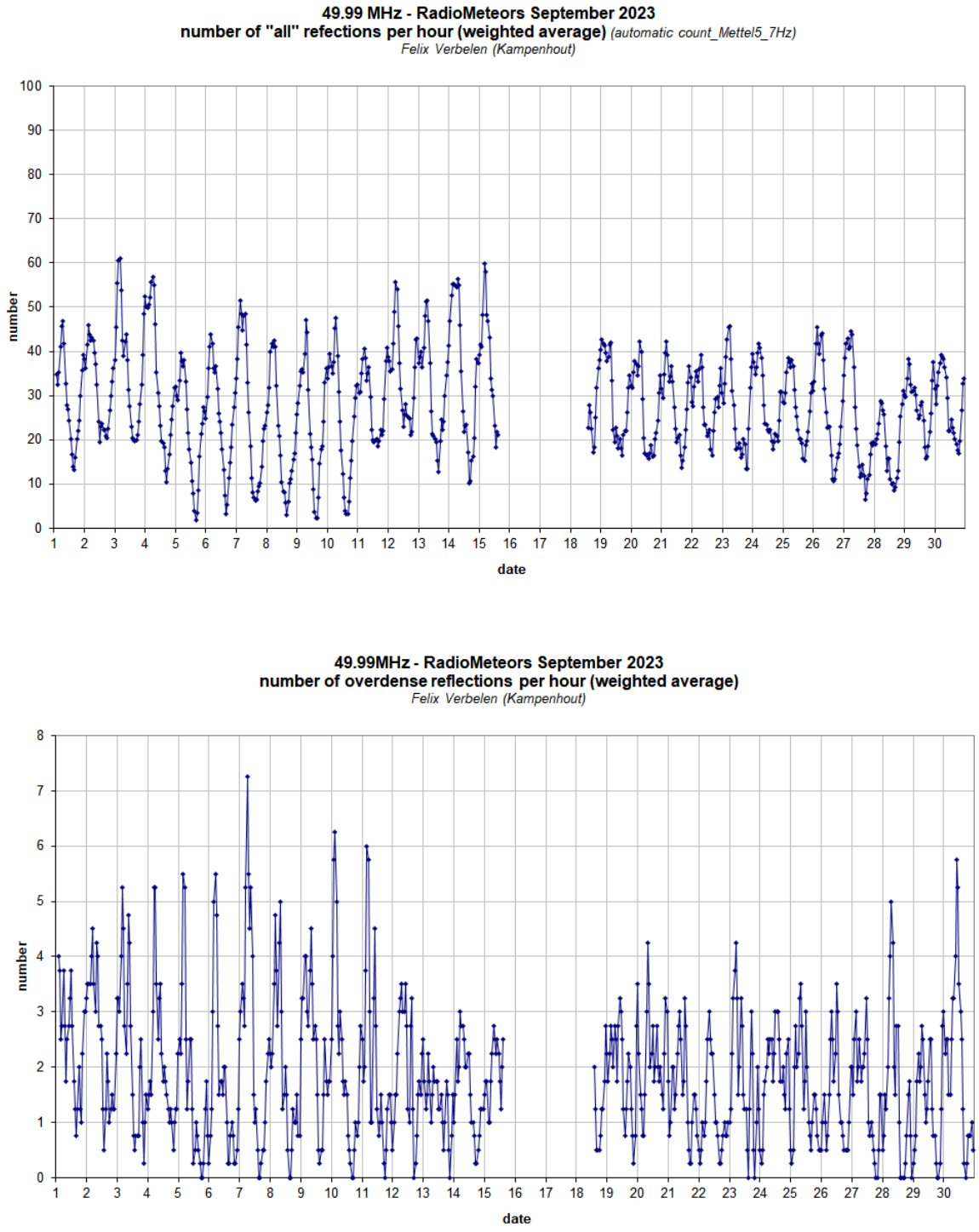

Figure 3 – The hourly numbers of "all" reflections counted automatically, and of manually counted "overdense" reflections, as observed here at Kampenhout (BE) on the frequency of our VVS-beacon (49.99 MHz) during September 2023.

 © eMeteorNews

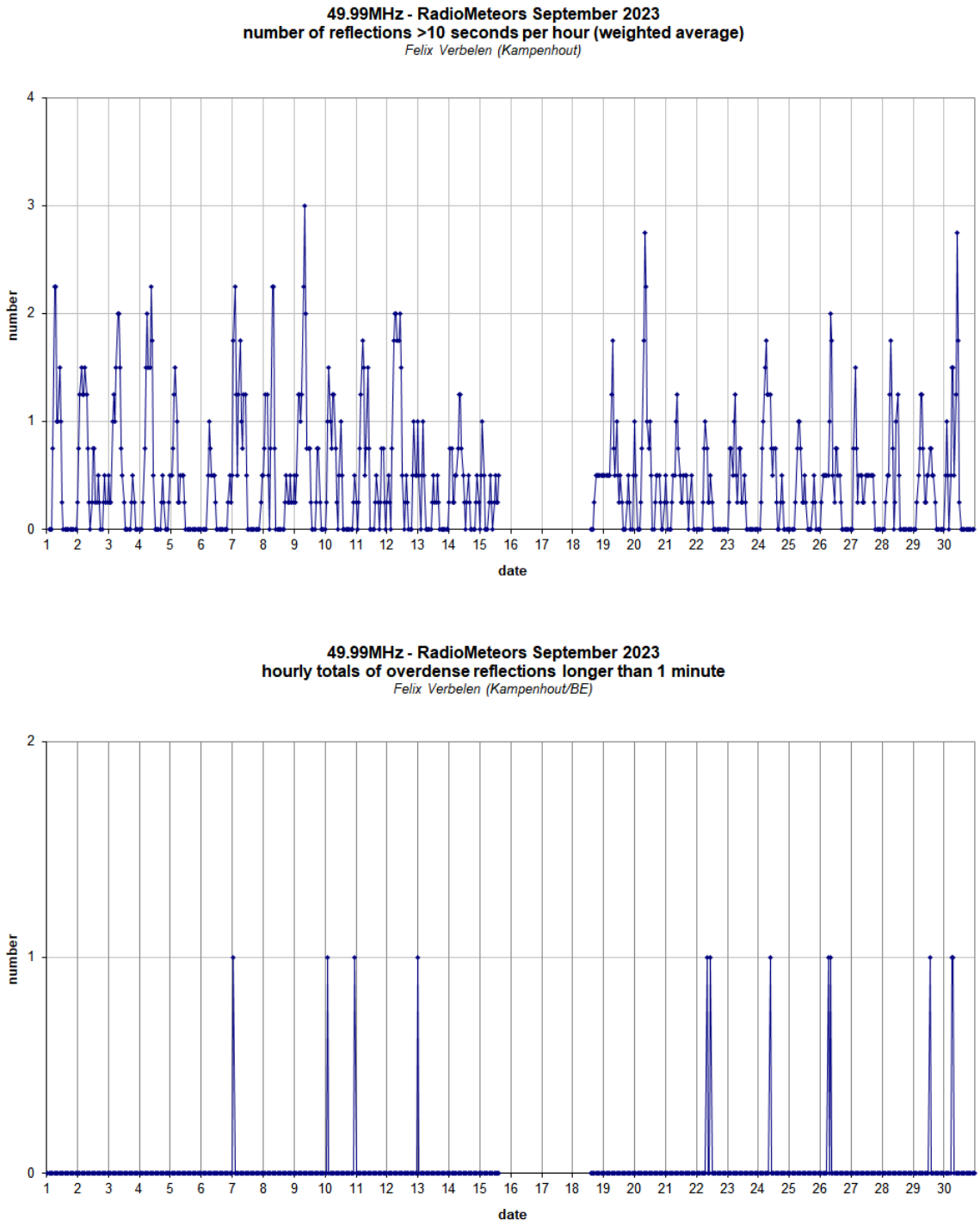

Figure 4 – The hourly numbers of overdense reflections longer than 10 seconds and longer than 1 minute, as observed here at Kampenhout (BE) on the frequency of our VVS-beacon (49.99 MHz) during September 2023.

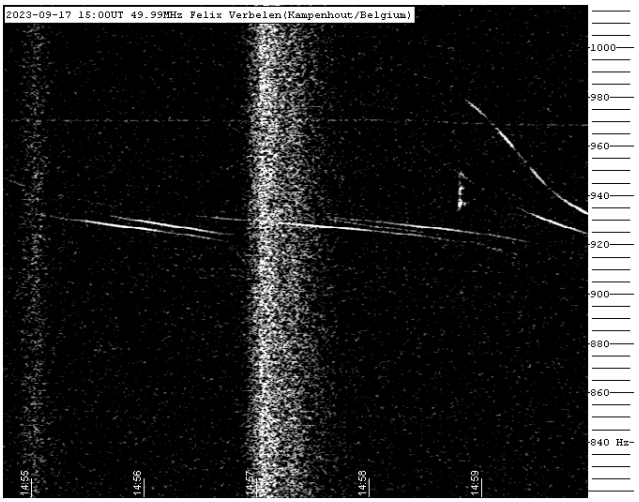

Figure 5 – Solar outburst 17 September 2023, 15^h00^m UT.

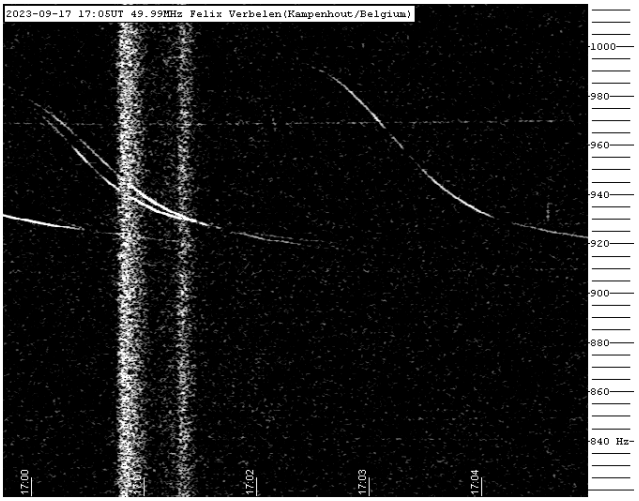

Figure 6 – Solar outburst 17 September 2023, 17^h05^m UT.

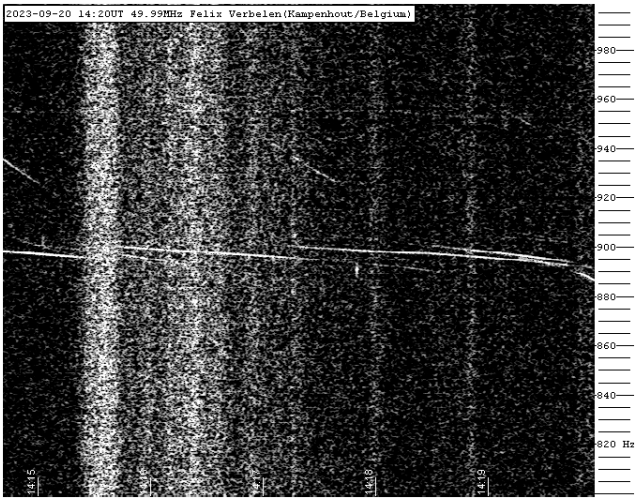

Figure 7 – Solar outburst 20 September 2023, 14^h20^m UT.

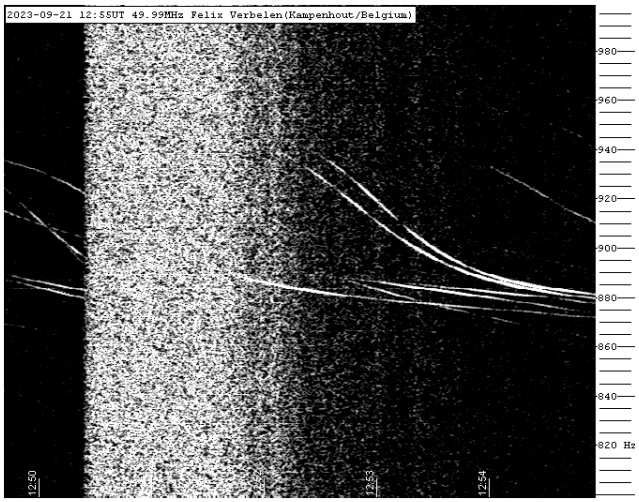

Figure 8 – Solar outburst 21 September 2023, 12^h55^m UT.

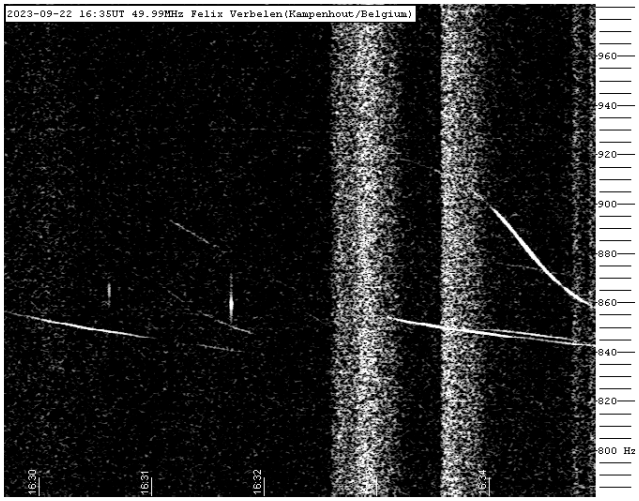

Figure 9 – Solar outburst 22 September 2023, 16^h35^m UT.

Figure 10 – Solar outburst 24 September 2023, 15^h00^m UT.

© eMeteorNews

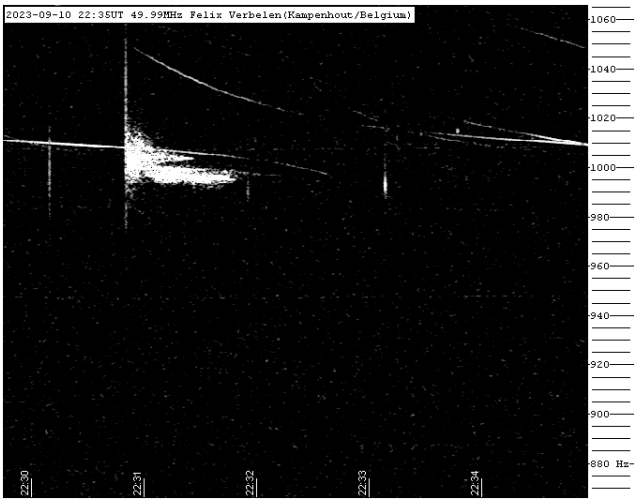

Figure 11 – Meteor echo 10 September 2023, 22^h35^m UT.

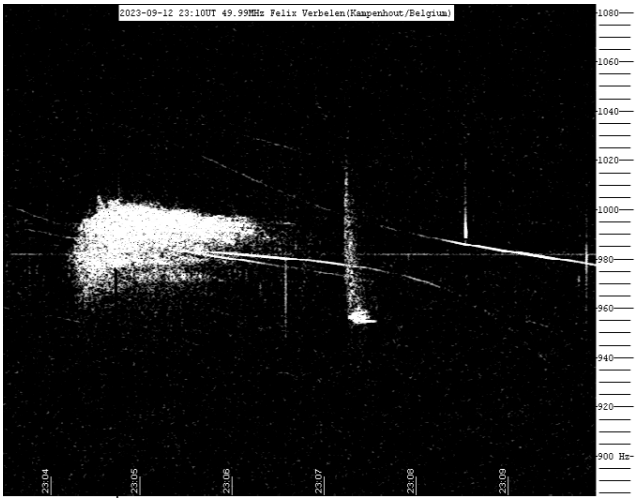

Figure 12 – Meteor echo 12 September 2023, 23^h10^m UT.

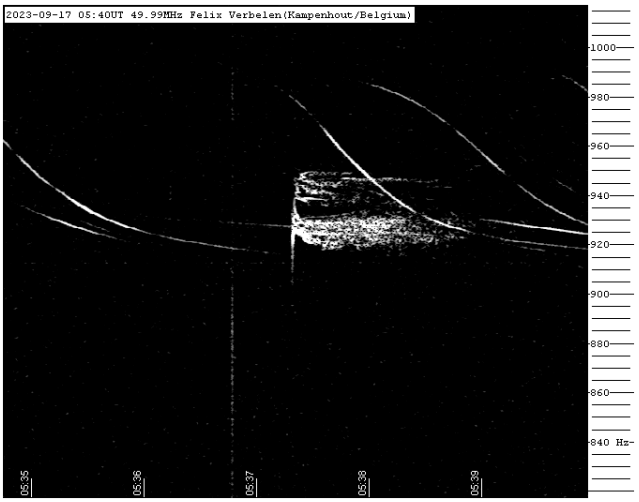

Figure 13 – Meteor echo 17 September 2023, 05^h40^m UT.

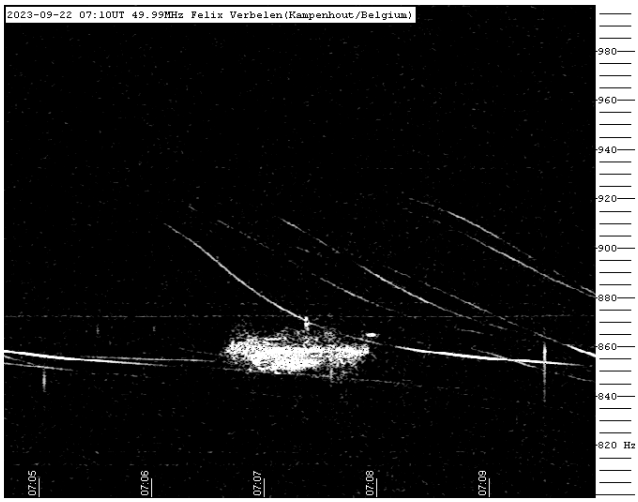

Figure 14 – Meteor echo 22 September 2023, 07^h10^m UT.

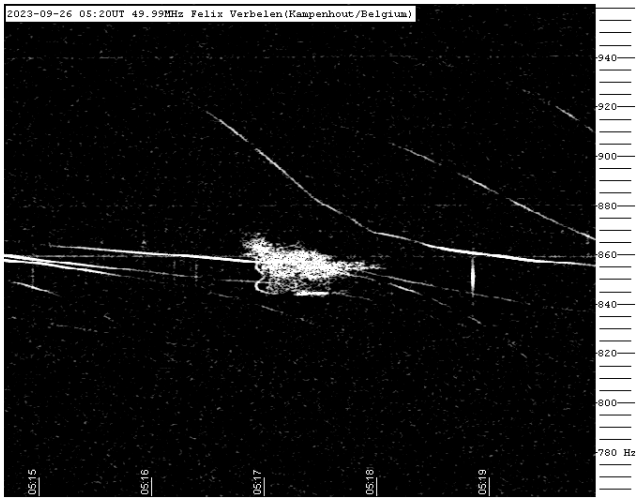

Figure 15 – Meteor echo 26 September 2023, 05^h20^m UT.

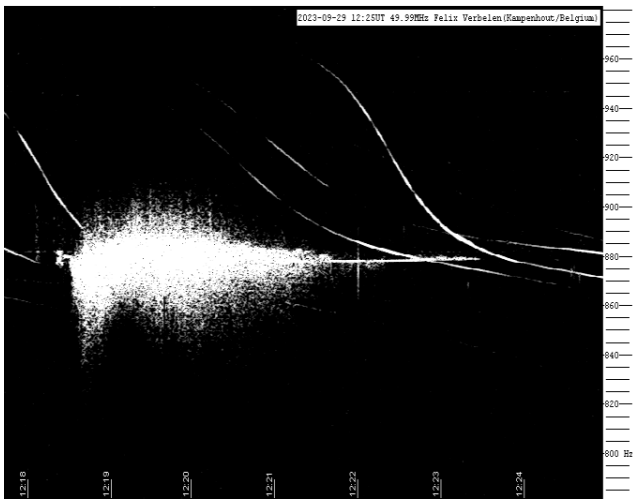

Figure 16 – Meteor echo 29 September 2023, 12^h25^m UT.

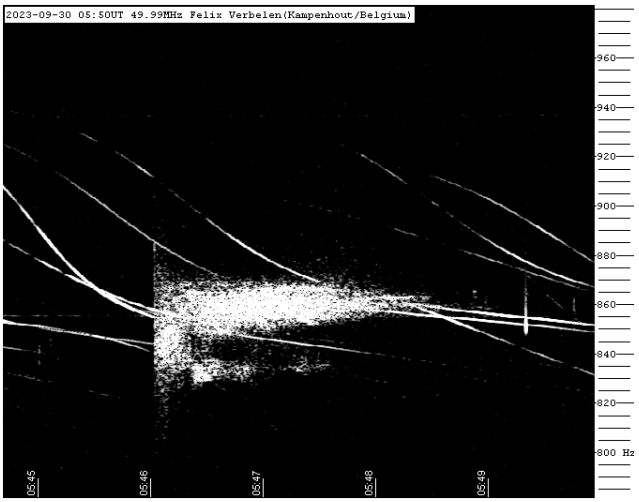

Figure 17 – Meteor echo 30 September 2023, 05^h50^m UT.

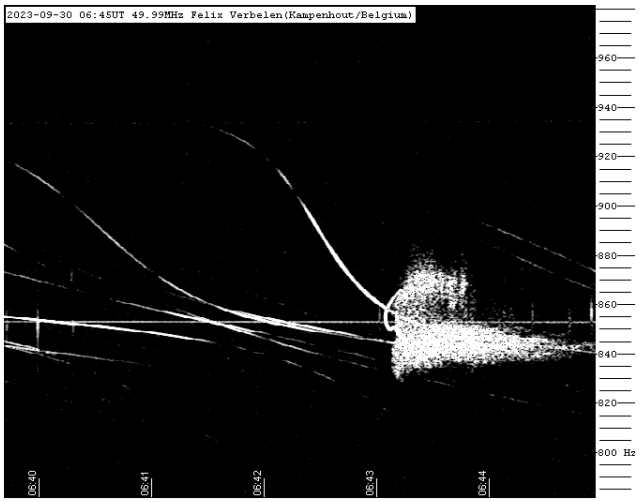

Figure 18 – Meteor echo 30 September 2023, 06^h45^m UT.

 © eMeteorNews

The mission of MeteorNews is to offer fast meteor news to a global audience, a swift exchange of information in all fields of active amateur meteor work without editing constraints. MeteorNews is freely available without any fees.

You are welcome to contribute to MeteorNews on a regular or casual basis, if you wish to. Anyone can become an author or editor, send an email to us. For more info read: https://meteornews.net/writing-content-for-emeteornews/

MeteorNews account manager: Richard Kacerek <rickzkm@gmail.com>.

The running costs for website hosting are covered by a team of sponsors. We want to thank the 2022-2023 sponsors: Anonymous (3x), Mikhail Bidnichenko, Gaetano Brando, TomB, Trevor C, Nigel Cunnington, Richard Glassner, Kevin Heider, Paul Hyde, K. Jamrogowicx, Dave Jones, Richard Kacerek, Richard Lancaster, Joseph Lemaire, Mark McIntyre, Hiroshi Ogawa, Paul Mohan, Stan Nelson, Lubos Neslusan, BillR, Whitham D. Reeve, John Schlin, Ann Schroyens and Denis Vida.

Contributing to this issue:

- Crivello S
- Johannink C
- Koseki M
- Kurenya I
- Miskotte K
- Stomeo E
- Terentjeva A
- Vandeputte M
- Verbelen F

ISSN 2570-4745 Online publication https://meteornews.net

Listed and archived with ADS Abstract Service: https://ui.adsabs.harvard.edu/search/q=eMetN

MeteorNews Publisher:

Valašské Meziříčí Observatory, Vsetínská 78, 75701 Valašské Meziříčí, Czech Republic

Copyright notices © 2023: The copyright of articles submitted to eMeteorNews remains with the authors